ESECMaSE

Enhanced **S**afety and **E**fficient **C**onstruction of **Ma**sonry **S**tructures in **E**urope

Project No. Coll – Ct - 2003 - 500291

ESECMaSE

Enhanced Safety and Efficient Construction of Masonry Structures in Europe

Horizontal Research Activities Involving SMEs

Collective Research

Work Package N°: 7

D 7.1a Test results on the behaviour of masonry under static (monotonic and cyclic) in plane lateral loads

Prof. Dr.-Ing. E. Fehling, Dipl.-Ing. J. Stuerz, Dipl.-Ing. A. Emami

Due date of deliverable: 10.04.2006
Actual submission date: 30.03.2007

Start date of project: 10.04.2004 Duration: 36 months

University of Kassel
Institute of Structural Engineering
Chair of Structural Concrete
Kurt-Wolters-Straße 3
34109 Kassel [draft 1]

Project co-funded by the European Commission within the Sixth Framework Programme (2002-2006)		
Dissemination Level		
PU	Public	X
PP	Restricted to other programme participants (including the Commission Services)	
RE	Restricted to a group specified by the consortium (including the Commission Services)	
CO	Confidential, only for members of the consortium (including the Commission Services)	

Contents:

1. Introduction

Static-cyclic tests with a test set-up as developed in WP 6 on different kinds of masonry (clay, calcium silicate and lightweight concrete) were carried out at Kassel University. The tests have been performed using different levels of vertical stresses and different specimen dimensions.

Because the static-cyclic tests of the ESECMaSE project were carried out at different laboratories, this deliverable is divided into three parts:

⇒ D 7.1a - University of Kassel (UNIK)

⇒ D 7.1b - Technical University of Munich (TUM)

⇒ D 7.1c - University of Pavia (UPavia)

Because of the satisfying results of the first three tests in WP 6.4, no more verification tests are deemed to be necessary in Kassel and Munich. Since the tests in total ten tests had been allocated for deliverable D 6.4, it was decided to perform additional tests in work package 7. On the other hand it was decided to analyse the walls which were intended for monotonic tests at a static cyclic load history, too, because these tests show more substantial results with just a little more effort. So 25 static cyclic tests on walls with a width of 175 mm or 300 mm and a height of 2.50 m were carried out at Kassel University.

2. Materials used

The first and the last layer of mortar of all tested walls were fabricated with a general purpose mortar Sakret ZM M10 according to DIN EN 998-2. The other kinds of mortar were specific to each kind of bricks.

2.1. Walls made of clay bricks

2.1.1. Units

Four different kinds of vertically perforated clay bricks have been used. Three of them have a width of 175 mm and a length of 363 mm, the fourth one has a width of 300 mm and a length of 249 mm. The height of the bricks depends on the mortar used and is 238 mm for general purpose mortar and 249 mm for thin layer mortar. The conventional clay brick is a HLZ-Plan–12–0.9–9DF. The optimised ones have different hole patterns but the same density.

As the first range of the optimised clay bricks had a smaller vertical compressive strength as the conventional bricks, a second range of optimised clay bricks with smaller holes was produced. For the strength values of the different kind of bricks see [4].

To represent bricks for exterior walls additional tests on Plan T10 with a thickness of 300 mm were achieved. This bricks have an allowable strength of 0.7 N/mm^2 according to approval Z-17.1-889.

conventional

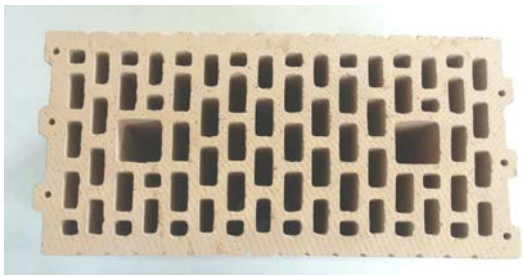

optimised

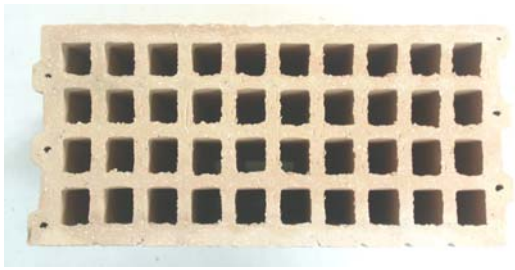

T10

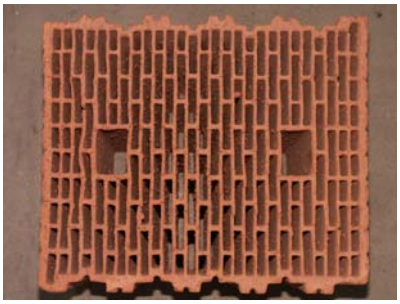

optimised 2

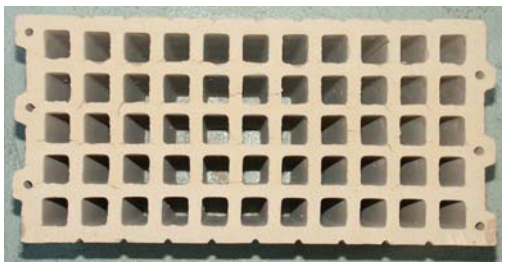

figure 1: different hole patterns of the clay bricks

The compressive strength of the T10 bricks were tested in three single brick tests. The results of these tests are given in table 1.

table 1: overview of the tests on clay bricks T10

specimen No.	**force [kN]**	**face [mm^2]**	**strength [N/mm^2]**	**average [N/mm^2]**
1	897.6	75910	11.8	10.3
2	631.8	76629	8.2	
3	835.1	76894	10.9	

2.1.2. Mortar

- General purpose mortar
  ready-mixed mortar M5 according to DIN EN 998-2
- Thin layer mortar
  Bellenberger Planziegel thin layer mortar
  Generally approved by the building authorities (DIBT Zul.-Nr. Z.17.1-261)
- Thin layer mortar
  Wienerberger Poroton thin layer mortar for bricks T10
  Generally approved by the building authorities (DIBT Zul.-Nr. Z.17.1-261)

2.2. Walls made of calcium silicate units

2.2.1. Units

Two different kinds of calcium silicate bricks were used. Each of them had a width of 175 mm, a length of 249 mm and a height 248 mm. The conventional calcium silicate bricks are KS-R-Plansteine 20–1.8-6 DF.

conventional

optimised

figure 2: different kinds of calcium silicate bricks

2.2.2. Mortar

- Thin layer mortar
  Mortar class M10 according to DIN EN 998-2

2.3. Walls made of LAC units

2.3.1. Units

Two different kinds of LAC bricks were used. Each of them had a width of 175 mm and a length of 249 mm. The height of the bricks depends on the used mortar and is 238 mm for general purpose mortar and 249 mm for thin layer mortar. The LAC bricks are Bisophon 17.5 VBL–12-2.0-6 DF.

figure 3: view of a LAC brick

2.3.2. Mortar

- General purpose mortar
  ready-mixed mortar M5 according to DIN EN 998-2
- Thin layer mortar
  Bisotherm heat-insulating thin layer mortar
  Mortar class M10 according to DIN EN 998-2

3. Static-cyclic tests

3.1. Test programme

25 wall tests were performed at Kassel University. 15 were based on clay bricks with a width of 175 mm (see table 2), two on calcium silicate units (see table 3), five on LAC units (see table 4) and three on clay bricks T10 (see table 5). All of these walls except one LAC wall were tested with a fixed support at the top of the wall, so that the point of zero moment is at mid height of the wall as described in WP6.3. One LAC wall (LAC-0M-dm-150-220-1) was tested without any fixed support at the top of the wall. So the moment on the bottom of the wall is 2.90 m · H, because of the lever arm between the bottom of the wall and the axis of the horizontal force.

For all combinations of units and mortar investigations of different wall lengths and different kinds of vertical loading were done. Table 2 up to table 5 represent all tests with their special boundary conditions.

For the walls made of T10 bricks the tests were carried out centric as well as eccentric (out of plane). In the eccentric case, only a portion of 20.0 cm of the wall thickness was loaded.

table 2: overview of the wall tests on clay bricks

No.	specimen	kind of brick	Length of the wall [m]	mortar	vertical stress [N/mm²]	M/Q/h
1	Hlz-nm-220-380-1	conventional	2,2	general purpose	1,00	0,5
2	Hlz-dm-220-380-1	conventional	2,2	thin layer	1,00	0,5
3	Hlz-nm-220-380-2	conventional	2,2	general purpose	1,00	0,5
4	Hlz-dm-220-380-2	conventional	2,2	thin layer	1,00	0,5
5	Hlz-opti-dm-220-380-1	optimized	2,2	thin layer	1,00	0,5
6	Hlz-opti-nm-220-380-1	optimised	2,2	general purpose	1,00	0,5
7	Hlz-opti-dm-110-190-1	optimised	1,1	thin layer	1,00	0,5
8	Hlz-opti-nm-110-190-1	optimised	1,1	general purpose	1,00	0,5
9	Hlz-opti-dm-220-95-1	optimised	2,2	thin layer	0,25	0,5
10	Hlz-opti2-dm-220-380-1	optimised 2	2,2	thin layer	1,00	0,5
11	Hlz-opti2-nm-220-380-1	optimised 2	2,2	general purpose	1,00	0,5
12	Hlz-opti2-dm-110-190-1	optimised 2	1,1	thin layer	1,00	0,5
13	Hlz-opti2-dm-110-95-1	optimised 2	1,1	thin layer	0,50	0,5
14	Hlz-opti2-dm-110-48-1	optimised 2	1,1	thin layer	0,25	0,5
15	Hlz-opti2-dm-220-95-1	optimised 2	2,2	thin layer	0,25	0,5

table 3: overview of the wall tests on calcium silicate bricks

No.	specimen	kind of brick	Length of the wall [m]	mortar	vertical stress [N/mm²]	M/Q/h
16	KS-125-220-1	conventional	1,25	thin layer	1,00	0,5
17	KS-opti-125-220-1	optimised	1,25	thin layer	1,00	0,5

table 4: overview of the wall tests on LAC

No.	specimen	kind of brick	Length of the wall [m]	mortar	vertical stress [N/mm²]	M/Q/h
18	LAC-nm-125-220-1	conventional	1,25	general purpose	1,00	0,5
19	LAC-dm-125-220-1	conventional	1,25	thin layer	1,00	0,5
20	LAC-nm-125-110-1	conventional	1,25	general purpose	0,50	0,5
21	LAC-dm-125-110-1	conventional	1,25	thin layer	0,50	0,5
22	LAC-0M-dm-125-220-1	conventional	1,25	thin layer	1,00	1,0

table 5: overview of the wall tests on clay bricks T10

No.	specimen	kind of brick	Length of the wall [m]	mortar	vertical stress [N/mm²]	M/Q/h
23	T10-exz-200-280-1	T10 (eccentric)	2.00	thin layer	0.70	0.5
24	T10-zen-200-280-1	T10 (centric)	2.00	thin layer	0.47	0.5
25	T10-exz-100-140-1	T10 (eccentric)	2.00	thin layer	0.70	0.5

3.2. Test procedure

Each test has been performed applying a load history as given in annex A. The horizontal force is under compression (negative value) when the hydraulic jack is moving from the left to the right hand side and under tension (positive value) when moving the other way around. In the following the distinctive features of each test are described.

3.2.1. Test No. 1

At a horizontal force of about +90 kN first cracks (see figure A1-1) were visible in the upper right corner of the wall. At the maximum horizontal force, the complete vertical force could not be carried by the wall anymore.

3.2.2. Test No. 2

At a horizontal force of about +100 kN first cracks were visible. The load history for this test is different to the other tests (see figure A2-3). Because of this, an analysis of the ductility of this wall was not possible.

3.2.3. Test No. 3

At a horizontal force of about +48 kN cracking was audible. The first visible cracks appeared at a horizontal force of about -102 kN in the bottom right corner (see figure A3-1). The end of the test is determined by the failure of the upper left corner of the wall (see figure A3-2).

3.2.4. Test No. 4

Within the vertical loading at a vertical force of -360 kN a cracking is audible. At a horizontal force of about +87 kN cracking became audible again. From a horizontal force of about +110 kN the cracking becomes louder. The first visible cracks appeared at a horizontal force of about -130 kN in the left upper corner (see figure A4-1). The end of the test is determined by the failure of the upper right corner of the wall (see figure A4-2).

3.2.5. Test No. 5

The first visible cracks appeared at a horizontal force of about 90 kN in the right upper corner (see figure A5-1). The end of the test is determined by cracks in the middle of the wall, where shells of the vertically perforated bricks fell off (see figure A5-2).

3.2.6. Test No. 6

At a horizontal force of about +62 kN became first cracking audible. The first visible cracks appeared at a horizontal force of about +65 kN (see figure A6-1). Within a horizontal force of -120 kN another cracking is audible for each cycle but no cracks are visible in this direction. The first visible cracks in this direction appeared at a horizontal force of about -150 kN.

The end of the test is determined by a decrease of the horizontal force in the compression direction (see figure A6-4).

3.2.7. Test No. 7

The first visible vertical crack appeared at a horizontal force of about +50 kN (see figure A7-1). The first visible cracks in the diagonal direction appeared at a horizontal force of about +58 kN in the middle of the wall. The end of the test is determined by cracks in the middle and in the right upper corner of the wall, where shells of the vertically perforated bricks fell down (see figure A7-2).

3.2.8. Test No. 8

At a horizontal force of about -53 kN first cracking was audible. The first visible cracks appeared at a horizontal force of about -55 kN. The end of the test is determined by cracks in the bottom left corner of the wall, where shells of the vertically perforated bricks fell off (see figure A8-2).

3.2.9. Test No. 9

At a horizontal force of about -63 kN a first cracking was audible and cracks appeared at in the bed joints of the wall (see figure A8-1). A sliding in the bed joints was visible (see figure A9-2). The end of the test is determined by cracks in the bottom right corner of the wall at a horizontal force of -66 kN.

3.2.10. Test No. 10

At a horizontal force of about +70 kN first cracking was audible. The first visible cracks appeared at a horizontal force of about -127 kN (see figure A10-1). The end of the test is determined by cracks in the bottom left and the upper right corner of the wall.

3.2.11. Test No. 11

At a horizontal force of about -134 kN first cracking was audible. The first visible cracks appeared at a horizontal force of about -140 kN (see figure A11-1). The end of the test is determined by cracks in the bottom right corner of the wall.

3.2.12. Test No. 12

At a horizontal force of -70 kN a sudden cracking over the total diagonal of the wall appeared (see figure A12-1). The end of the test is determined by this first crack.

3.2.13. Test No. 13

The first visible cracks appeared at a horizontal force of about -41 kN (see figure A13-1). The end of the test is determined by cracks over the whole diagonal length (see figure A13-2).

3.2.14. Test No. 14

No cracking in the bricks is visible. Only a gapping at the bottom (see figure A14-1) and at the top of the wall could be detected.

3.2.15. Test No. 15

Already at a horizontal force of about -10 kN first cracking was audible. The first visible cracks appeared at a horizontal force of about +70 kN in the bed joints of the wall.

3.2.16. Test No. 16

The first visible cracks in the units appeared at a horizontal force of about +86 kN (see figure A16-1). The end of the test is determined by cracks over the whole diagonal length (see figure A16-2) .

3.2.17. Test No. 17

The first visible cracks in the units appeared at a horizontal force of about -81 kN (see figure A17-1). The end of the test is determined by a drop-out of a part of a unit in the bottom left corner of the wall (see figure A17-2) .

3.2.18. Test No. 18

First visible cracks in the units appeared at the failure of the wall (see figure A18-1).

3.2.19. Test No. 19

First visible cracks in the units appeared at the failure of the wall (see figure A19-1).

3.2.20. Test No. 20

First visible cracks in the units appeared at the failure of the wall (see figure A20-1).

3.2.21. Test No. 21

First visible cracks in the units appeared at the failure of the wall (see figure A21-1).

3.2.22. Test No. 22

The first visible cracks in the units appeared at a horizontal force of about -48 kN (see figure A22-1). The end of the test is determined by cracks along the bed and the head joints (see figure A22-2).

3.2.23. Test No. 23

Already at a horizontal force of about ±60 kN a first cracking is audible. The first visible cracks appeared at a horizontal force of about -100 kN in the first layer of the wall.

3.2.24. Test No. 24

The first visible cracks appeared at a horizontal force of about +115 kN and -120 kN in the corners of the diagonals of the wall. At a horizontal force of about -125 kN further cracks appeared in the middle of the wall. With the decreasing of the maximum horizontal load new cracks over the diagonal of the wall appeared abruptly at -80 kN.

3.2.25. Test No. 25

The first visible cracks appeared at a horizontal force of about -36 kN on the face side of head side of the first layer. With the increasing of the horizontal deformation diagonal cracks appeared at the loaded face side. The overlaying face side of the wall showed no cracks.

3.3. Compensation of parasitic / energy dissipation due to the test-setup

In general, the test-setup should show the most feasible stiffness in proportion to the test specimen to widely exclude effects from the configuration on the measurement results. Because the presently tested wall panels are relatively stiff, it is additionally necessary to measure the wall deformations to a rigid measuring frame, which is decoupled from the remaining test-setup.

It has also to be considered that each hinged connection within the test-setup cannot be formed without any friction. Thus, based on the test-setup energy is dissipated, which can be detected in the hysteresis curve of the test specimen.

So in this setup a minor part of the horizontal load is carried by friction in the hinges of the vertical cylinders through the testing frame but not through the specimen. This force is determined for each time step within the test by the measured deformation of the test frame and the defined spring stiffness, and it has to be substracted from the measured force.

A further result is that due to the inclination of the vertical cylinders a horizontal force occurs (second order theory). This effort is also measured by the load cell of the horizontal cylinder, and on the other hand by the deformation of the testing frame. Hence the balance of force is warranted and a further consideration of the effects based on the second order theory is not necessary.

Energy is also being dissipated by friction in the above mentioned moment-shear force-hinge, which connects the horizontal cylinder with the load distribution girder. At this a minor rate of the vertical loads is applied as a vertical shear force on the horizontal cylinder by friction within the PTFE-steel-sliding joint of the hinge. The shear force itself can be defined by measuring the vertical deformation of the horizontal cylinder and with the knowledge of the spring stiffness. From these data the hysteresis of the moment-shear force-joint can be derived, which enables to calculate the dissipated energy.

Thus an adjusted hysteresis curve of the masonry wall can be determined, in which all energy dissipation rates caused by the test-setup are eliminated. Figure 4 shows the hysteresis of specimen No. 14 as measured hysteresis and as adjusted hysteresis curve (with compensation of parasitic energy dissipation), respectively. Herewith it can be shown that the adjusted hysteresis curve is not shaped as “bellied” as the measured hysteresis, i. e. a minor part of energy is dissipated compared to the measured, unadjusted values. The load bearing capacity values as determined from both curves differ just marginally.

For defining the adjusted hysteresis curve, both the vertical deformations of the horizontal cylinder and the horizontal deformation of the testing frame must be measured. However, this had been done for test specimen No. 14 only. In the following the other test results are displayed as measured hysteresis for this reason. At this it should be noted that the damping of the masonry wall and the energy dissipation, respectively, are over-estimated by the measured raw-data.

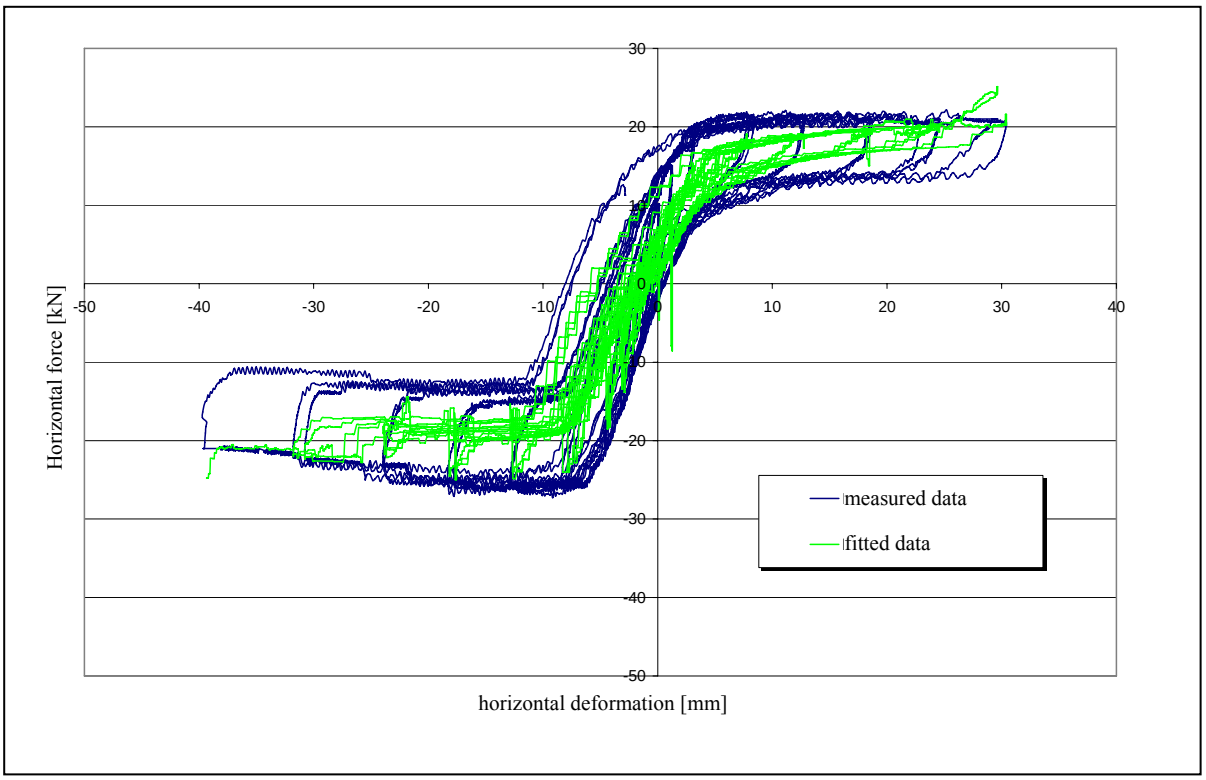

figure 4: Comparison between the adjusted and the measured hysteresis

The peaks of revised curve result from numerical problems. Smoothing functions can calendar this peaks, but this leads to a deformation of the hysteresis curve.

4. Test results

4.1. Comparison of the maximum horizontal force

Table 6 up to table 9 show the results of the 25 wall tests. Herein the horizontal force of the first visible crack on the wall and the maximum force are displayed. Furthermore the maximum deformations [d_{u1} and d_{u2}] to both sides on top of the wall are given.

The hysteresis curves and the crack patterns of all walls are given in annex A.

table 6: overview of the test results on clay bricks

No.	specimen	first crack H_C [kN]	maximum force H_F [kN]	H_C / H_F [-]	H_F / V [-]	d_{u1} [mm]	d_{u2} [mm]
1	Hlz-nm-220-380-1	90	160	0.56	0.42	3.1	2.7
2	Hlz-dm-220-380-1	100	140	0.57	0.37	3.3	4.5
3	Hlz-nm-220-380-2	102	118	0.86	0.31	7.0	5.6
4	Hlz-dm-220-380-2	130	147	0.88	0.39	7.0	5.7
5	Hlz-opti-dm-220-380-1	90	120	0.75	0.32	6.7	6.5
6	Hlz-opti-nm-220-380-1	149	149	1.00	0.39	6.9	7.8
7	Hlz-opti-dm-110-190-1	50	60	0.83	0.32	12.1	11.1
8	Hlz-opti-nm-110-190-1	55	56	0.98	0.29	15.9	10.8
9	Hlz-opti-dm-220-95-1	63	72	0.88	0.76	13.6	9.9
10	Hlz-opti2-dm-220-380-1	127	150	0.85	0.39	7.9	4.9
11	Hlz-opti2-nm-220-380-1	140	162	0.86	0.43	9.3	6.9
12	Hlz-opti2-dm-110-190-1	70	70	1.00	0.37	5.8	7.8
13	Hlz-opti2-dm-110-95-1	41	43	0.95	0.45	15.4	15.6
14	Hlz-opti2-dm-110-48-1	25	25	1.00	0.53	> 25	> 30
15	Hlz-opti2-dm-220-95-1	70	75	0.93	0.74	13.5	11.5

table 6: overview of the test results on calcium silicate bricks

No.	specimen	first crack H_C [kN]	maximum force H_F [kN]	H_C / H_F [-]	H_F / V [-]	d_{u1} [mm]	d_{u2} [mm]
16	KS-125-220-1	86	91	0.95	0.41	15.9	15.8
17	KS-opti-125-220-1	81	86	0.94	0.39	10.8	12

table 7: overview of the test results on LAC bricks

No.	specimen	first crack H_C [kN]	maximum force H_F [kN]	H_C / H_F [-]	H_F / V [-]	d_{u1} [mm]	d_{u2} [mm]
18	LAC-nm-150-220-1	90	90	1.00	0.41	16.7	17.2
19	LAC-dm-150-220-1	98	98	1.00	0.45	16.7	18.0
20	LAC-nm-150-110-1	55	55	1.00	0.50	19.0	19.8
21	LAC-dm-150-110-1	51	51	1.00	0.46	17.0	20.8
22	LAC-0M-dm-150-220-1	48	49	0.98	0.22	23.0	18.4

table 8: overview of the test results on T10 bricks

No.	specimen	first crack H_C [kN]	maximum force H_F [kN]	H_C / H_F [-]	H_F / V [-]	d_{u1} [mm]	d_{u2} [mm]
23	T10-exz-200-280-1	100	107	0.93	0.38	8.8	8.8
24	T10-zen-200-280-1	115	125	0.92	0.45	11.1	13.1
25	T10-exz-100-140-1	36	47	0.77	0.34	19.6	20.7

To compare the load bearing capacity of all walls tested with a restraint due to the floor slabs and a width of 175 mm, the values l' and τ' may be adopted.

$$l' = \alpha \cdot l_w / h_w \tag{1}$$

$$\alpha = \frac{\sigma_v}{f_k} \tag{2}$$

$$\tau' = \frac{H_F}{f_k \cdot A_w} \tag{3}$$

with: σ_v = normal stress due to vertical loading of the wall
f_k = compressive strength of masonry
l_w = length of the wall
h_w = height of the wall
H_F = maximum horizontal force
A_w = base area of the wall

In figure 4 τ' is displayed against l'. Here it can be seen, that the load bearing capacity of the wall is increasing with l'. So a higher vertical loading and a larger wall length lead to a higher load bearing capacity of the wall.
For the used kind of bricks with an unit strength of 12 N/mm^2 and 20 N/mm^2 and different kinds of mortar it can be shown, that by the value α a standardisation of the test results can be done. For the walls made of T10-Bricks only the loaded surface is taken into account for the calculation l' and τ'.

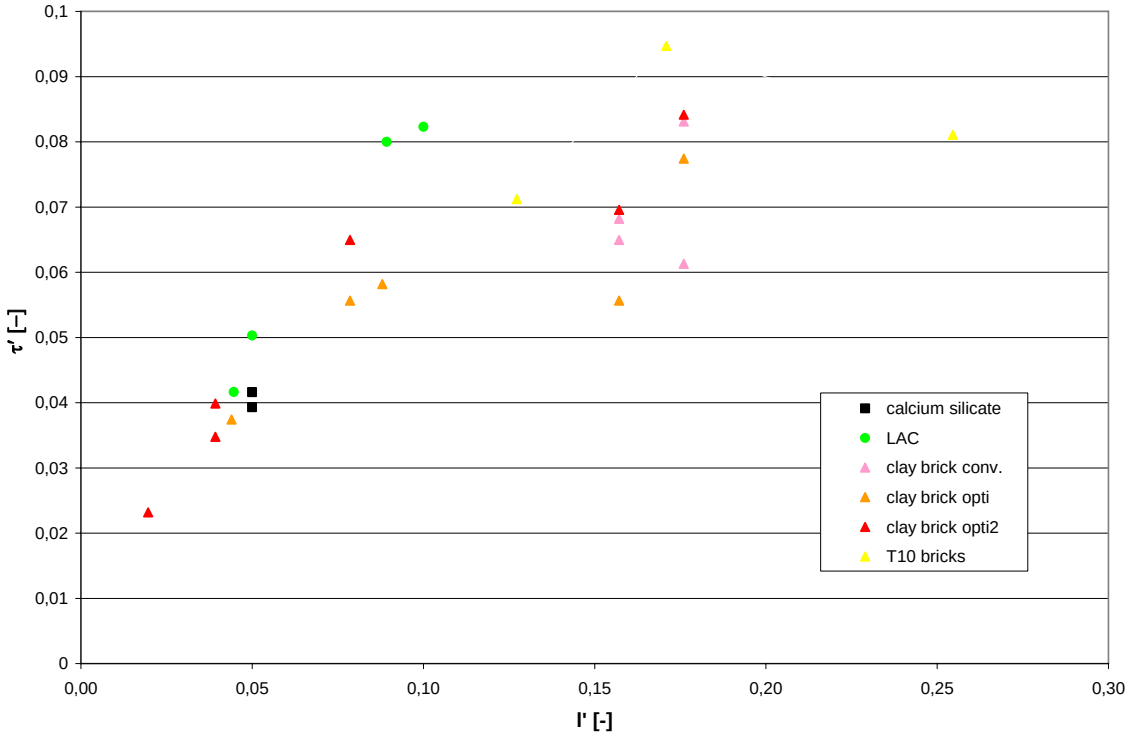

figure 5: comparison of the load bearing capacity

4.2. Comparison of the different kinds of mortar

The clay bricks and the LAC units were used in two different unit heights so that on the one hand thin layer mortar and on the other hand general purpose mortar M5 could be used. To compare the influence of the two different kinds of mortar on the shear bearing capacity of masonry walls, the hysteresis curves of walls with the identical boundary conditions but different kinds of mortar, are displayed in figure 6 and figure 7.

Figure 5 indicates that the wall with general purpose mortar and clay bricks opti2 has a higher shear bearing capacity as the wall with thin layer mortar and clay bricks opti2. In contrast, the wall with general purpose mortar and conventional clay bricks has a lower shear bearing capacity as the wall with thin layer mortar and conventional clay bricks.

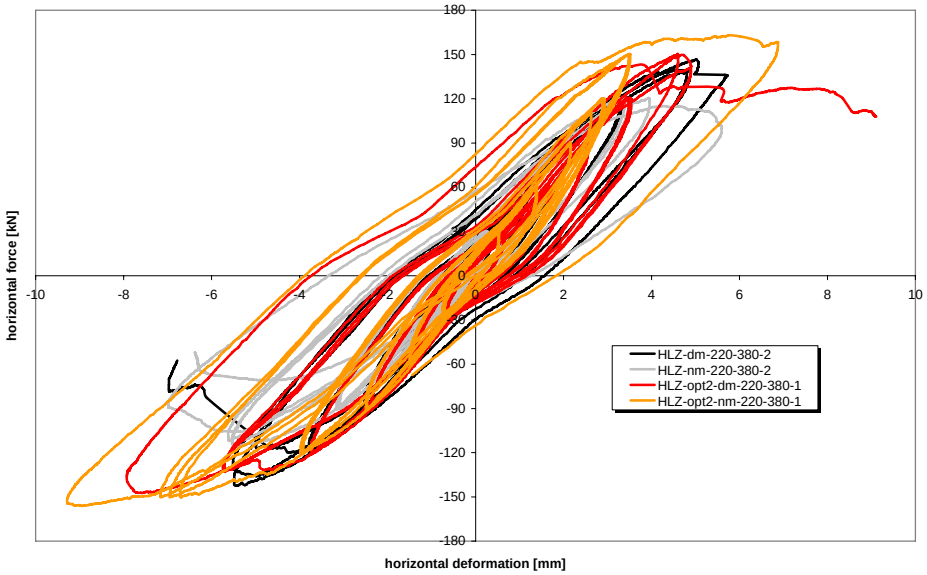

figure 6: comparison of different kinds of mortar with clay bricks

In figure 7 the comparison of two LAC walls with two different kinds of mortar is displayed. It can be shown, that the difference between both hysteresis curves is quite small.

The scattering of the wall tests, depending on the units used, can be estimated from 10% up to 20%. Hence a significant influence of the two different kinds of mortars could not be observed.

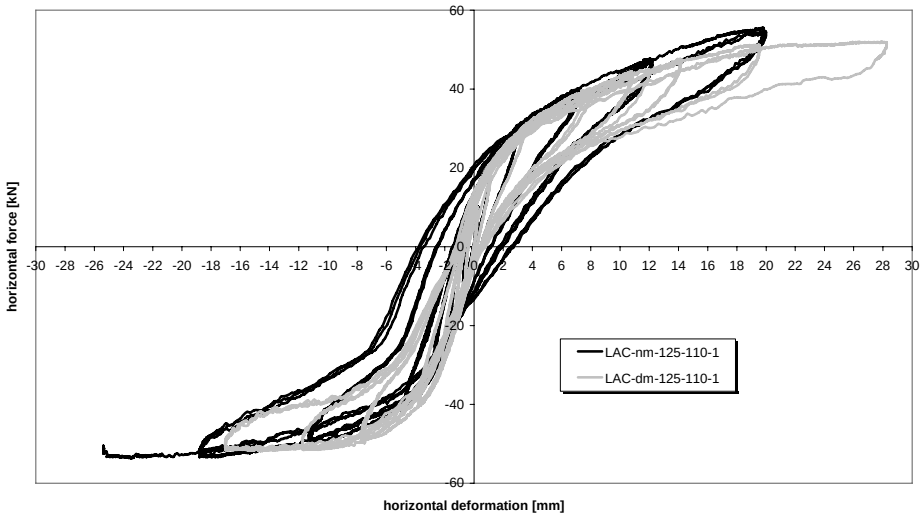

figure 7: comparison of different kinds of mortar with LAC units

4.3. Comparison of the different levels of vertical loading

While the walls of LAC units were tested at two different levels of stress, the clay bricks were tested at three different levels of stress of the vertical loading. Each wall type was tested at a vertical stress of 0.25 N/mm^2, 0.5 N/mm^2 or 1.0 N/mm^2 (see table 1 up to table 3). Figure 8 displays the comparison of two 2.20 m long walls of clay bricks opti2 at a vertical loading of 0.25 N/mm^2 and 1.0 N/mm^2. As can be seen from the figure the wall with a fourth of the vertical loading of the other wall has about half of the maximum horizontal force capacity, but a much higher deformation capacity.

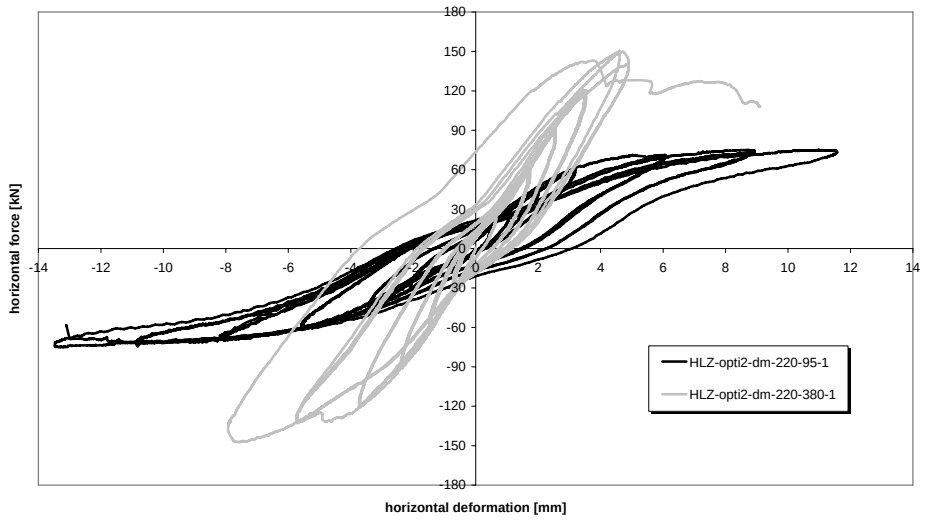

figure 8: comparison of different kinds of vertical loading (wall length 2,20 m)

Figure 9 displays three walls with a length of 1.10 m made of clay bricks opti2. The three levels of vertical loading show three different hysteresis curves. With a decreasing vertical loading the maximum horizontal force is decreasing too, whilst the deformation capacity of the wall is getting larger.

For LAC units a similar behaviour for the two different levels of vertical loading (0.5 N/mm^2 and 1.0 N/mm^2) is indicated in figure 10.

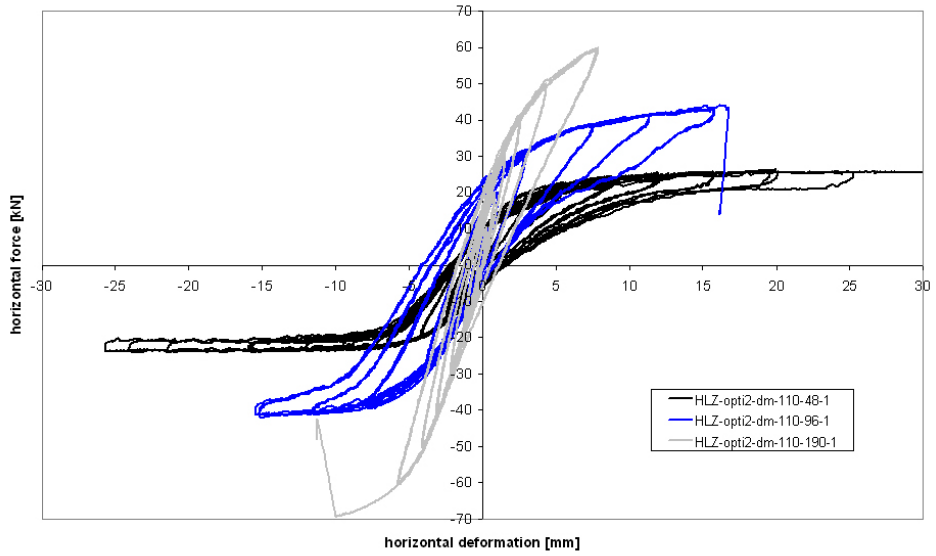

figure 9: comparison of different kinds of vertical loading (wall length 1,10 m)

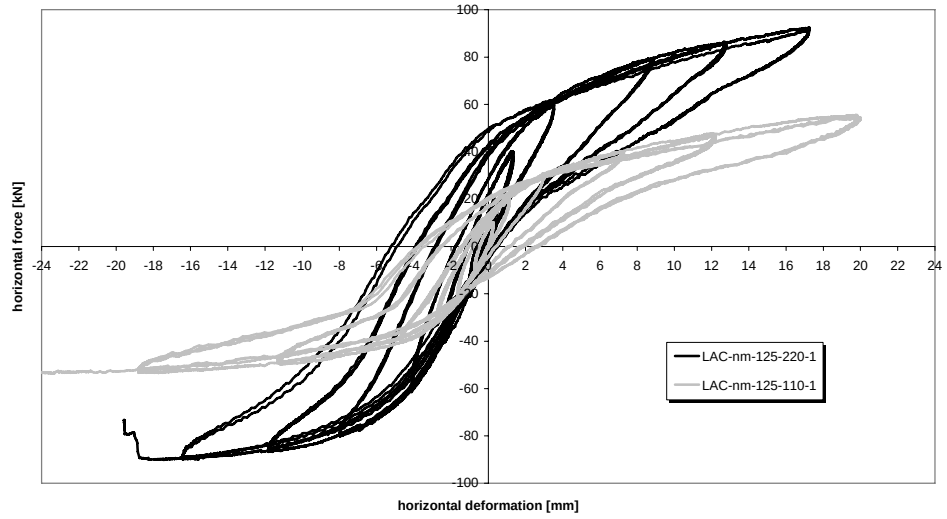

figure 10: comparison of different kinds of vertical loading (wall length 1,25 m)

4.4. Comparison of the different kinds of restraint

One test with no clamping due to the floor slabs in comparison to the other tests has been performed. In figure 11 the results of this wall are compared to a wall with the same boundary conditions but a point of zero moment at mid height of the wall. For a short wall with a length of 1.25 m it can be shown, that the restraint of the upper beam leads to a significantly higher shear capacity of the wall. Due to the fact that bending failure is decisive for this kind of walls, a linear dependency of the height of the point of zero moment on the maximum horizontal force is consequential.

For walls with another kind of failure, e. g. tension failure of the bricks or sliding failure in shear, the influence of the point of zero moment on the shear bearing capacity of masonry walls is definitely minor than in this case.

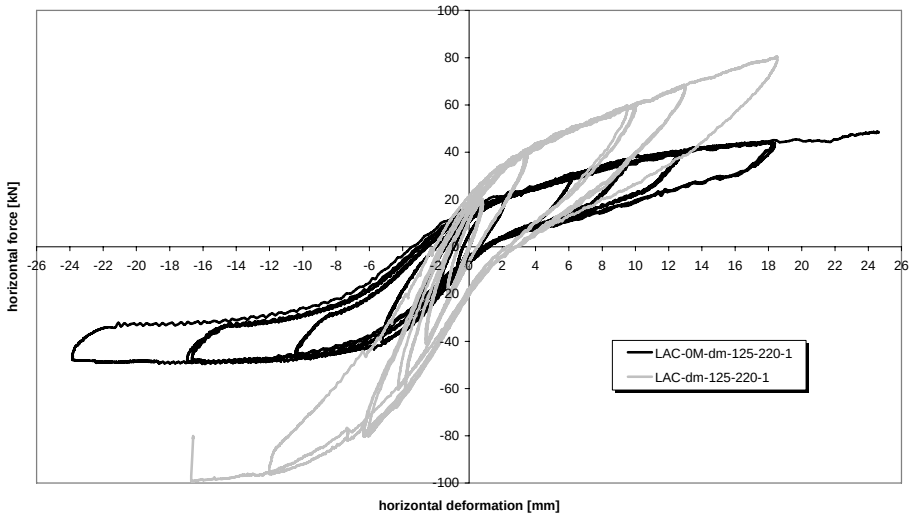

figure 11: comparison of different kinds of restraint

4.5. Validation of the optimising of units

The two optimising steps of clay bricks (see WP 2) are displayed in figure 12 for a wall with a length of 2.20 m and a vertical loading of 1.0 N/mm^2. In this case it can be shown, that the first optimising step (green hysteresis curve) led to a lower shear bearing capacity of the wall. Therefore the second optimising step was needed and results in the red hysteresis curve. The results of the wall with clay bricks opti2 show at least in the third quadrant the highest horizontal force.

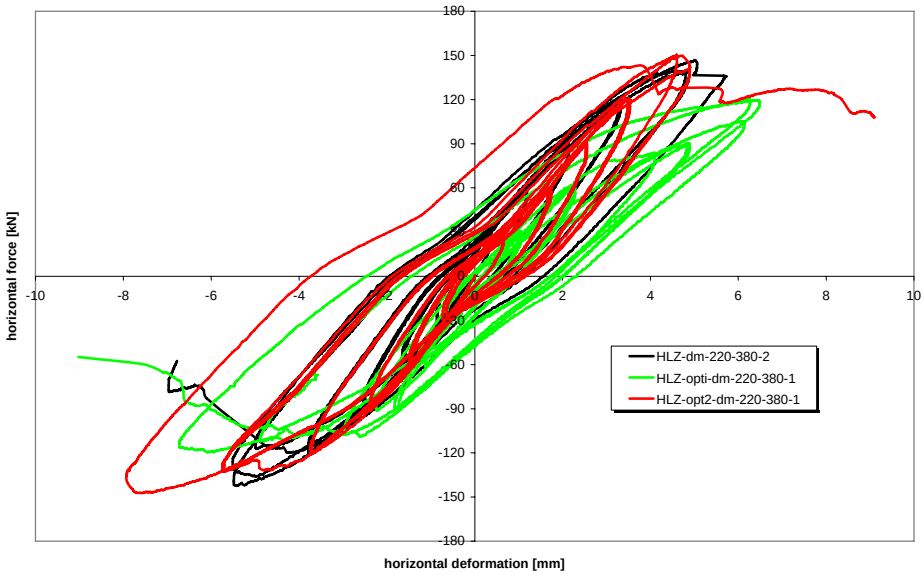

figure 12: comparison of different kind of vertically perforated bricks

The hysteresis curves of the two walls of calcium silicate units are pictured in figure 13. The comparison of the optimised and the conventional units show almost no difference.

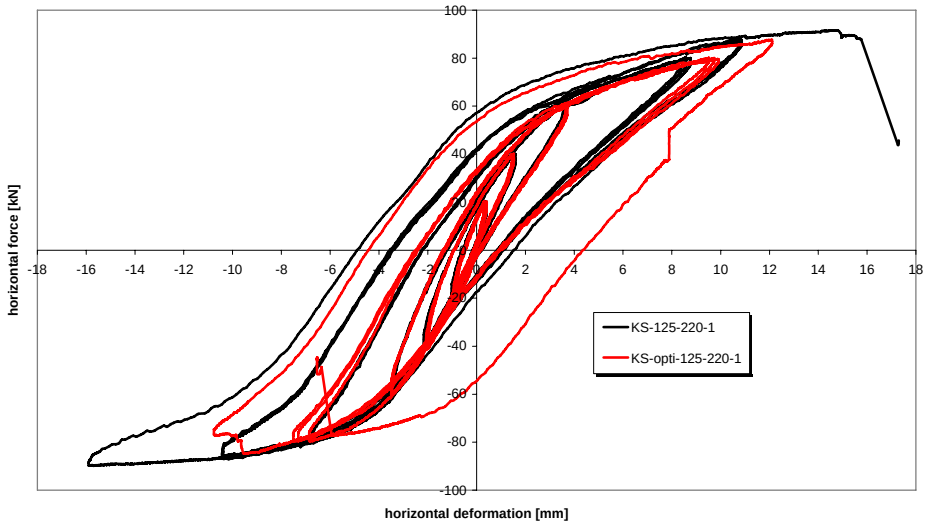

figure 13: comparison of different kind of calcium silicate units

4.6. Comparison of the deformation

For the comparison of the deformation behaviour of the walls, an enveloping curve of the hysteresis curves had to be made. The enveloping curves of all walls are displayed in annex A. Furthermore the curves were reduced to an idealised bilinear curve as shown in figure 15.

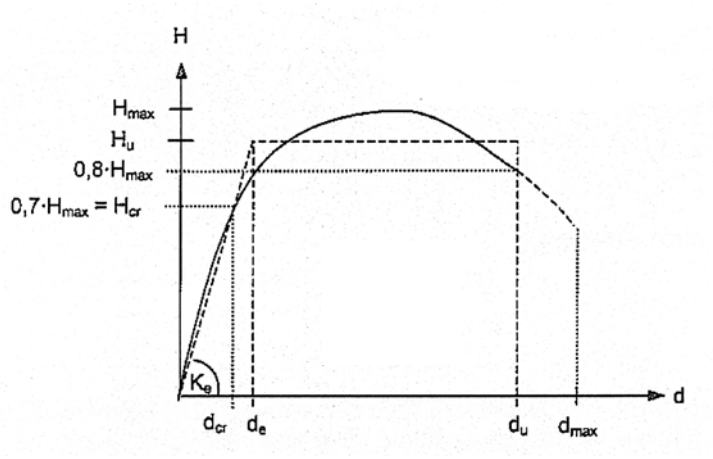

figure 14: idealised bilinear curve for the experimental envelope [7]

To get this bilinear curve the knowledge of the initial stiffness K_e of the wall is necessary.

$$K_e = \frac{H_{cr}}{d_{cr}} \tag{4}$$

The edge of the elastic deformation d_e can be calculated by the plateau of resistance H_u and the initial stiffness K_e. The plateau of resistance is determined by the principle of the equivalent energy.

$$d_e = \frac{H_u}{K_e} \tag{5}$$

The ductility μ of the walls can be calculated by the knowledge of deformations d_u and d_e (see figure 13).

$$\mu = \frac{d_u}{d_e} \tag{6}$$

Figure 15 exemplifies the approach for the calculation of the ductility for test No. 14.

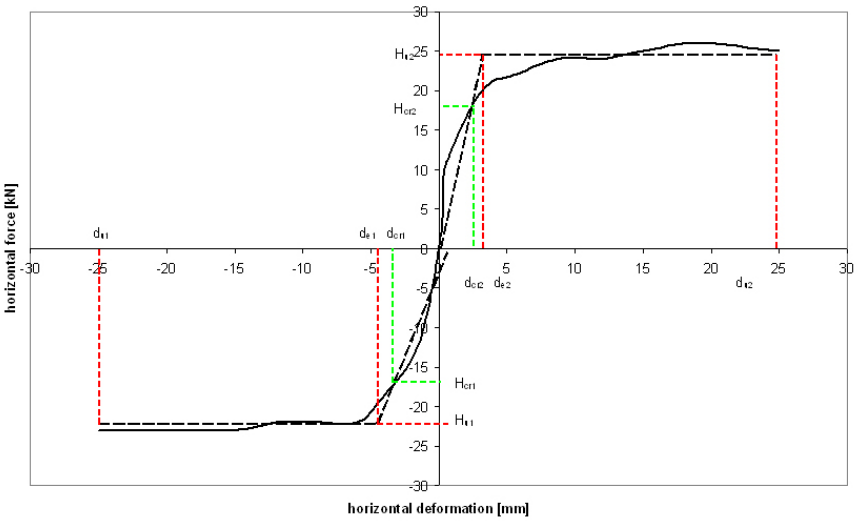

figure 15: example idealised bilinear curve

In table 9 up to table 12 an overview of the deformation behaviour of all tested walls is given. In case of test No. 2 the load history was different to the load history of the other tests and so the hysteresis is not significant for the validation of the deformation behaviour of this wall. All values in these tables are given with the indices 1 and 2. The values with index 1 correspond to the part of curve in the third quadrant, the index 2 corresponds to the first quadrant.

table 9: overview of the deformation behaviour of clay bricks

No.	specimen	d_{u1} [mm]	d_{u2} [mm]	d_{cr1} [mm]	d_{cr2} [mm]	H_{cr1} [kN]	H_{cr2} [kN]	K_{e1} [N/m]	K_{e2} [N/m]	H_{u1}	H_{u2}	d_{e1} [mm]	d_{e2} [mm]	μ_1 [-]	μ_2 [-]
1	Hlz-nm-220-380-1	3.1	2.7	1.45	1.5	112	105	77	70	148	130	1.9	1.9	1.6	1.5
2	Hlz-dm-220-380-1	3.3	4.5												
3	Hlz-nm-220-380-2	7.0	5.6	2.9	1.9	80	83	28	44	105	110	3.8	2.5	1.8	2.2
4	Hlz-dm-220-380-2	7.0	5.7	2.9	2.6	99	102	34	39	120	130	3.5	3.3	2.0	1.7
5	Hlz-opti-dm-220-380-1	6.7	6.5	1.8	4.1	83	83	46	20	104	102	2.3	5.0	3.0	1.3
6	Hlz-opti-nm-220-380-1	6.9	7.8	2.1	3.6	103	84	49	23	130	100	2.7	4.3	2.6	1.8
7	Hlz-opti-dm-110-190-1	12.1	11.1	6.8	3.5	41	39	6	11	51	49	8.5	4.4	1.4	2.5
8	Hlz-opti-nm-110-190-1	15.9	10.8	3.6	2.9	39	35	11	12	45	47	4.2	3.9	3.8	2.8
9	Hlz-opti-dm-220-95-1	13.6	9.9	3.2	2	46	50	14	25	55	63	3.8	2.5	3.6	3.9
10	Hlz-opti2-dm-220-380-1	7.9	4.9	2.9	3	102	105	35	35	130	129	3.7	3.7	2.1	1.3
11	Hlz-opti2-nm-220-380-1	9.3	6.9	3.2	2.8	109	114	34	41	140	148	4.1	3.6	2.3	1.9
12	Hlz-opti2-dm-110-190-1	5.8	7.8	3.6	2.8	48	41	13	15	63	51	4.7	3.5	1.2	2.2
13	Hlz-opti2-dm-110-95-1	15.4	15.6	4	3	29	31	7	10	38	39	5.2	3.8	2.9	4.1
14	Hlz-opti2-dm-110-48-1	> 25	> 30	2.5	3	17	18	7	6	23	24	3.4	4.0	7.4	7.5
15	Hlz-opti2-dm-220-95-1	13.5	11.5	4.2	2.3	53	53	13	23	68	70	5.4	3.0	2.5	3.8

table 10: overview of the deformation behaviour of calcium silicate units

No.	specimen	d_{u1} [mm]	d_{u2} [mm]	d_{cr1} [mm]	d_{cr2} [mm]	H_{cr1} [kN]	H_{cr2} [kN]	K_{e1} [N/m]	K_{e2} [N/m]	H_{u1}	H_{u2}	d_{e1} [mm]	d_{e2} [mm]	μ_1 [-]	μ_2 [-]
16	KS-125-220-1	15.9	15.8	4	4.2	62	62	16	15	85	83	5.5	5.6	2.9	2.8
17	KS-opti-125-220-1	10.8	12	3.8	4	60	61	16	15	78	75	4.9	4.9	2.2	2.4

table11: overview of the deformation behaviour of LAC units

No.	specimen	d_{u1} [mm]	d_{u2} [mm]	d_{cr1} [mm]	d_{cr2} [mm]	H_{cr1} [kN]	H_{cr2} [kN]	K_{e1} [N/m]	K_{e2} [N/m]	H_{u1}	H_{u2}	d_{e1} [mm]	d_{e2} [mm]	μ_1 [-]	μ_2 [-]
18	LAC-nm-150-220-	16.7	17.2	5	4.2	62	63	12.4	15	82	81	6.6	5.4	2.5	3.2
19	LAC-dm-150-220-1	16.7	18	4.8	7.8	67	56	13.96	7.2	92	69	6.6	9.6	2.5	1.9
20	LAC-nm-150-110-1	19	19.8	4.1	6.8	37	39	9.0	5.7	50	48	5.5	8.4	3.4	2.4
21	LAC-dm-150-110-1	17	20.8	3.2	6.2	36	36	11.3	5.8	50	48	4.4	8.3	3.8	2.5
22	LAC-0M-dm-150-220-1	23	18.4	4	7.2	34	32	8.5	4.4	47	40	5.5	9	4.2	2.0

table12: overview of the deformation behaviour of the T10 bricks

No.	specimen	d_{u1} [mm]	d_{u2} [mm]	d_{cr1} [mm]	d_{cr2} [mm]	H_{cr1} [kN]	H_{cr2} [kN]	K_{e1} [N/m]	K_{e2} [N/m]	H_{u1}	H_{u2}	d_{e1} [mm]	d_{e2} [mm]	μ_1 [-]	μ_2 [-]
23	T10-exz-200-280-1	8.8	8.8	1,7	1,9	72	80	42,35	42,1	100	95	2,3	2,2	3,82	4
24	T10-zen-200-280-1	11.1	13.1	2,2	2,3	98	90	44,54	39,1	115	105	2,7	2,9	4,11	4,5
25	T10-exz-100-140-1	19.6	20.7	2,5	2,1	33	32	13,2	15,2	40	42	3,1	3,1	6,32	6,7

Figure 16 compares the ductility of all tested walls with clamping due to the floor slabs. The ductility calculated by equation (6) is shown against the value l' calculated by equation (1). The graph shows an enhancement of the ductility by decreasing l'. So the deformation capacity and the ductility of masonry walls increases at a shorter wall length and a lower vertical loading of the wall. Because there is only one test result with a very low value of l' of 0.05, this disproportionate enhancement of ductility has to be verified by further tests.

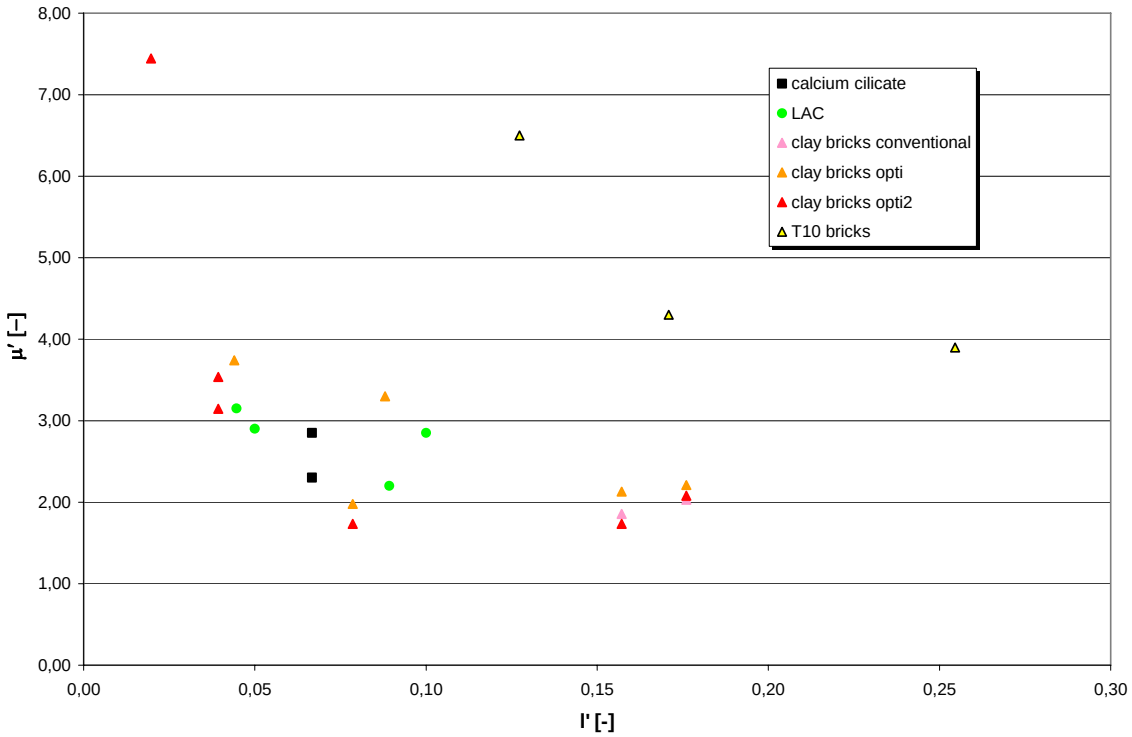

figure 16: comparison of the deformation capacity

5. Conclusions

The wall tests carried out at Kassel University show the whole range of masonry failure behaviour under shear loads. The crack patterns given in annex A show sliding failure between bricks and mortar, bending failure of the walls and tension failure of the bricks.

In chapter 3 the test programme and the test procedures are given. The audible and visible cracking and failure behaviour for each wall is specified.

In chapter 4 the walls with different boundary conditions are compared to each other. The comparison of the bearing capacity of the walls is given by the comparison of l'. It can be stated, that a higher vertical loading and a larger wall length lead to a higher load bearing capacity of the wall.

The comparison of the different kinds of mortar shows, that a significant influence of the two different kinds of mortar could not be observed. The scattering of the results of the wall tests, depending on the units used, can be estimated from 10% up to 20%, possible distinctions are in the range of the scattering of the masonry.

The comparison of the different kinds of loading confirms, that at decreasing vertical loading the maximum horizontal force is decreasing and the deformation capacity of the wall is growing.

The validation the optimised units (see work package 2) shows that neither an increase of the bearing capacity nor the ductility of the walls can be specified.

6. Bibliography

[1] Fehling, E.; Stürz, J.: Theoretical Investigation on Stress States of Masonry Structures Subjected to Static and Dynamic Shear Loads (Lateral Loads), Analysis of Terraced House; Technical report of the collective research project ESECMaSE, 2005

[2] Fehling, E.; Stürz, J. ; Schermer, D.: Theoretical Investigation on Shear Tests Methods, Construction of test setup for shear tests for validation of proposed method; Technical report of the collective research project ESECMaSE, 2006

[3] Fehling, E.; Stürz, J. ; Schermer, D.: Theoretical Investigation on Shear Tests Methods, Series of shear tests for validation; Technical report of the collective research project ESECMaSE, 2006

[4] Grabowski, S.: Tests on the relevant material properties on improved clay units; Technical report of the collective research project ESECMaSE, 2006

[5] Graubner, C.-A.; Kranzler, T.; Schubert, P.; Simon, E.: Festigkeitseigenschaften von Mauerwerk, Teil 3: Schubfestigkeit von Mauerwerksscheiben; Mauerwerk-Kalender 2005; Ernst & Sohn; 2005

[6] Jäger, W.; Schöps, P.: Kosteneinsparung durch Ansatz realitätsnaher Bemessungskonzepte für die Schubbeanspruchung von Mauerwerksbauten; Frauenhofer IRB Verlag; 2005

[7] Ötes, A.; Löring, S.: Tastversuche zur Identifizierung des Verhaltensfaktors von Mauerwerksbauten für den Erdbebennachweis; Abschlussbericht; Universität Dortmund; Lehrstuhl für Tragkonstruktionen; 2003

[8] Schermer, D.: Verhalten von unbewehrtem Mauerwerk unter Erdbebenbeanspruchung; Dissertation; TU München, Institut für Baustoffe und Konstruktionen, Lehrstuhl für Massivbau; 2004

[9] Schermer, D.: Theoretical Investigation on Stress States of Masonry Structures Subjected to Static and Dynamic Shear Loads (Lateral Loads), Analysis of Apartment House; Technical report of the collective research project ESECMaSE, 2005

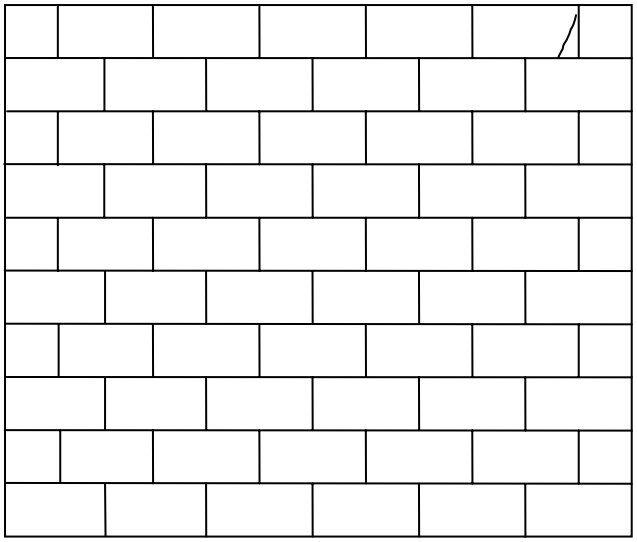

figure A1-1: first cracks at about 90 kN of test No. 1

figure A1-2: crack pattern of test No. 1

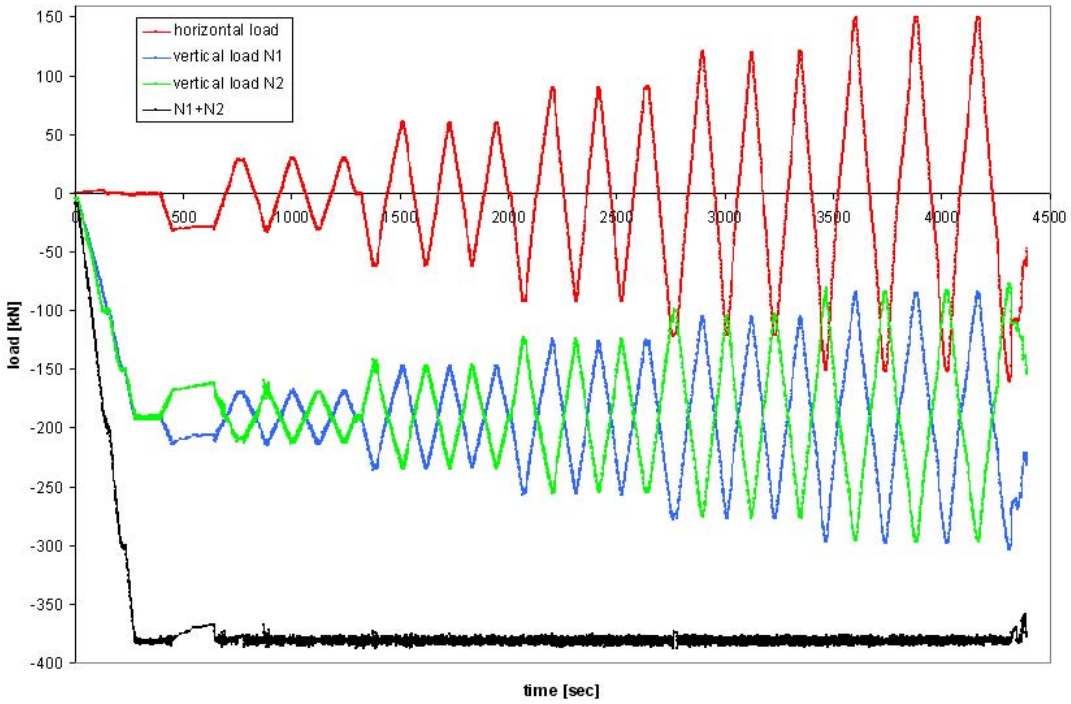

figure A1-3: load history of wall No. 1

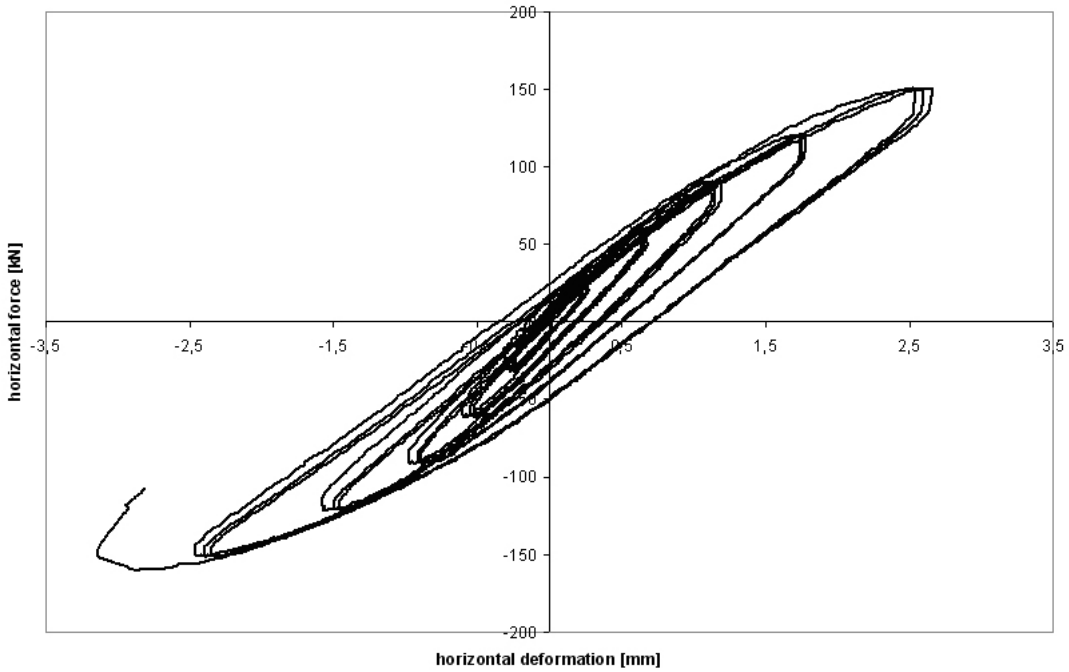

figure A1-4: hysteresis of wall No. 1

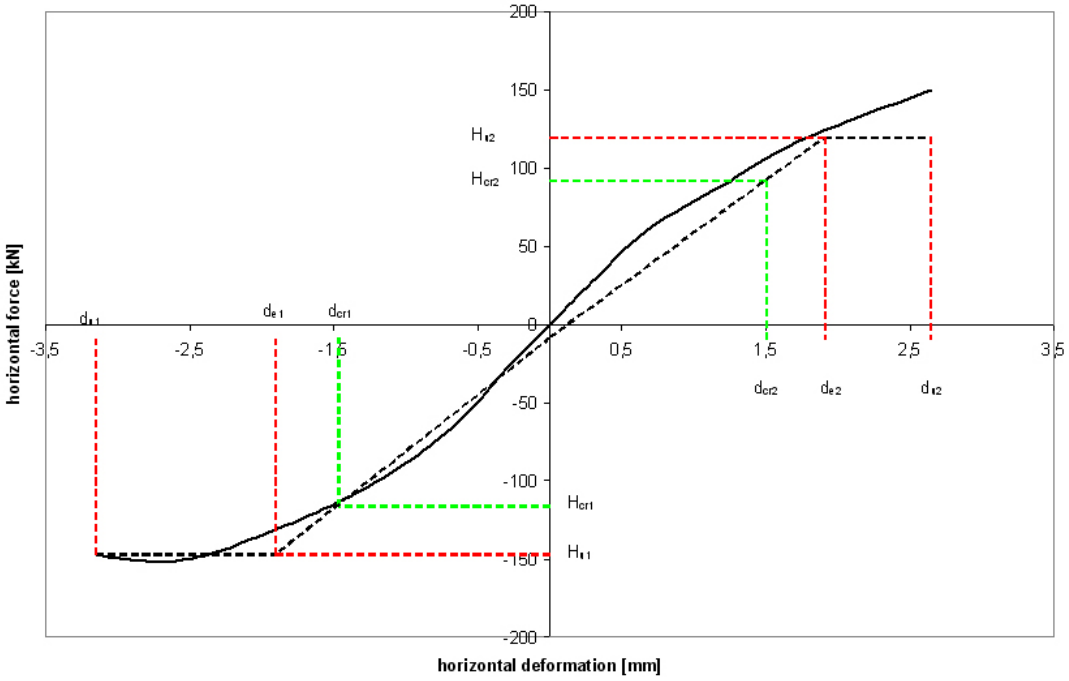

figure A1-5: enveloping curve of wall No. 1

figure A2-1: crack pattern of test No. 2

figure A2-2: detail of the crack pattern of test No. 2

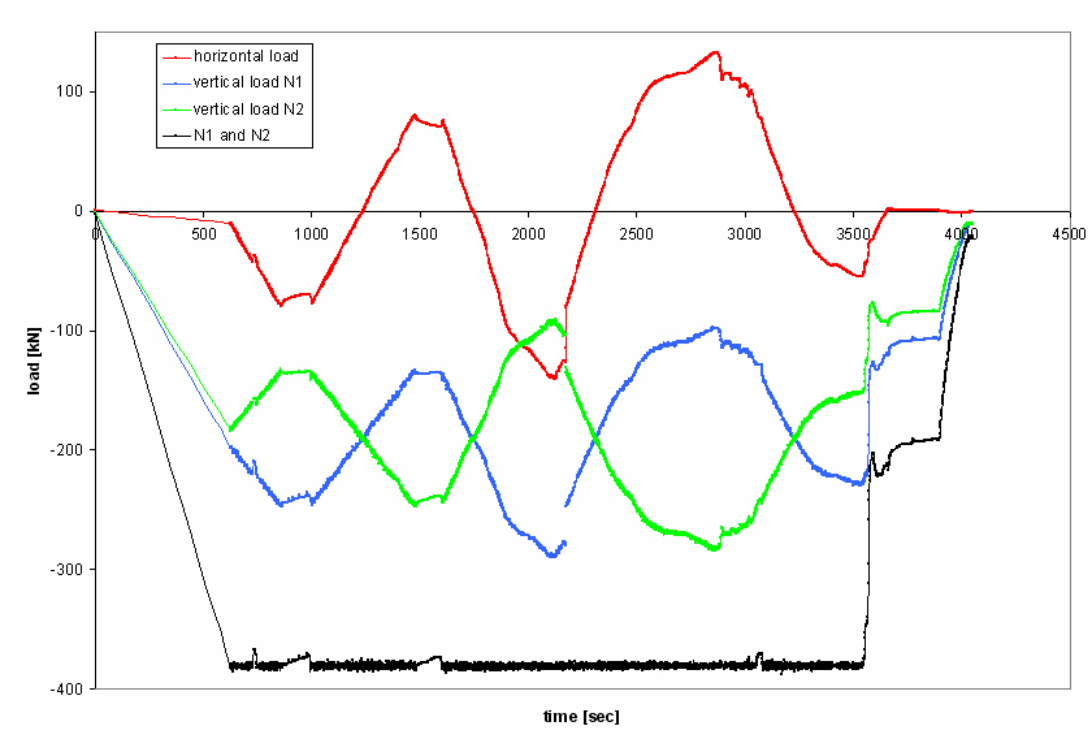

figure A2-3: load history of wall No. 2

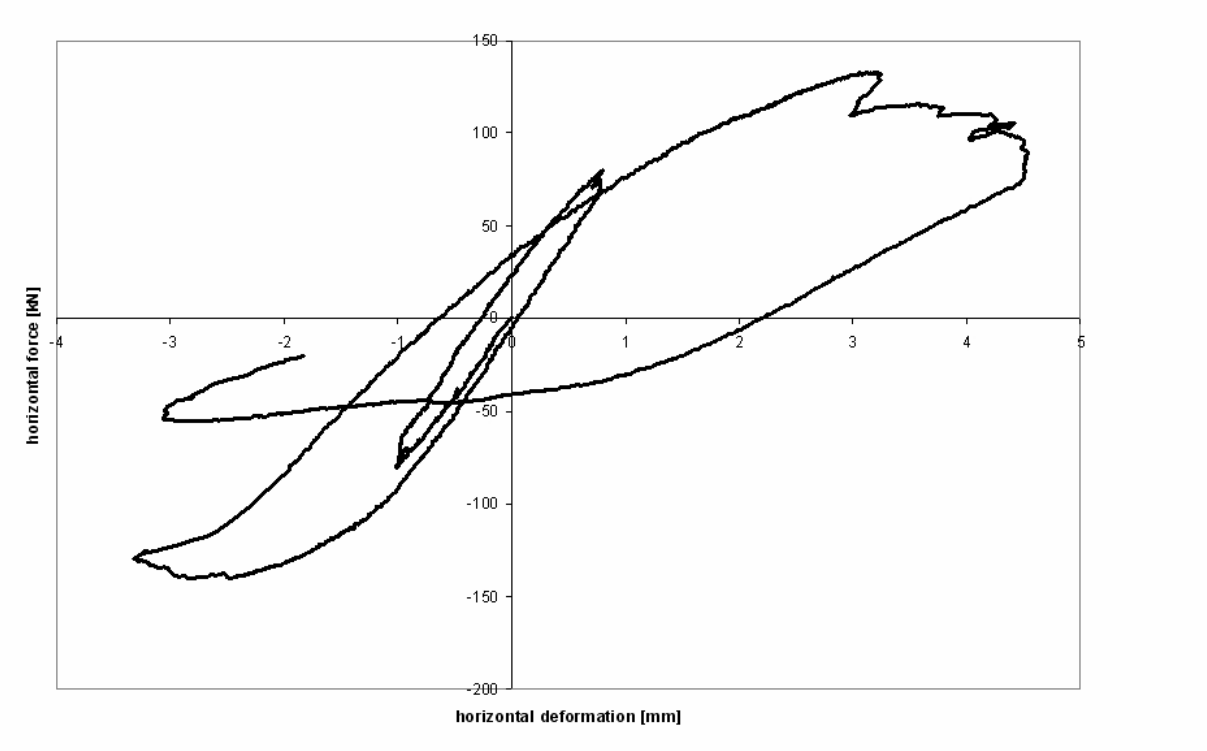

figure A2-4: hysteresis of wall No. 2

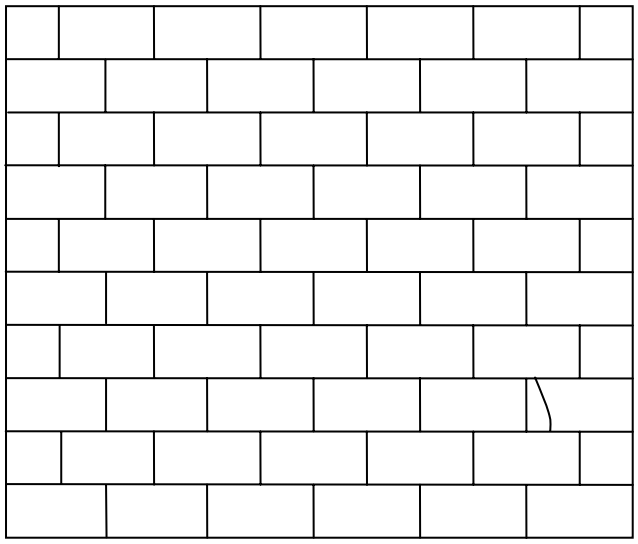

figure A3-1: first cracks at about -102 kN of test No. 3

figure A3-2: crack pattern of test No. 3

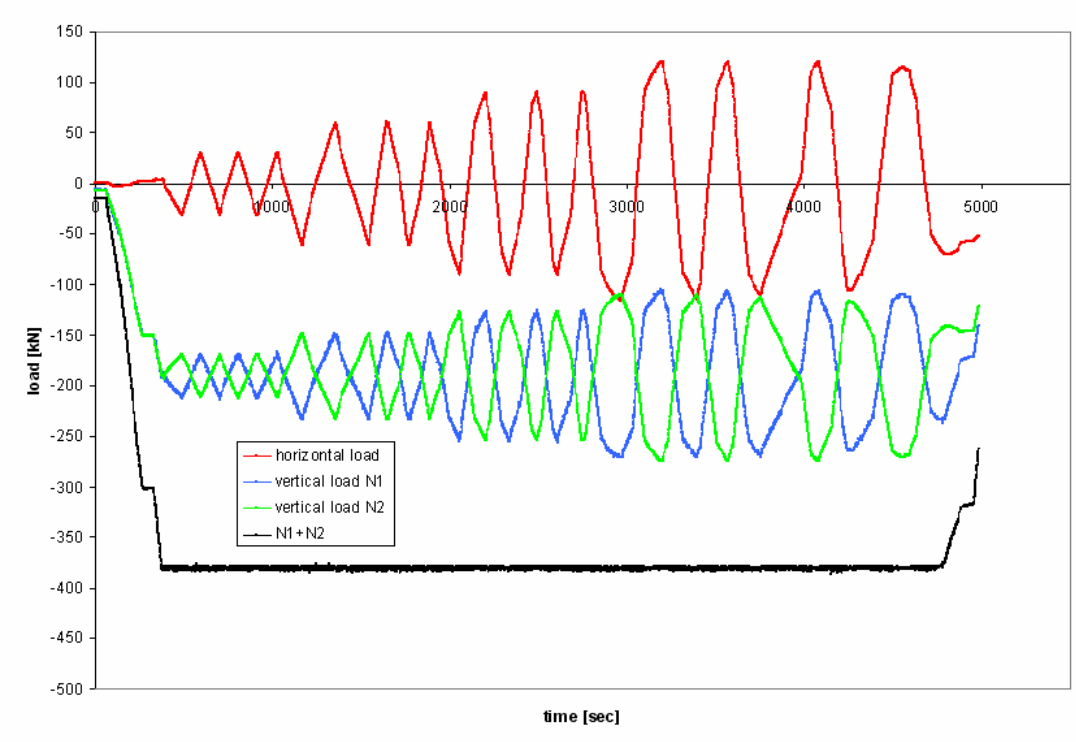

figure A3-3: load history of wall No. 3

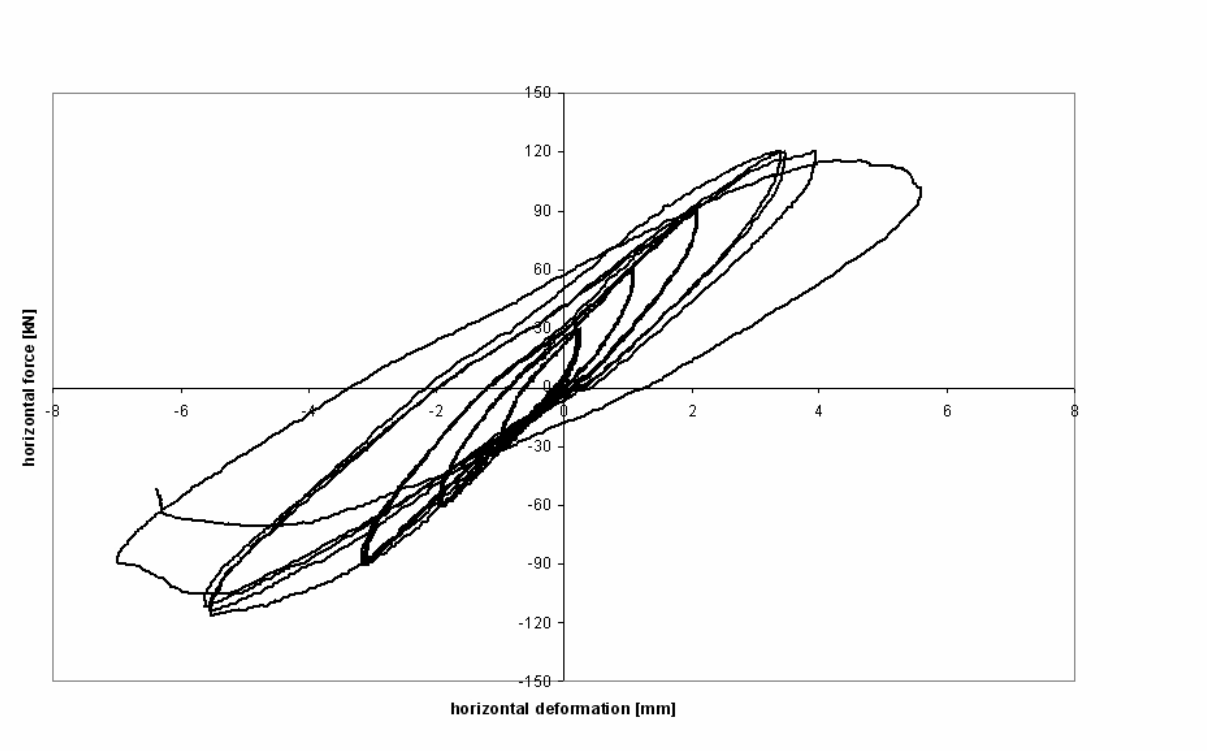

figure A3-4: hysteresis of wall No. 3

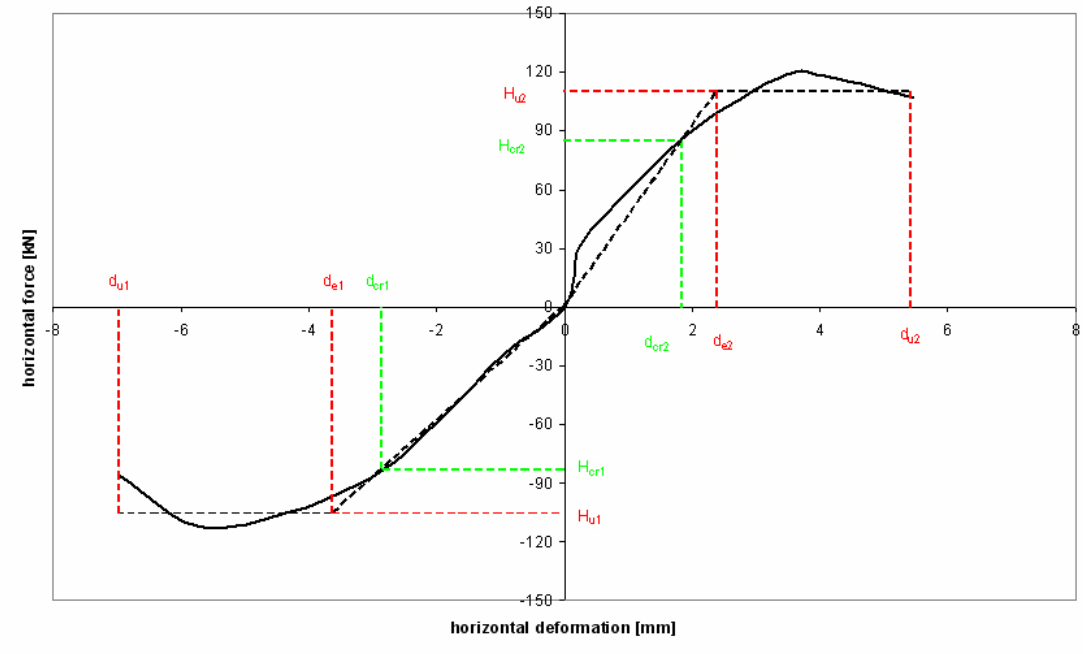

figure A3-5: enveloping curve of wall No. 3

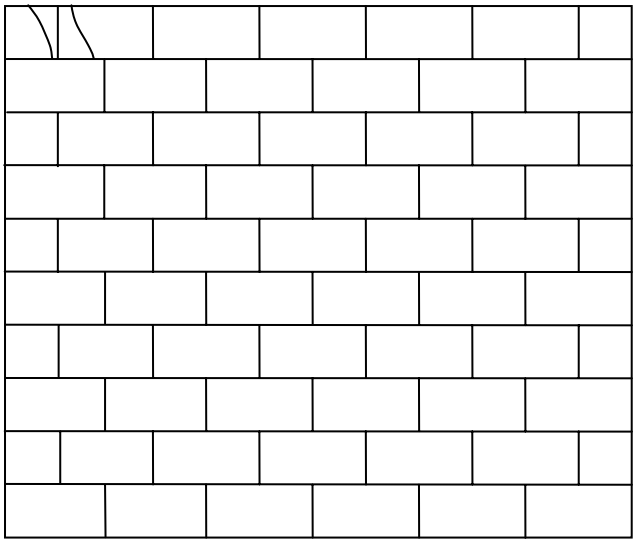

figure A4-1: first cracks at about -130 kN of test No. 4

figure A4-2: crack pattern of test No. 4

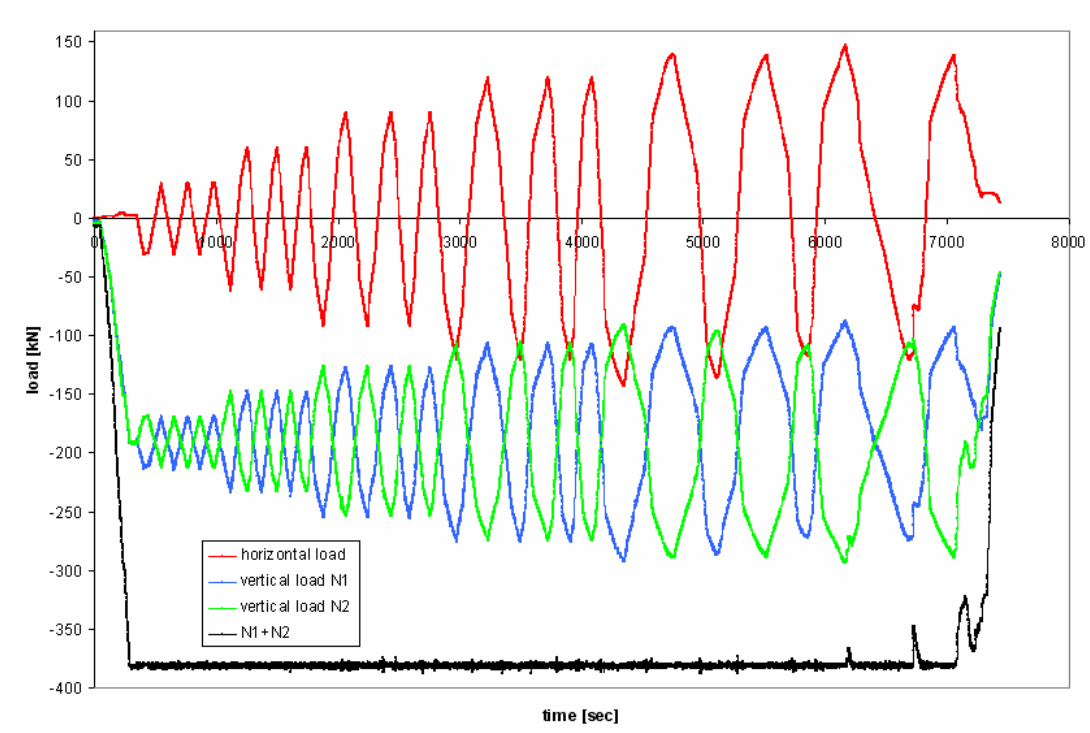

figure A4-3: load history of wall No. 4

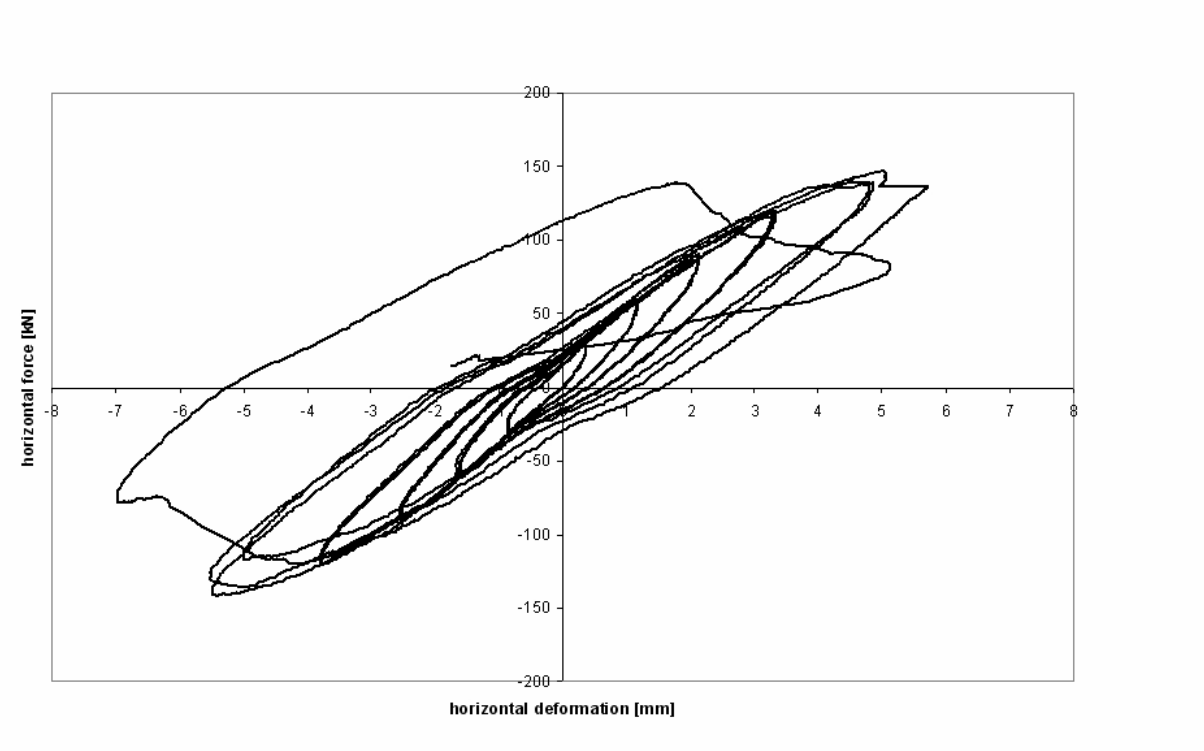

figure A4-4: hysteresis of wall No. 4

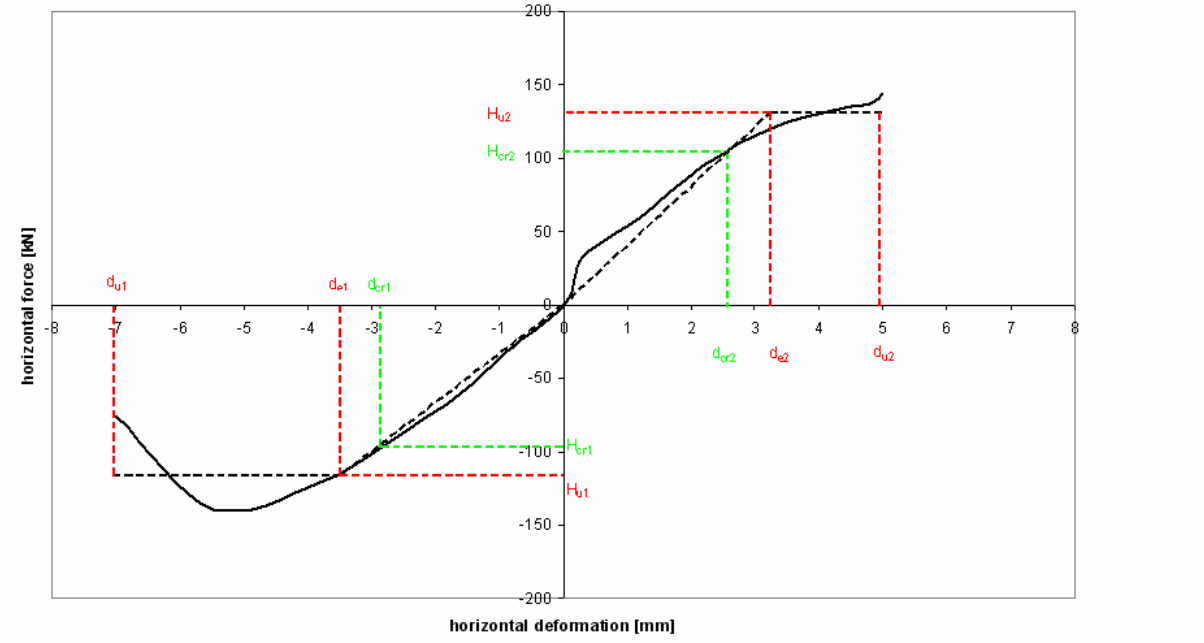

figure A4-5: enveloping curve of wall No. 4

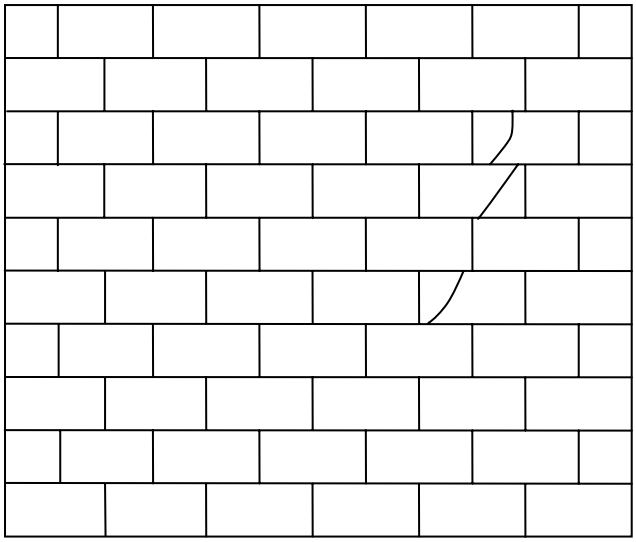

figure A5-1: first cracks at about 90 kN of test No. 5

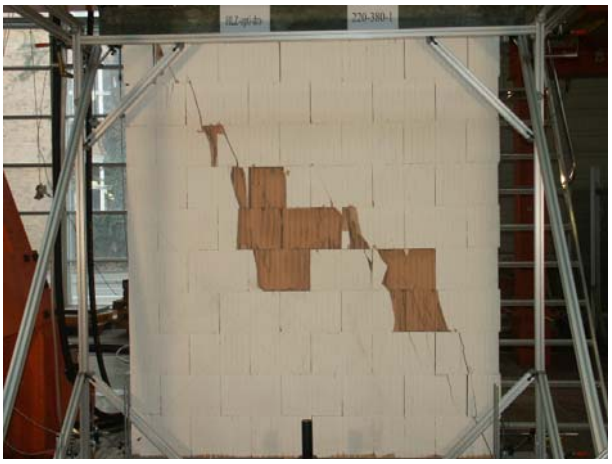

figure A5-2: crack pattern of test No. 5

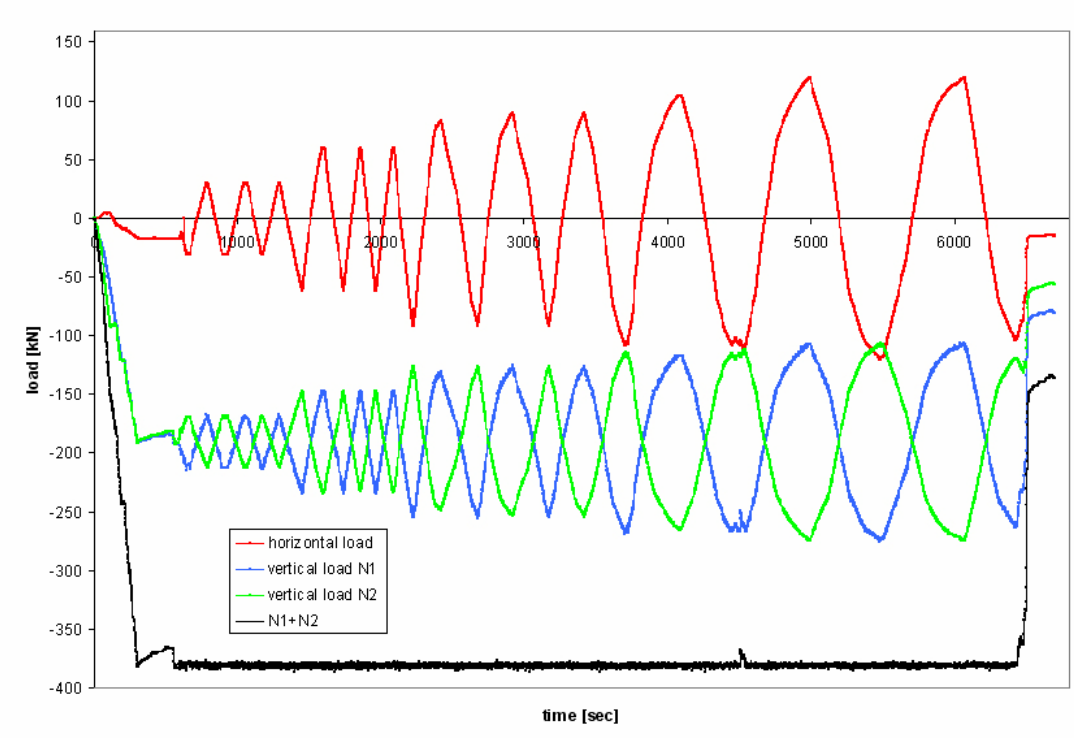

figure A5-3: load history of wall No. 5

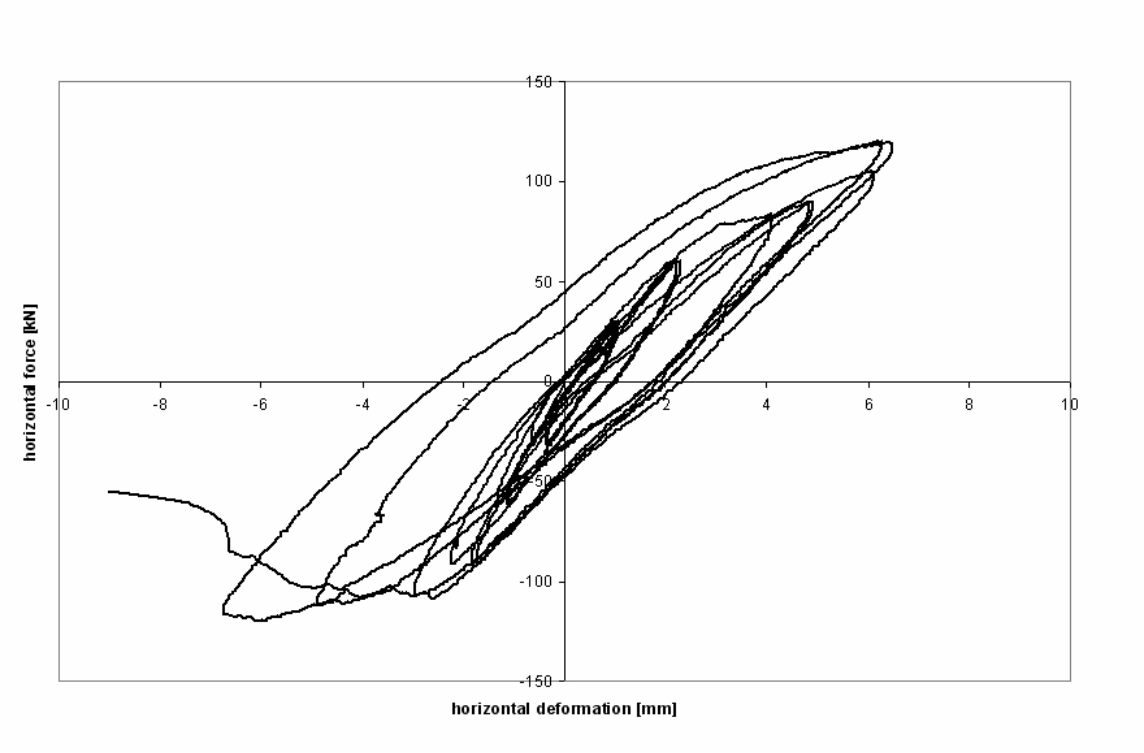

figure A5-4: hysteresis of wall No. 5

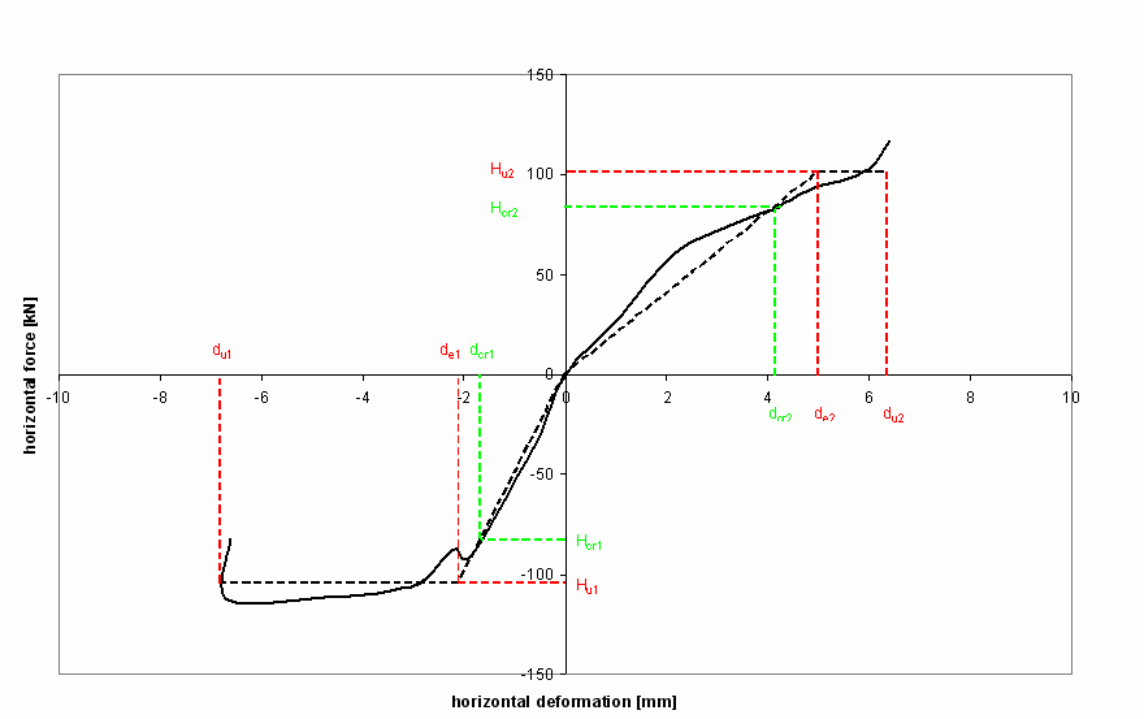

figure A5-5: enveloping curve of wall No. 5

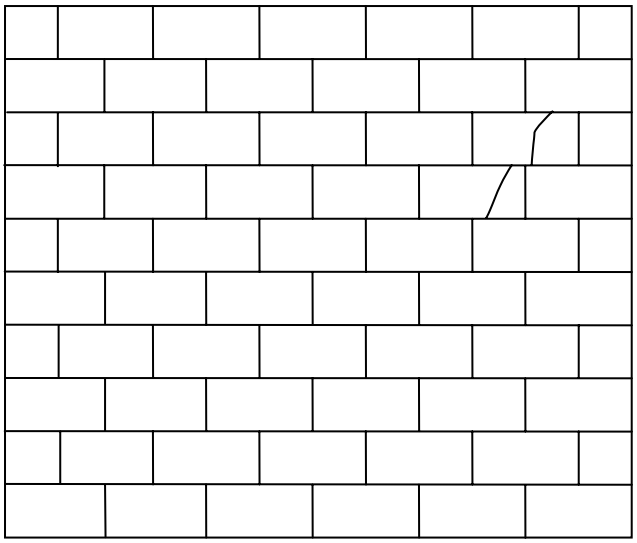

figure A6-1: first cracks at about -149 kN of test No. 6

figure A6-2: crack pattern of test No. 6

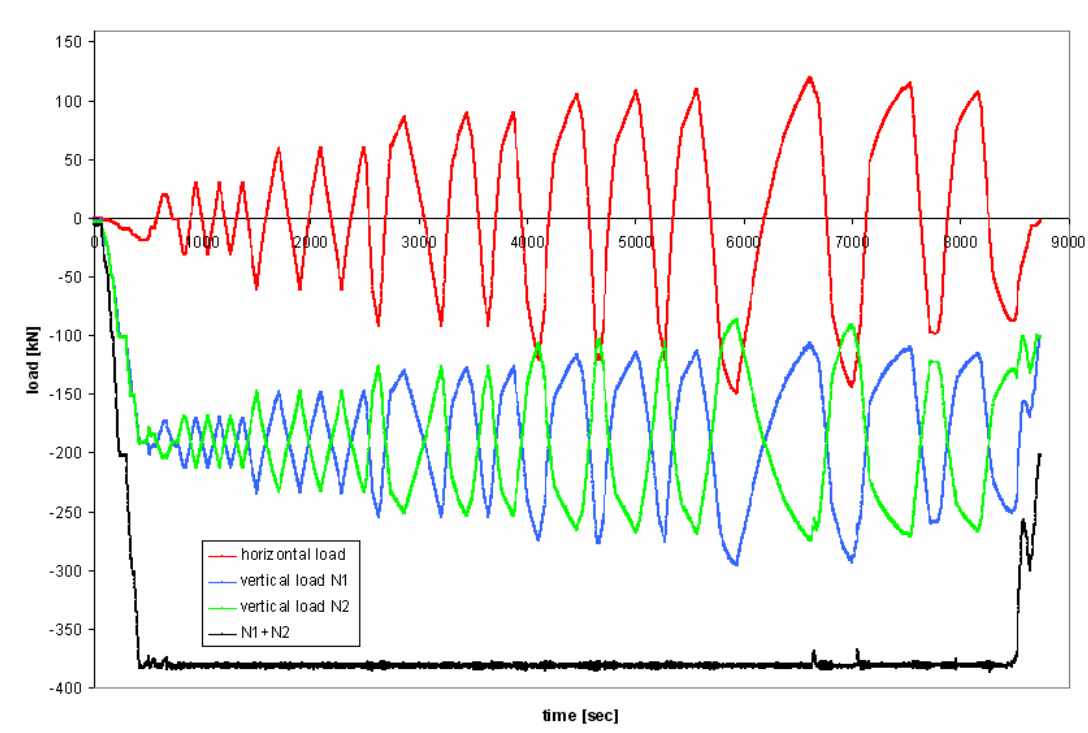

figure A6-3: load history of wall No. 6

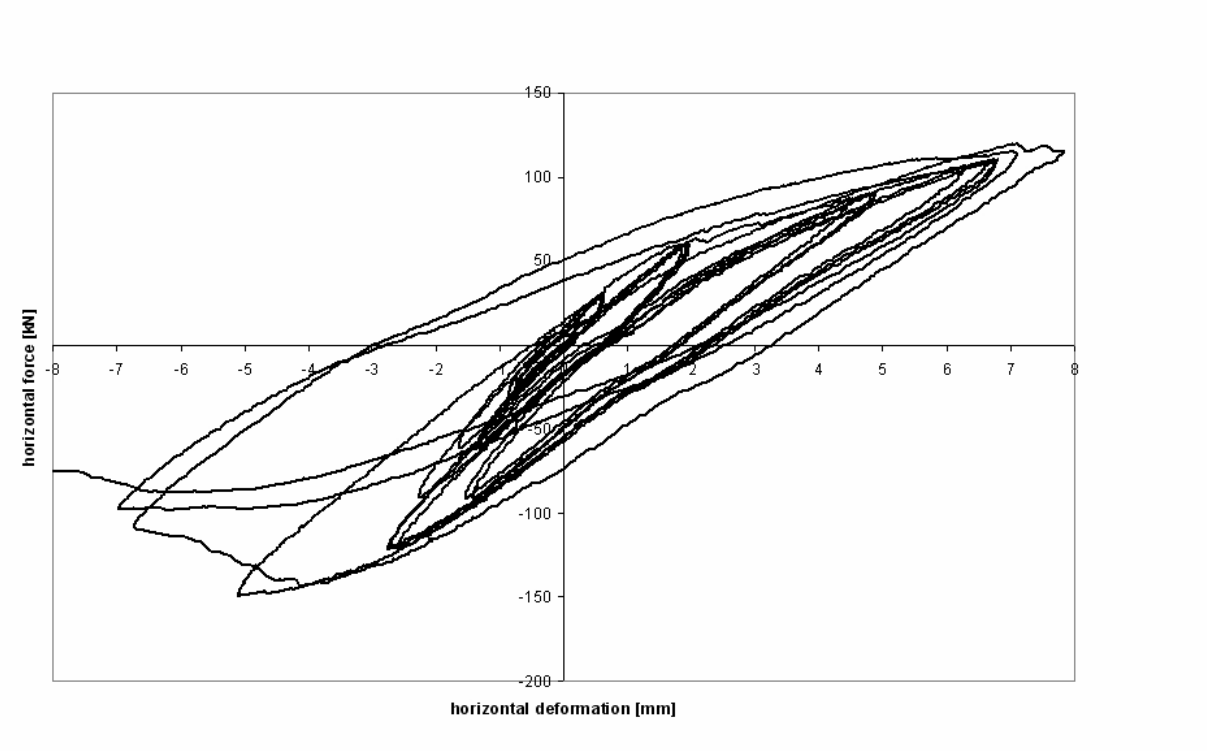

figure A6-4: hysteresis of wall No. 6

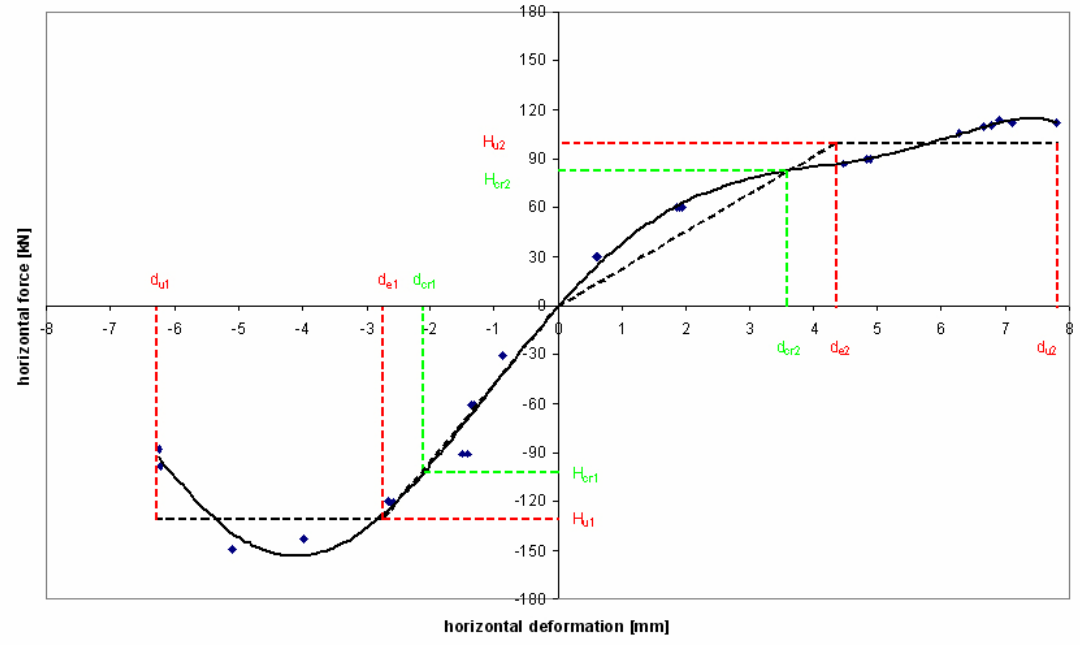

figure A6-5: enveloping curve of wall No. 6

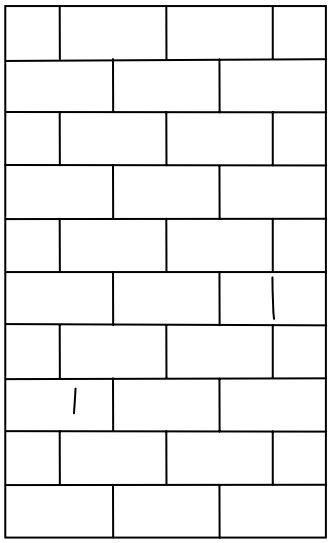

figure A7-1: first cracks at about 50 kN of test No. 7

figure A7-2: crack pattern of test No. 7

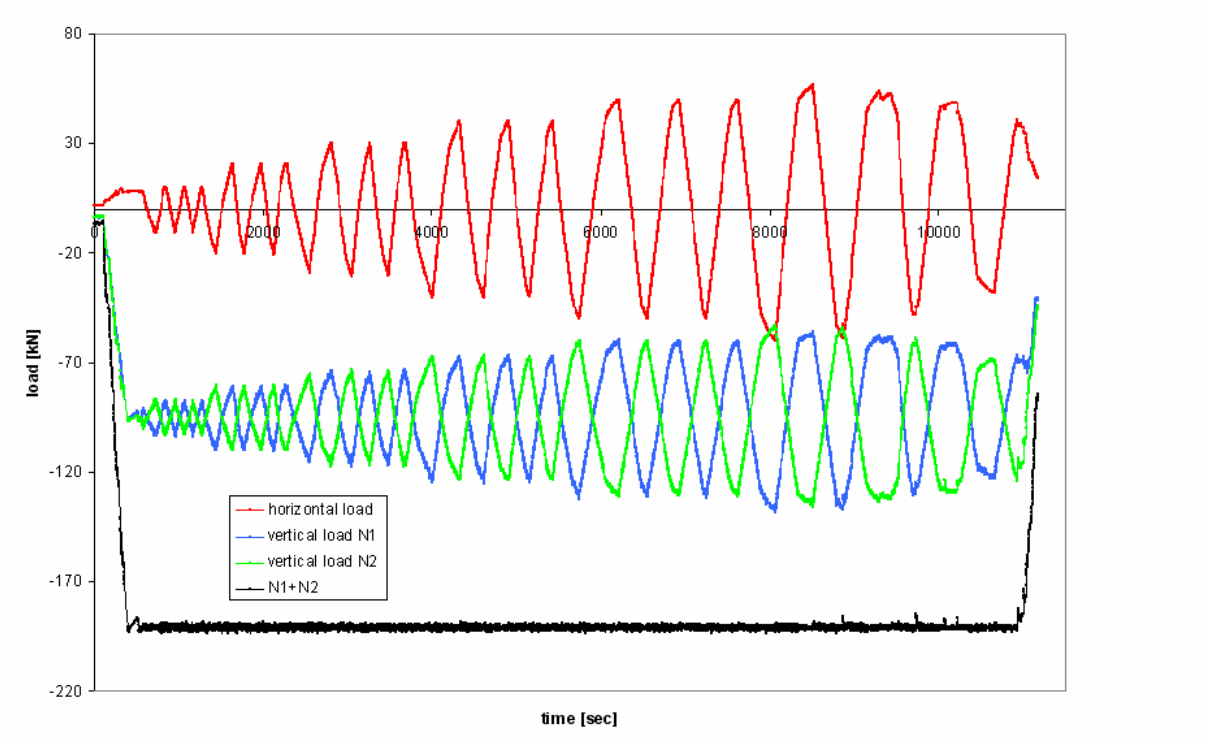

figure A7-3: load history of wall No. 7

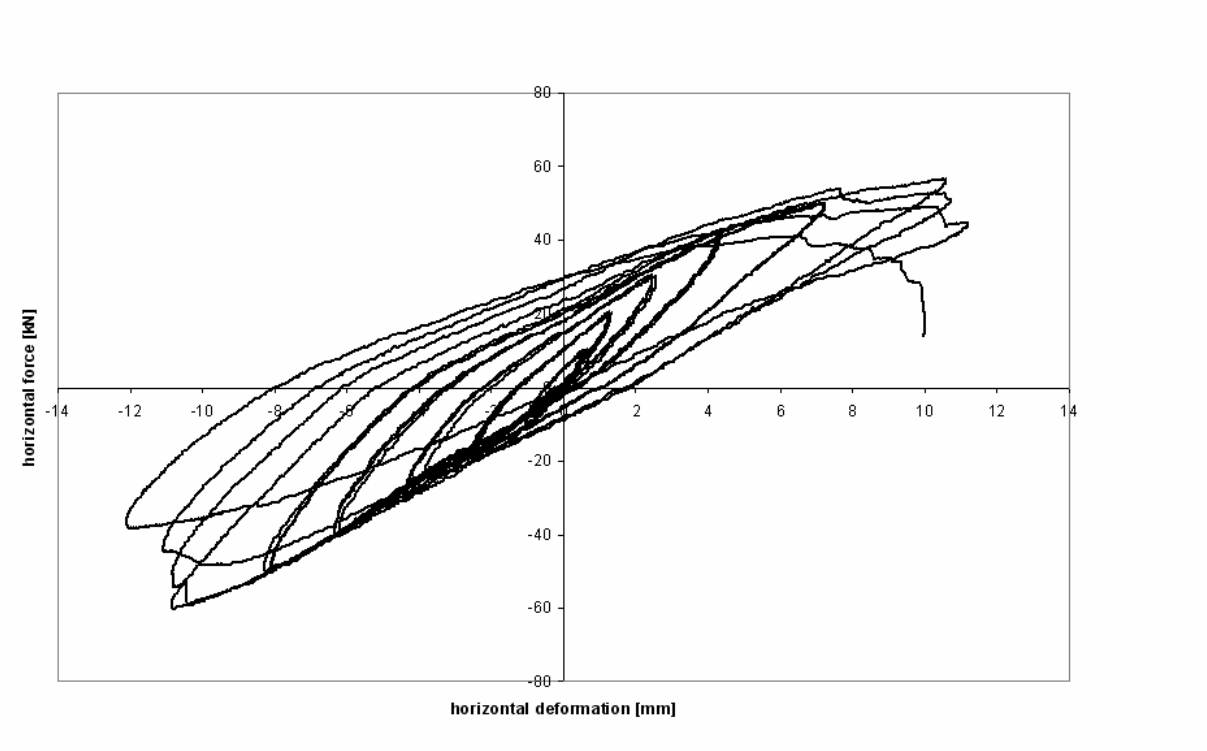

figure A7-4: hysteresis of wall No. 7

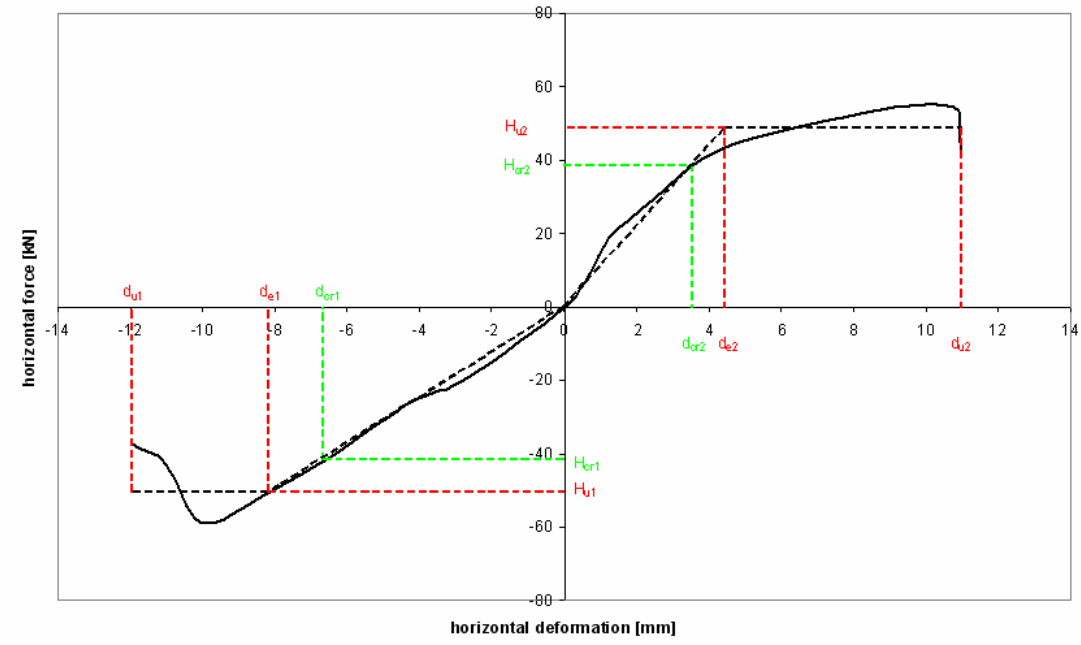

figure A7-5: enveloping curve of wall No. 7

figure A8-1: crack pattern of test No. 8

figure A8-2: failure of test No. 8

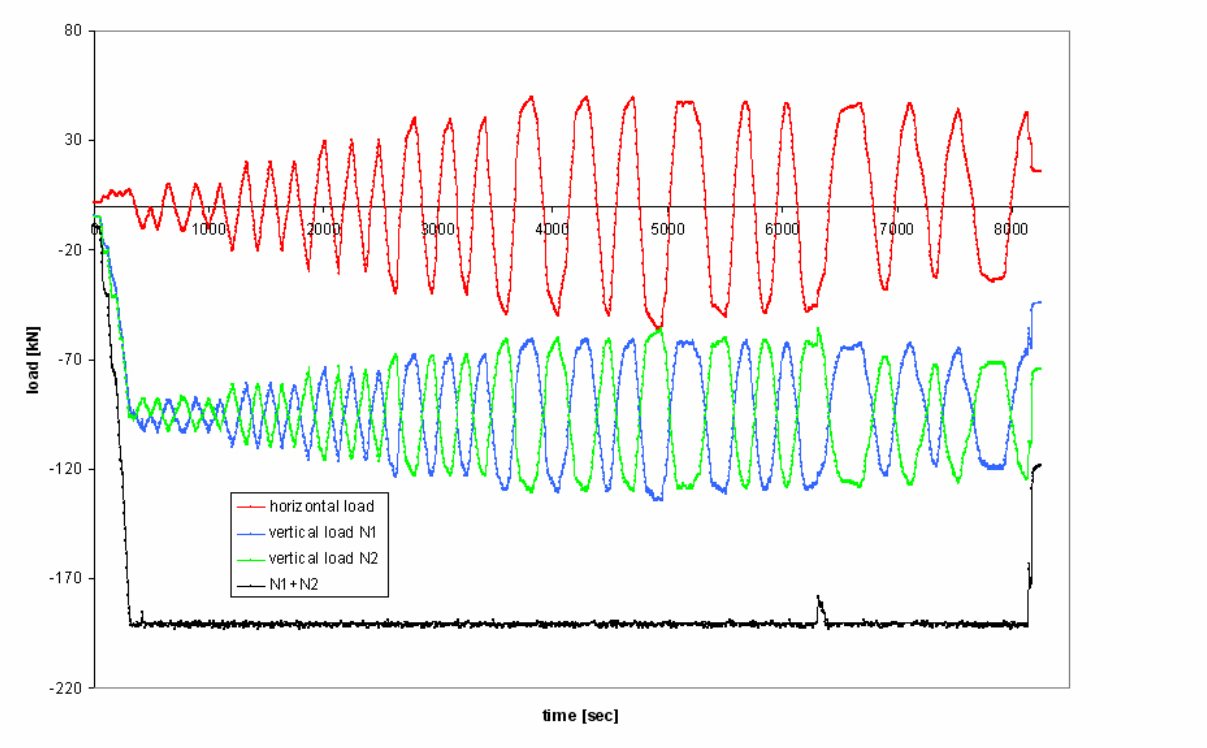

figure A8-3: load history of wall No. 8

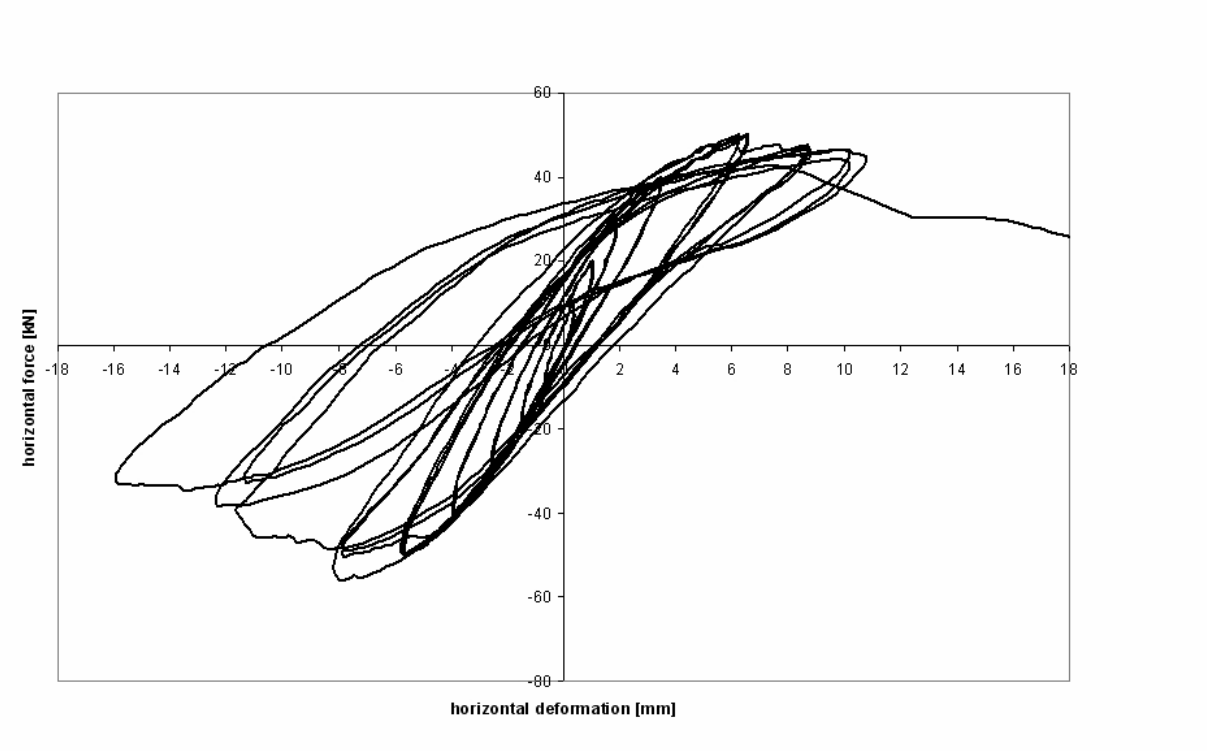

figure A8-4: hysteresis of wall No. 8

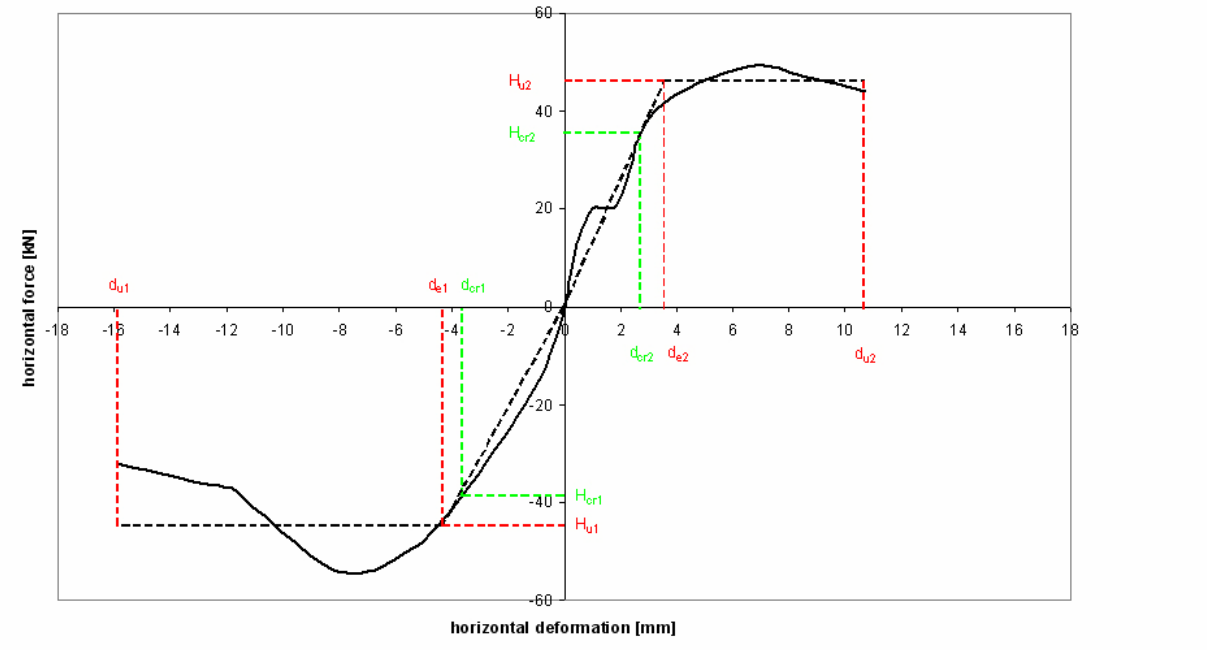

figure A8-5: enveloping curve of wall No. 8

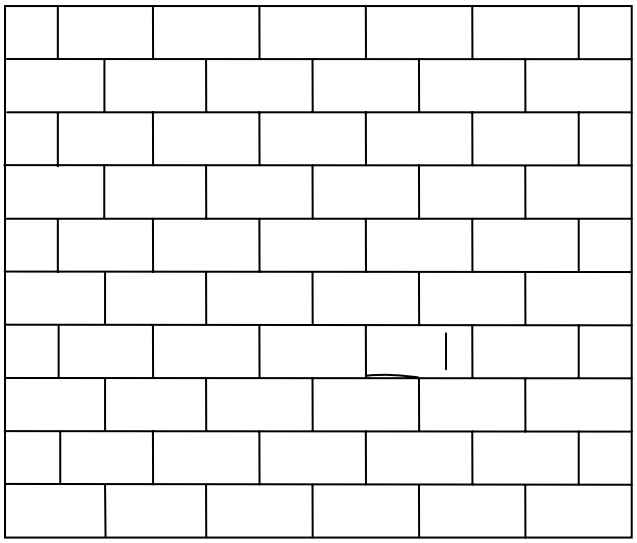

figure A9-1: first cracks at about -63 kN of test No. 9

figure A9-2: crack pattern of test No. 9

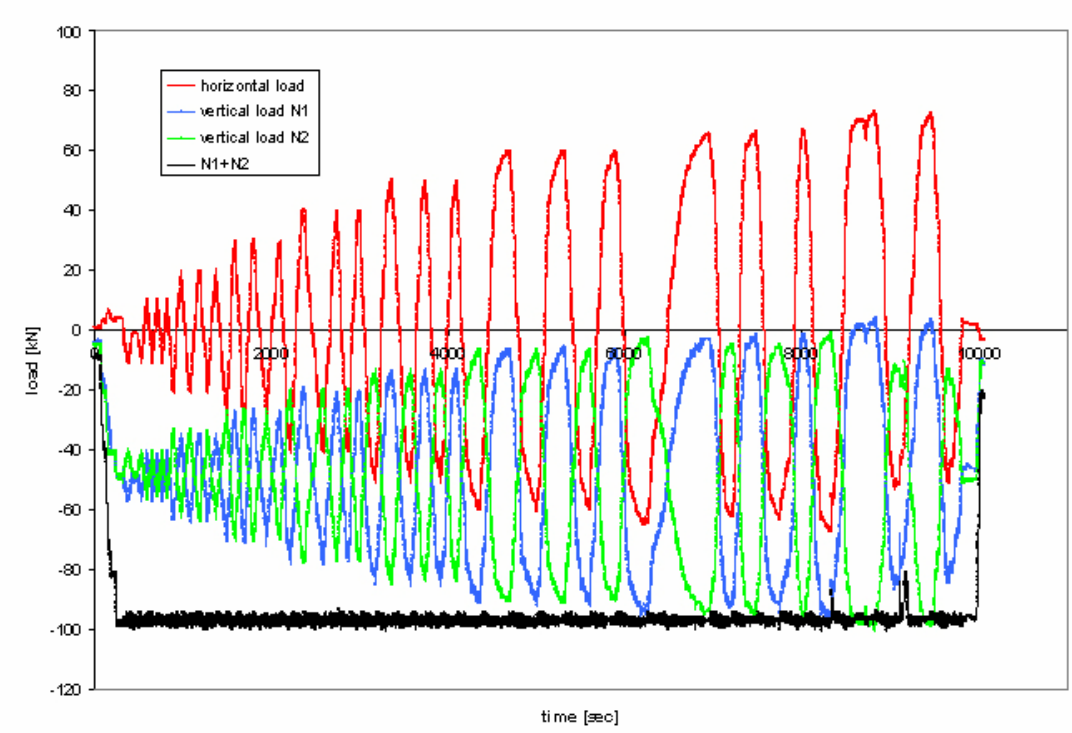

figure A9-3: load history of wall No. 9

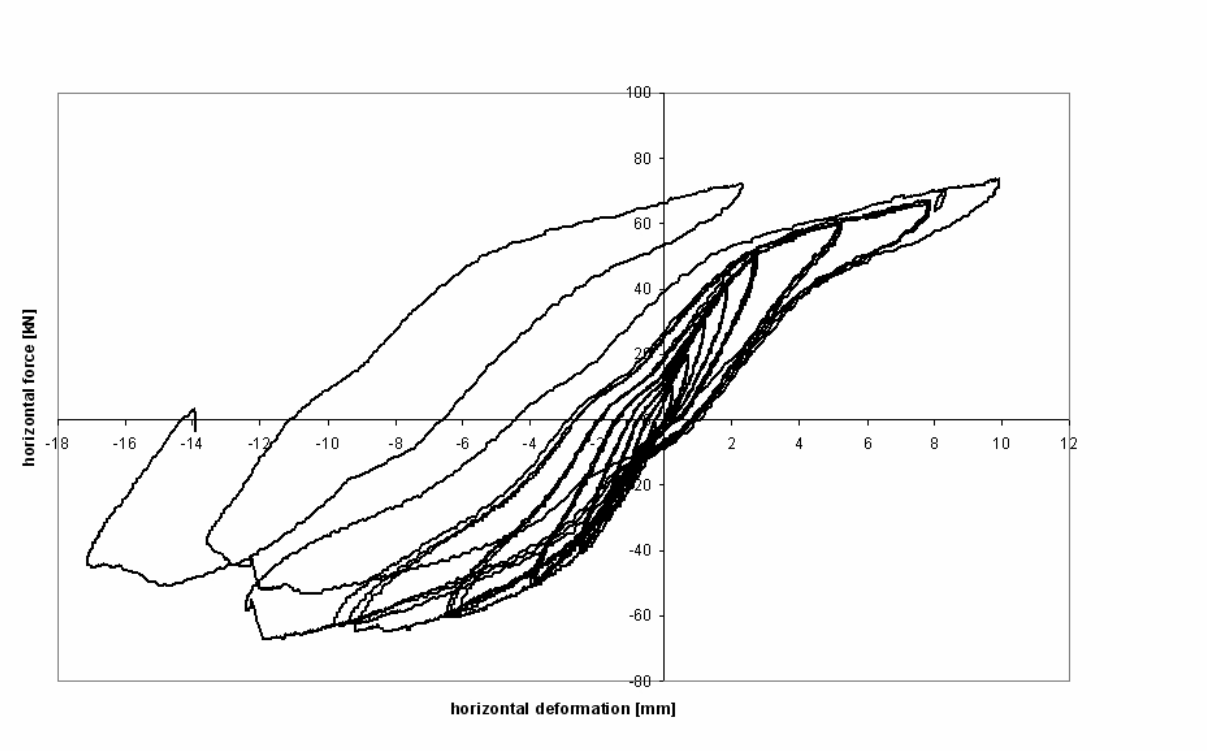

figure A9-4: hysteresis of wall No. 9

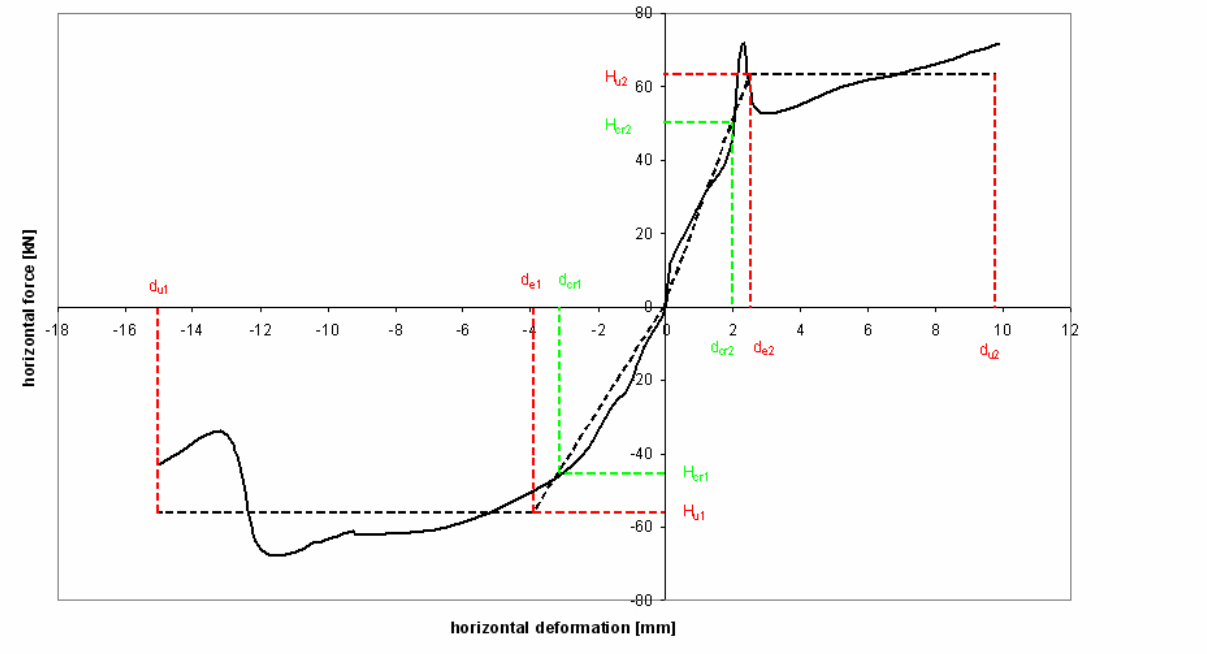

figure A9-5: enveloping curve of wall No. 9

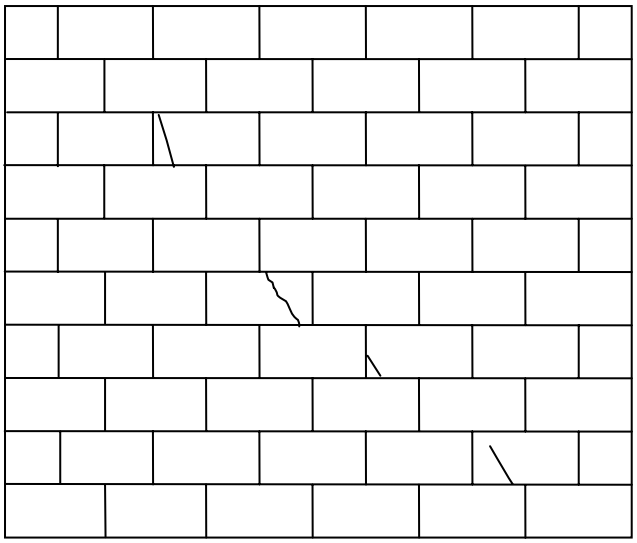

figure A10-1: first cracks at about -127 kN of test No. 10

figure A10-2: crack pattern of test No. 10

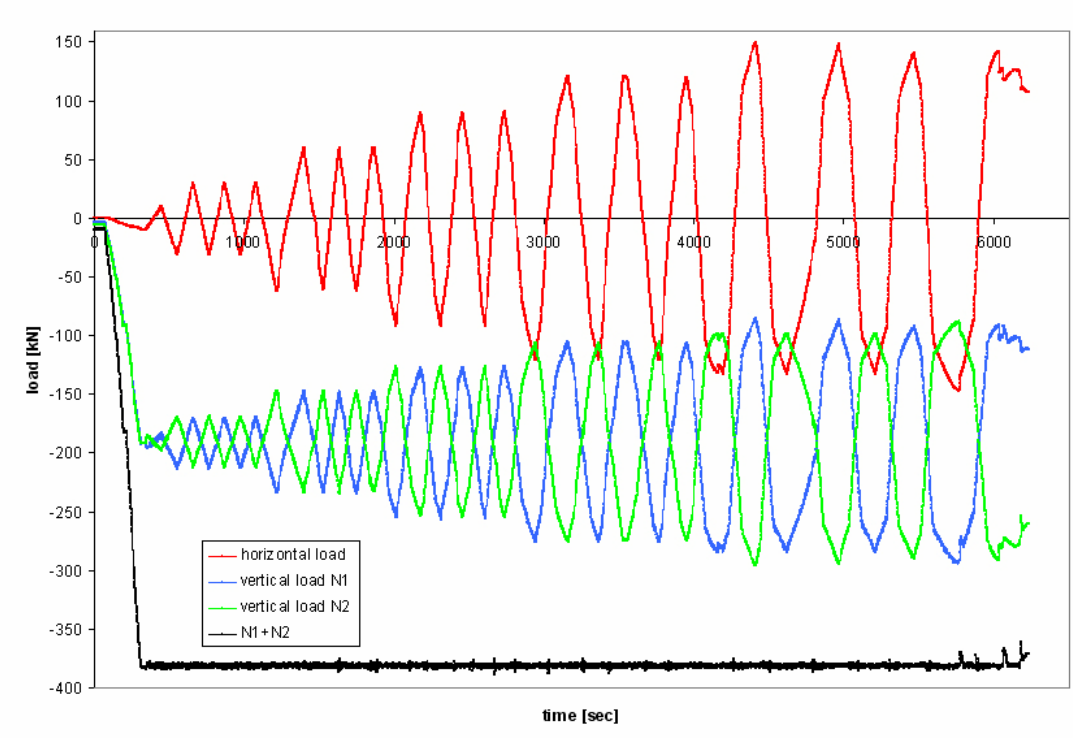

figure A10-3: load history of wall No. 10

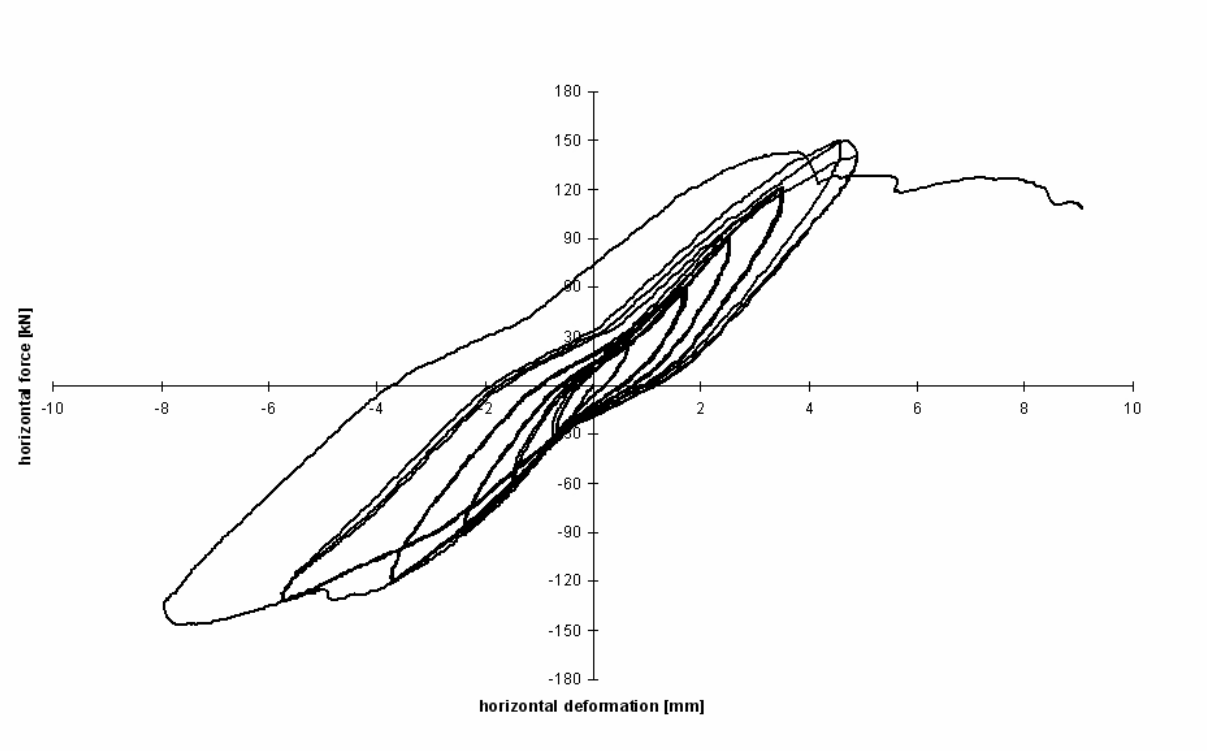

figure A10-4: hysteresis of wall No. 10

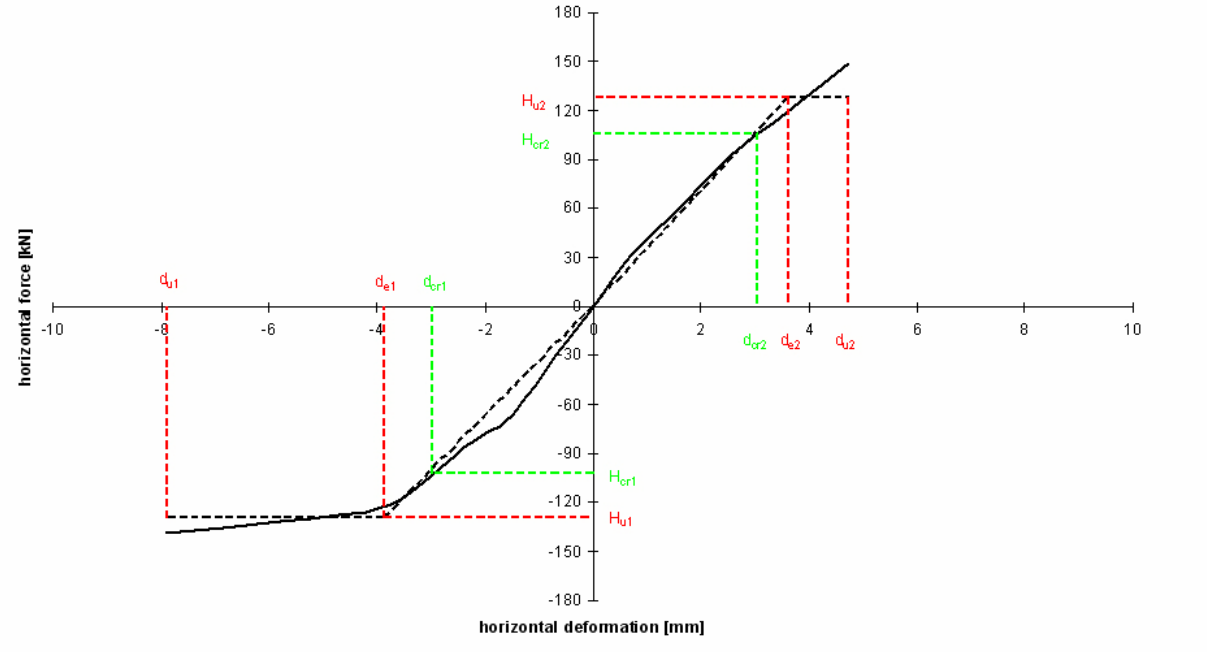

figure A10-5: enveloping curve of wall No. 10

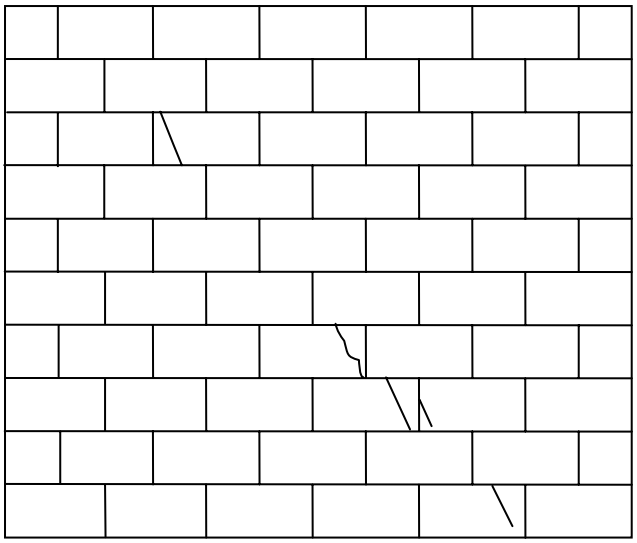

figure A11-1: first cracks at about 140 kN of test No. 11

figure A11-2: crack pattern of test No. 11

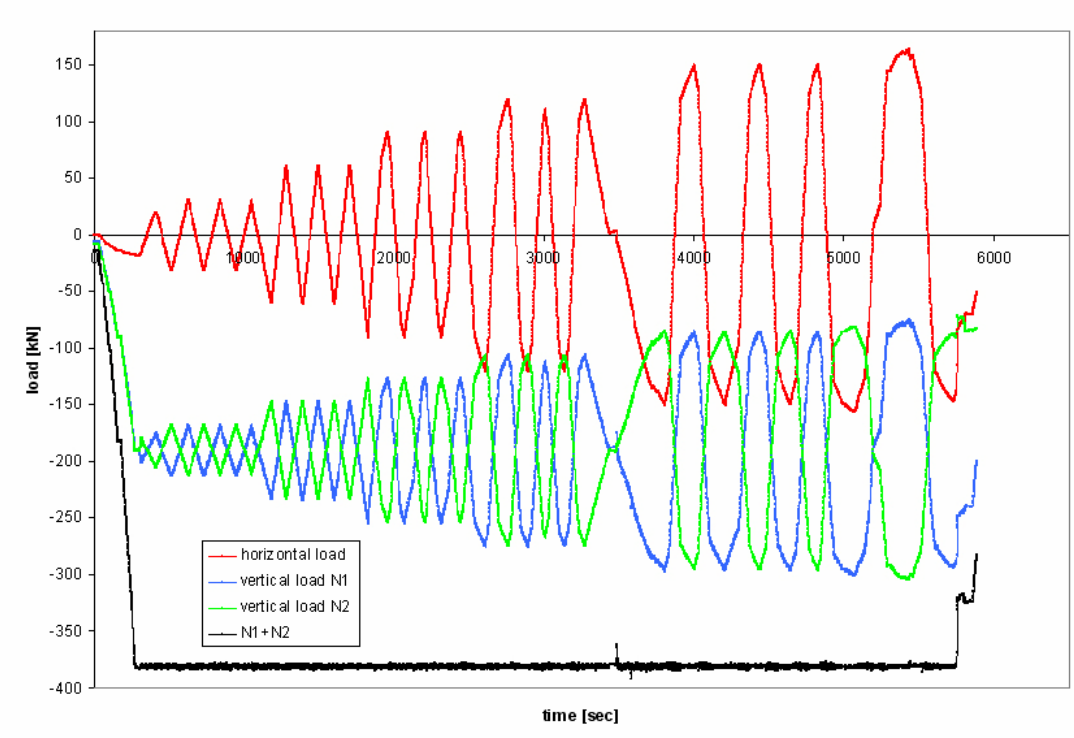

figure A11-3: load history of wall No. 11

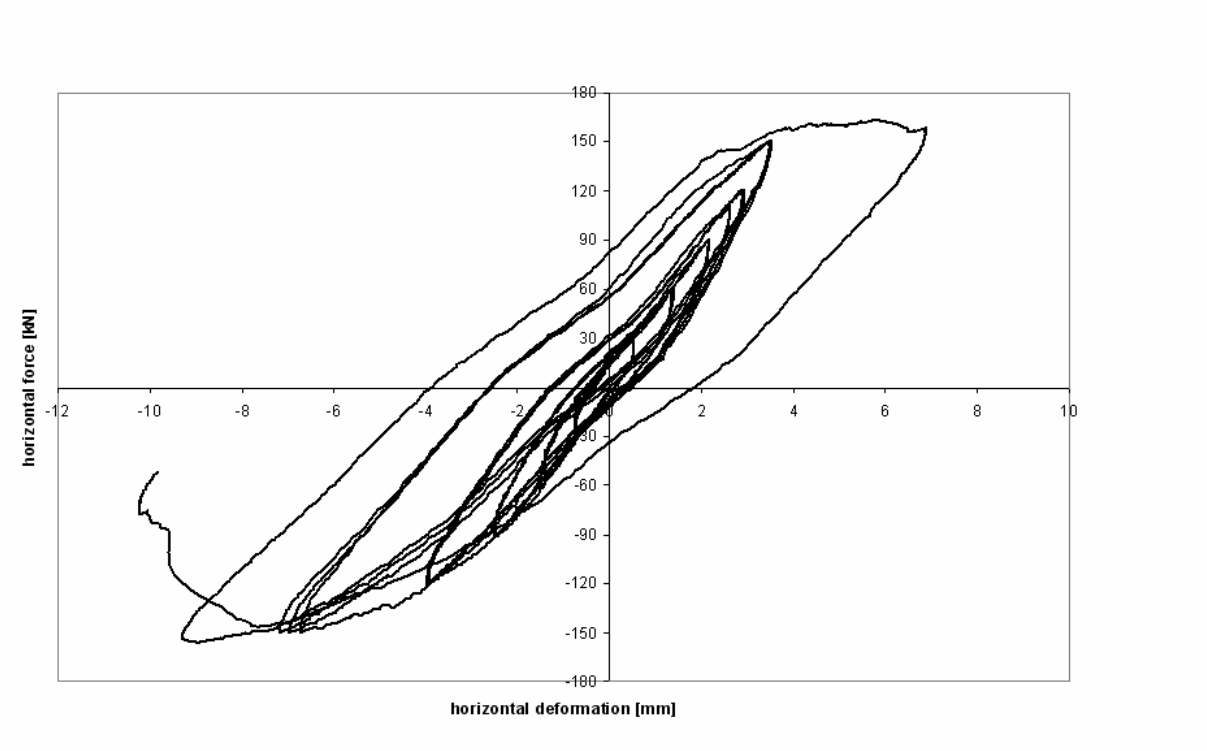

figure A11-4: hysteresis of wall No. 11

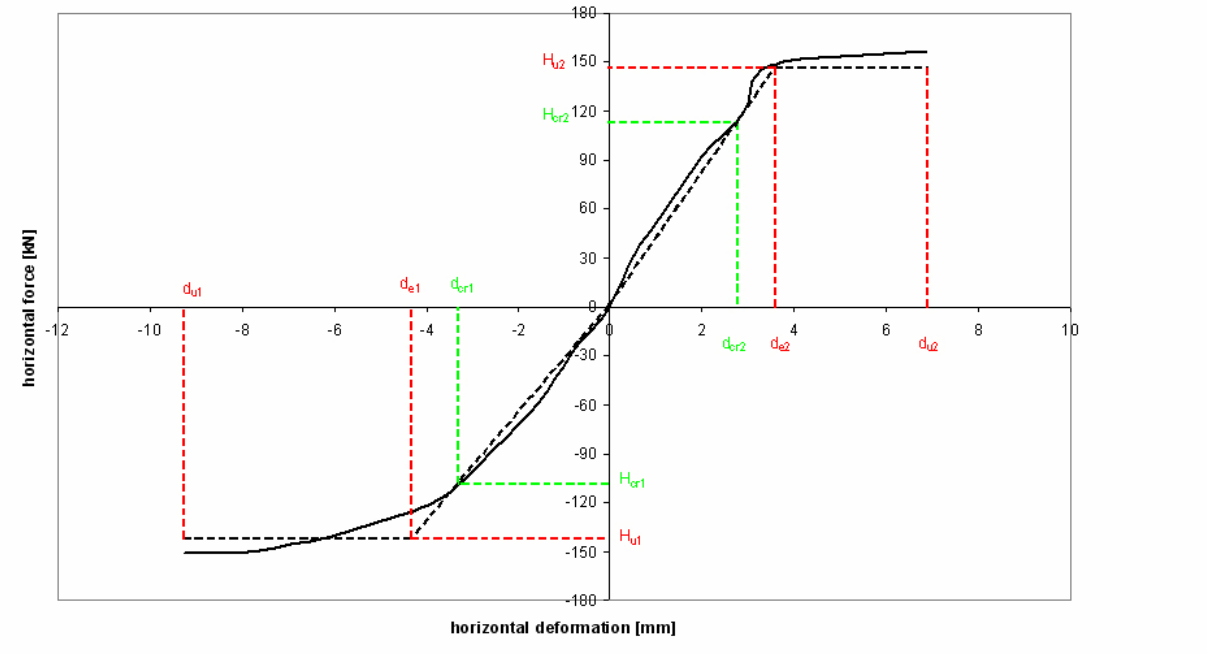

figure A11-5: enveloping curve of wall No. 11

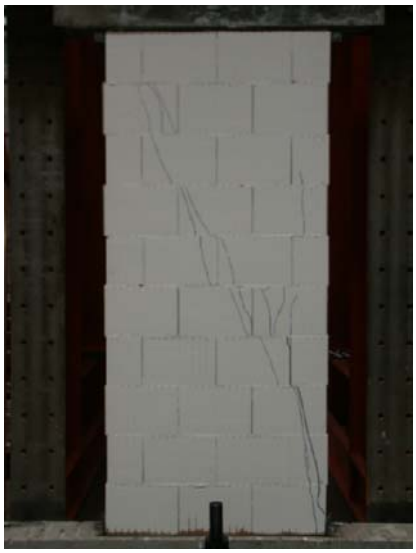

figure A12-1: first cracks at about -70 kN of test No. 12

figure A12-2: detail of the crack pattern of test No. 12

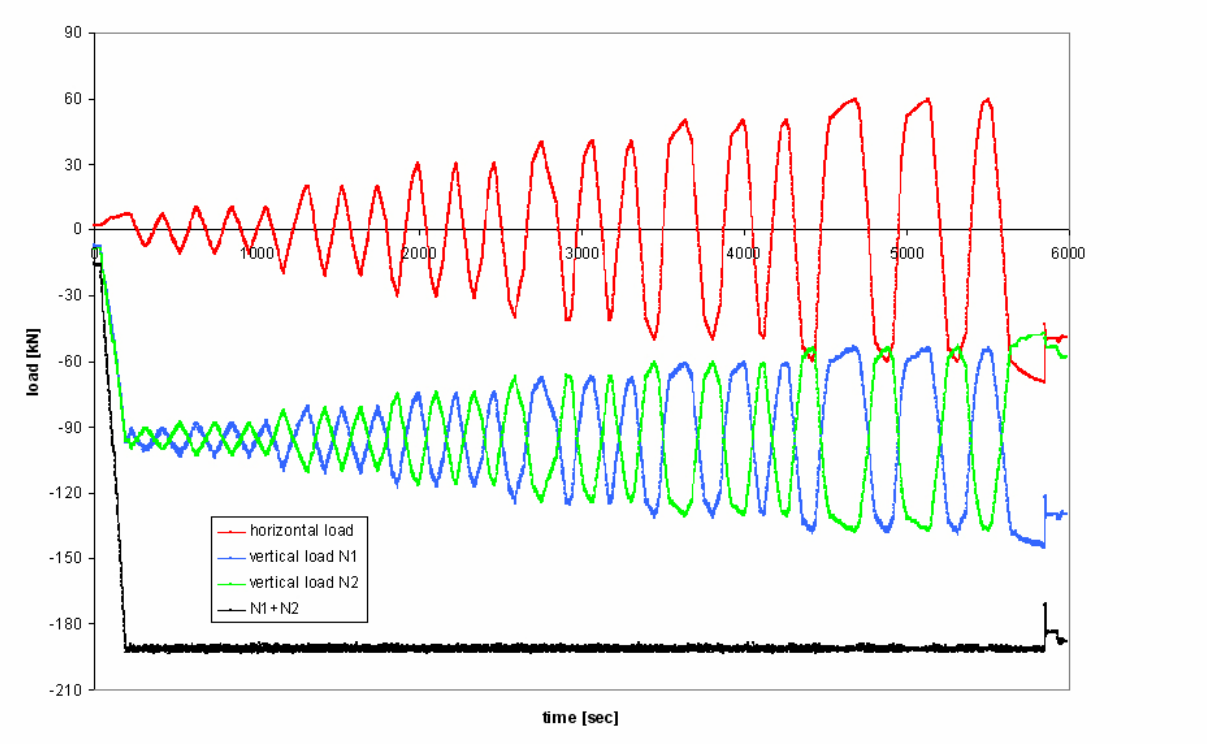

figure A12-3: load history of wall No. 12

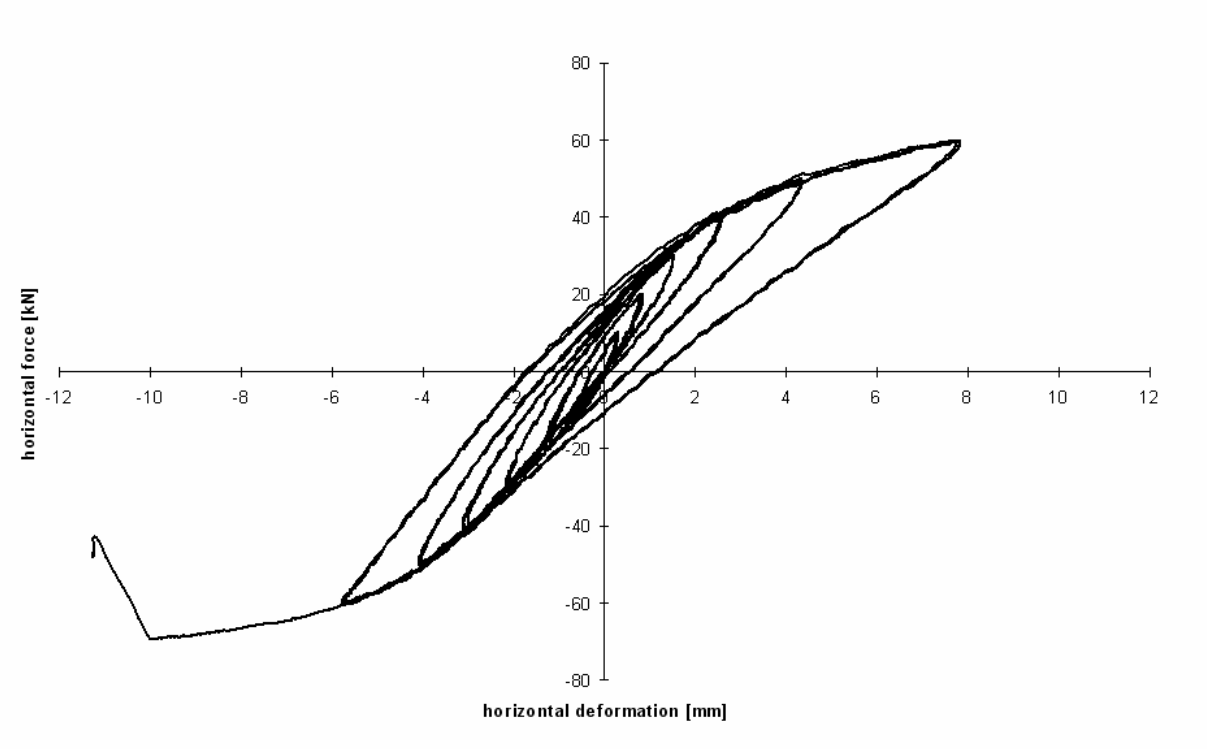

figure A12-4: hysteresis of wall No. 12

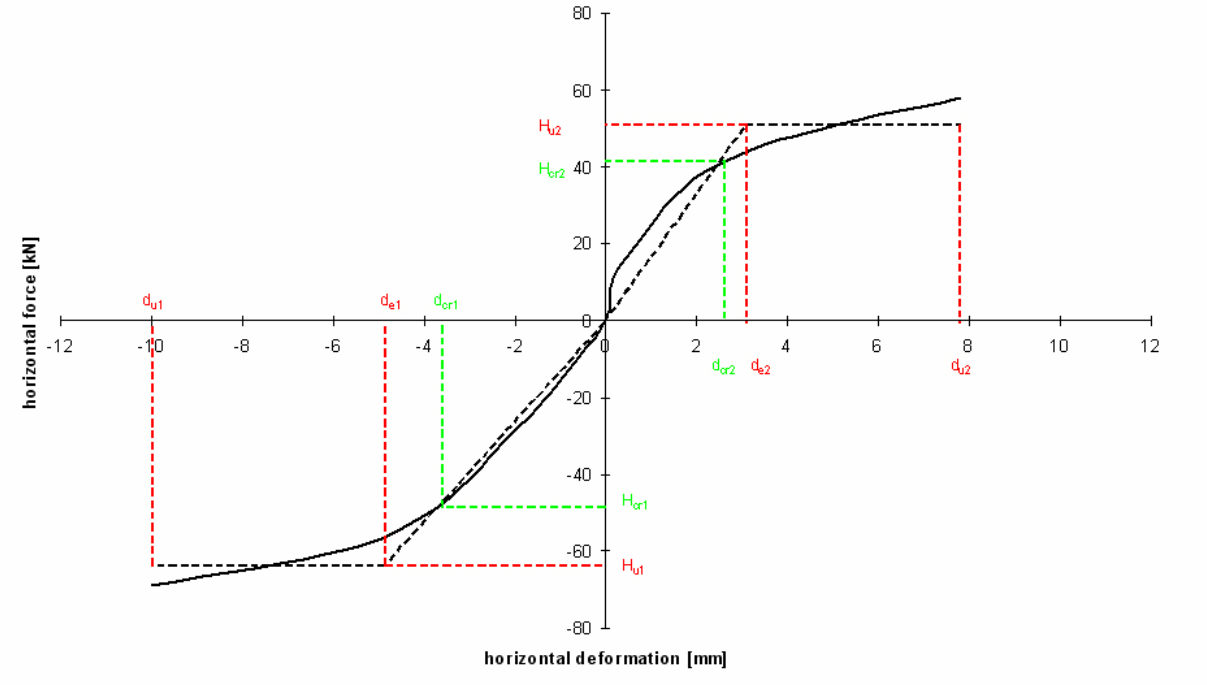

figure A12-5: enveloping curve of wall No. 12

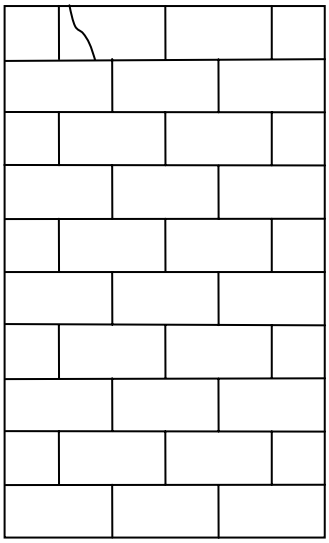

figure A13-1: first cracks at about -41 kN of test No. 13

figure A13-2: crack pattern of test No. 13

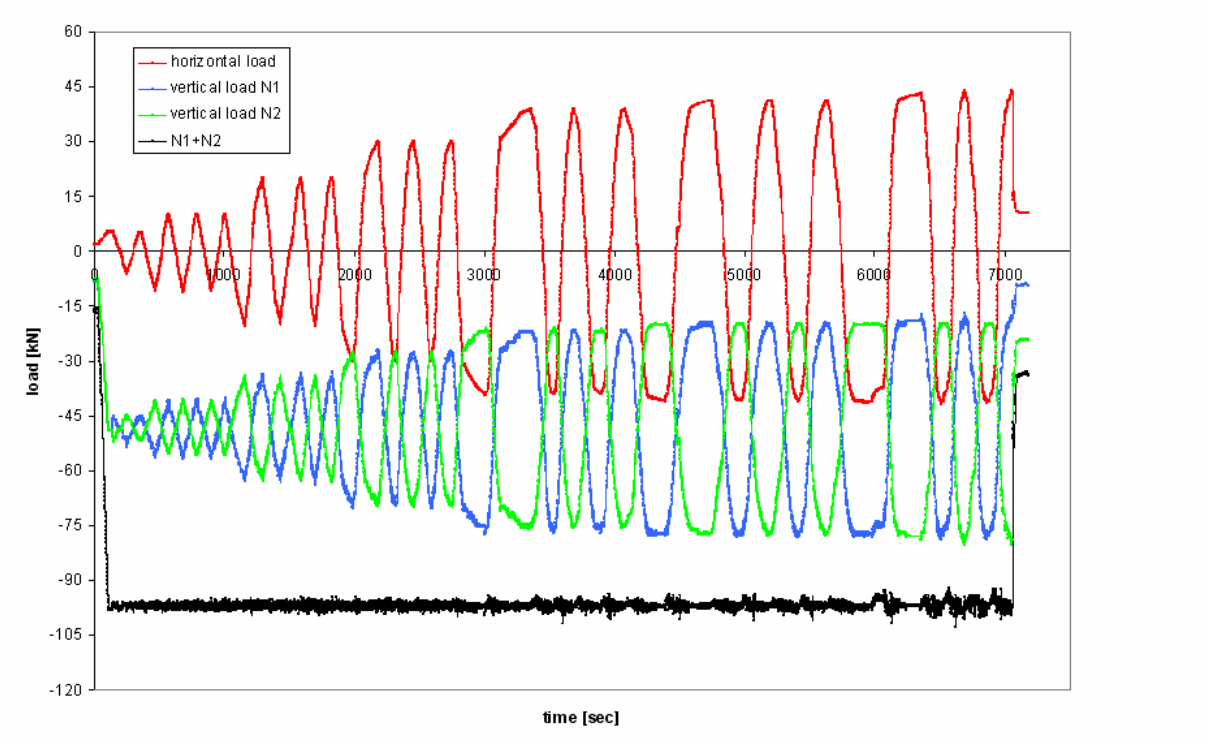

figure A13-3: load history of wall No. 13

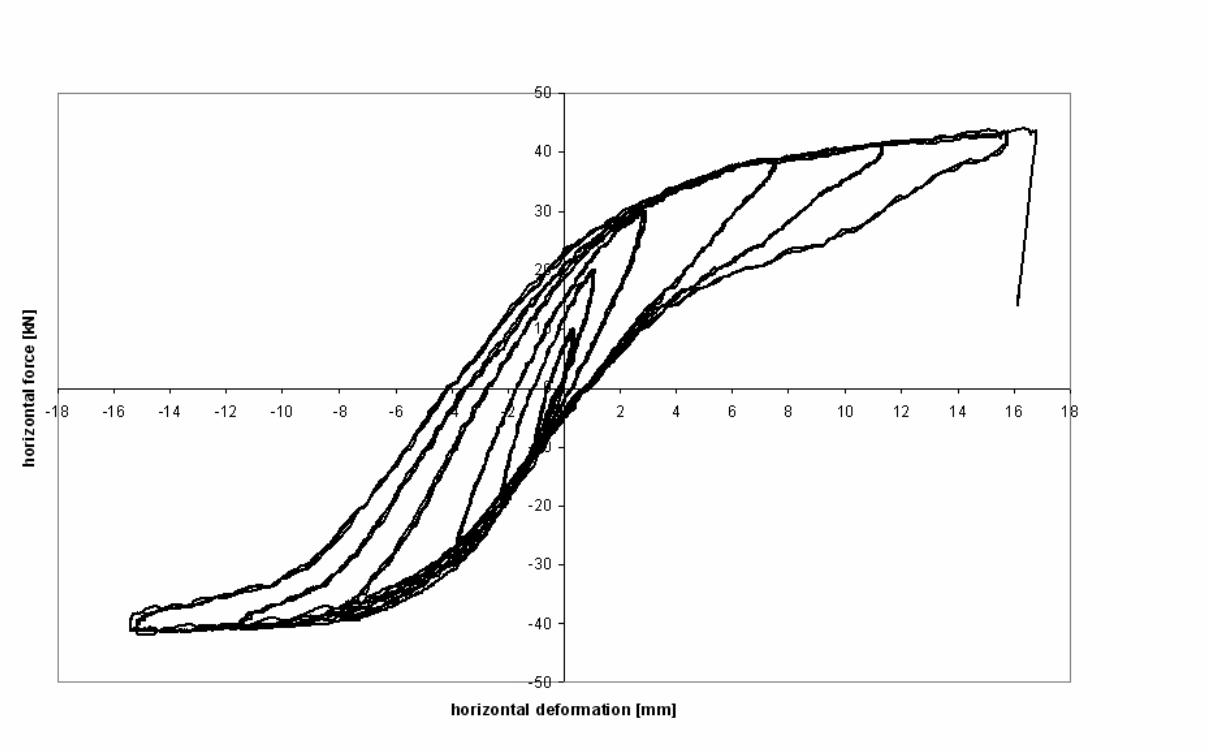

figure A13-4: hysteresis of wall No. 13

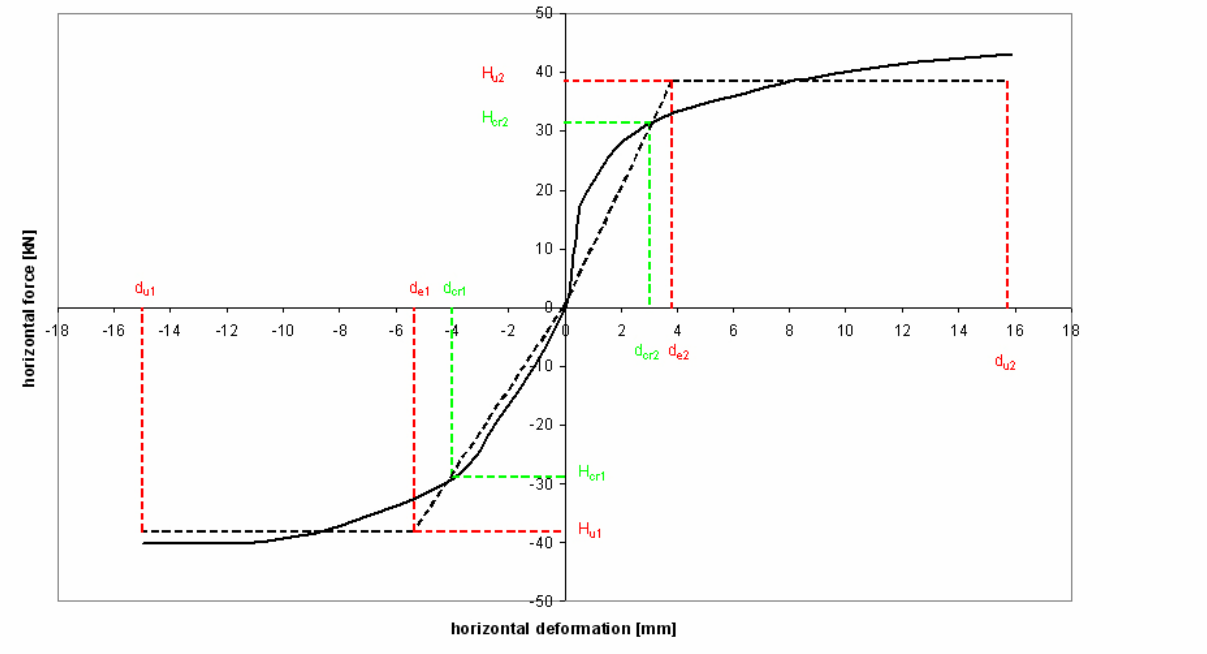

figure A13-5: enveloping curve of wall No. 13

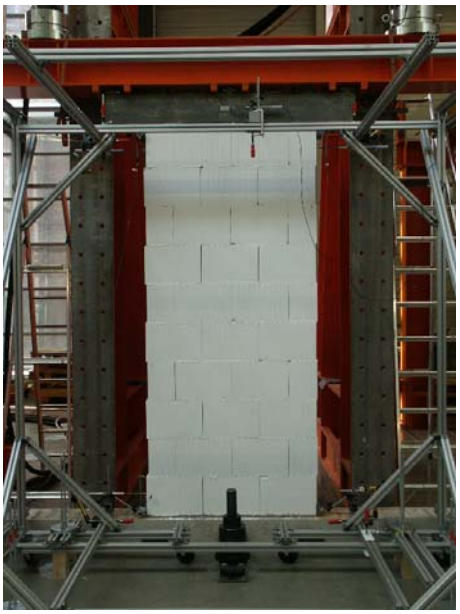

figure A14-1: view of the test specimen No. 14

figure A14-2: gapping of test No. 14

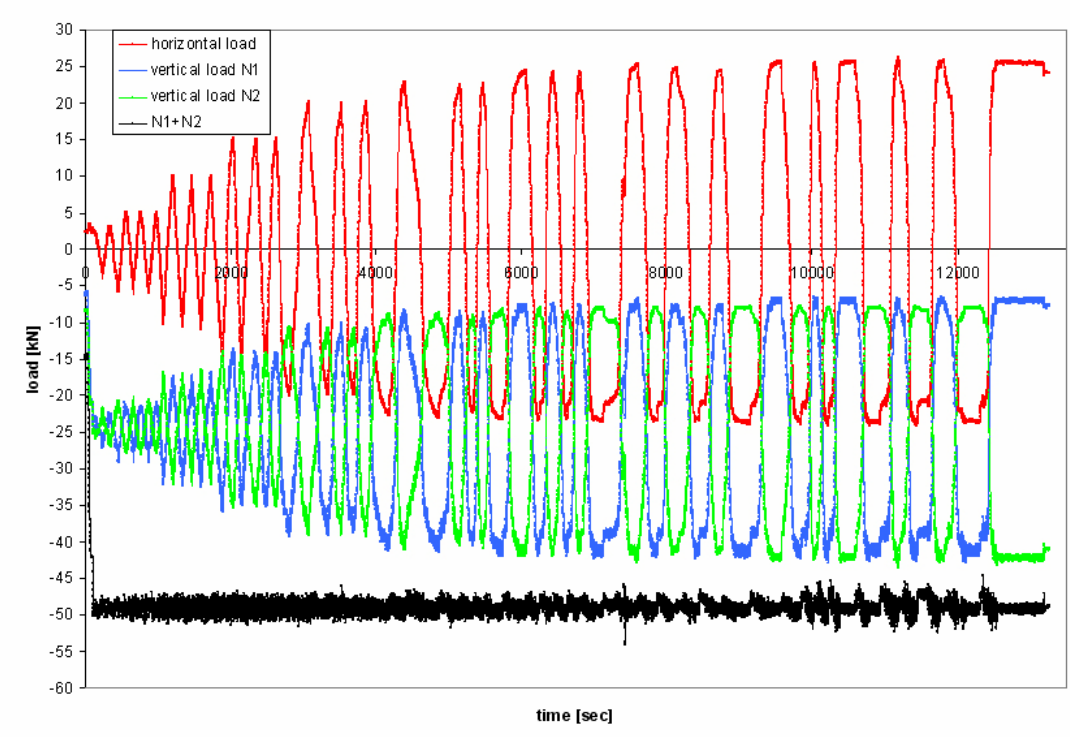

figure A14-3: load history of wall No. 14

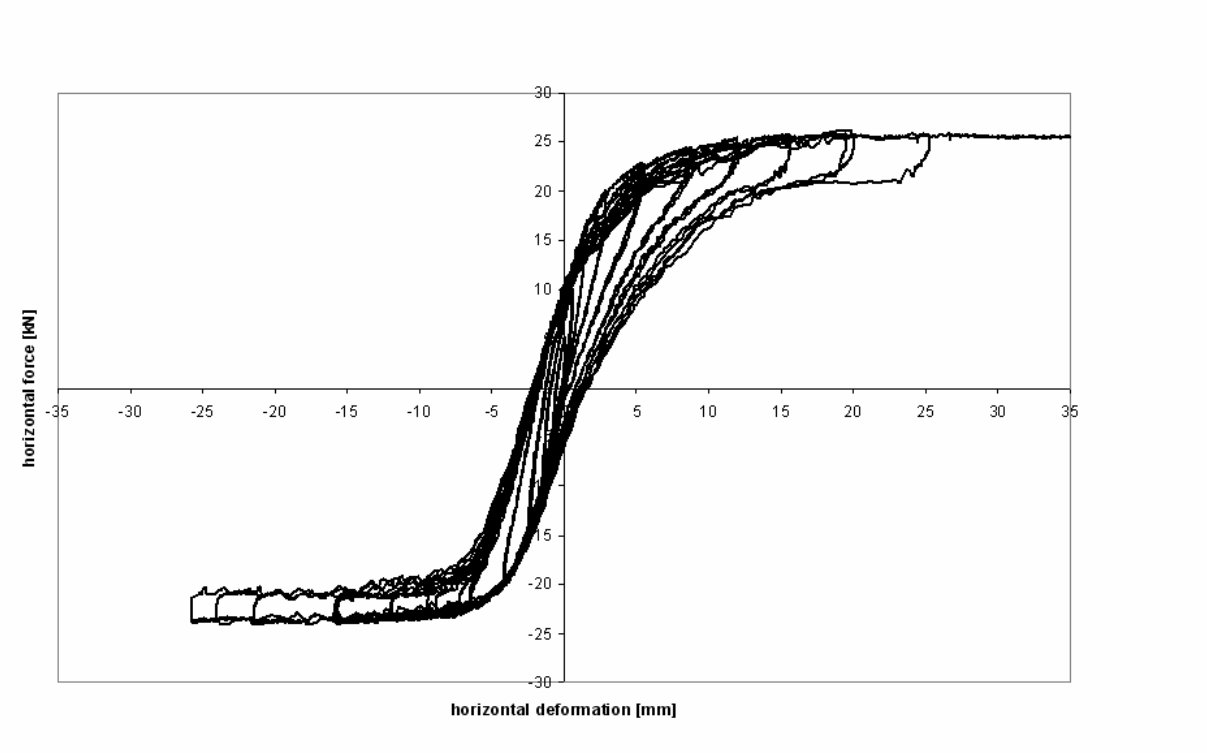

figure A14-4: hysteresis of wall No. 14

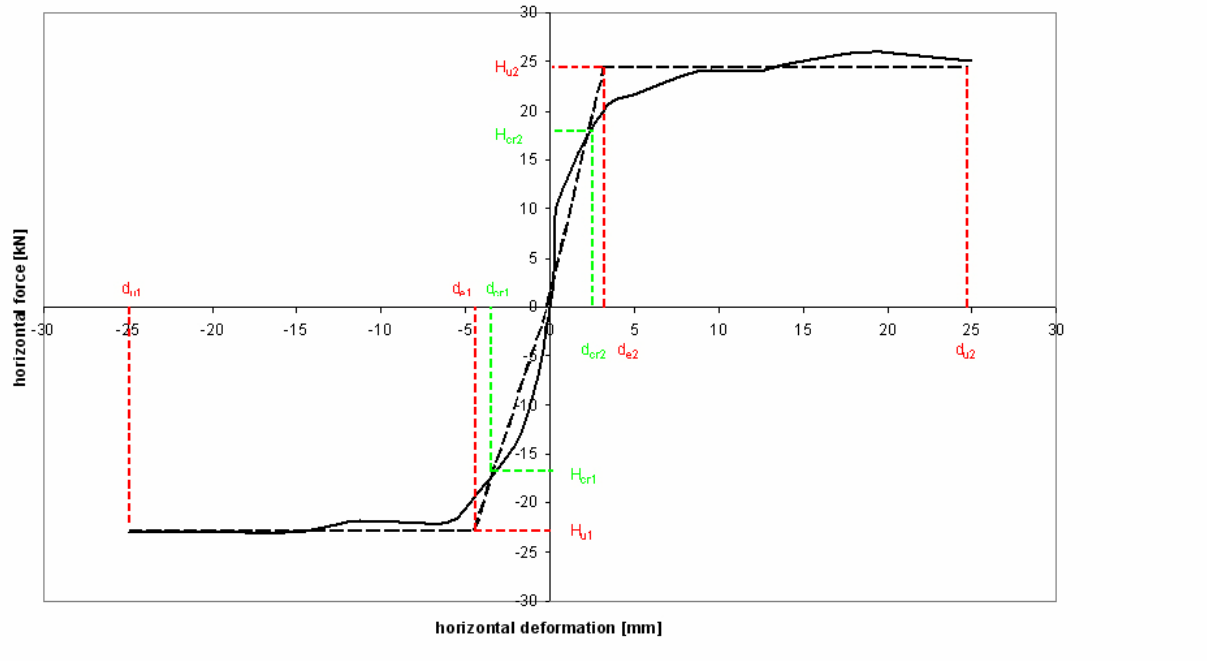

figure A14-5: enveloping curve of wall No. 14

figure A15-1: first cracks at about 70 kN of test No. 15

figure A15-2: crack pattern of test No. 15

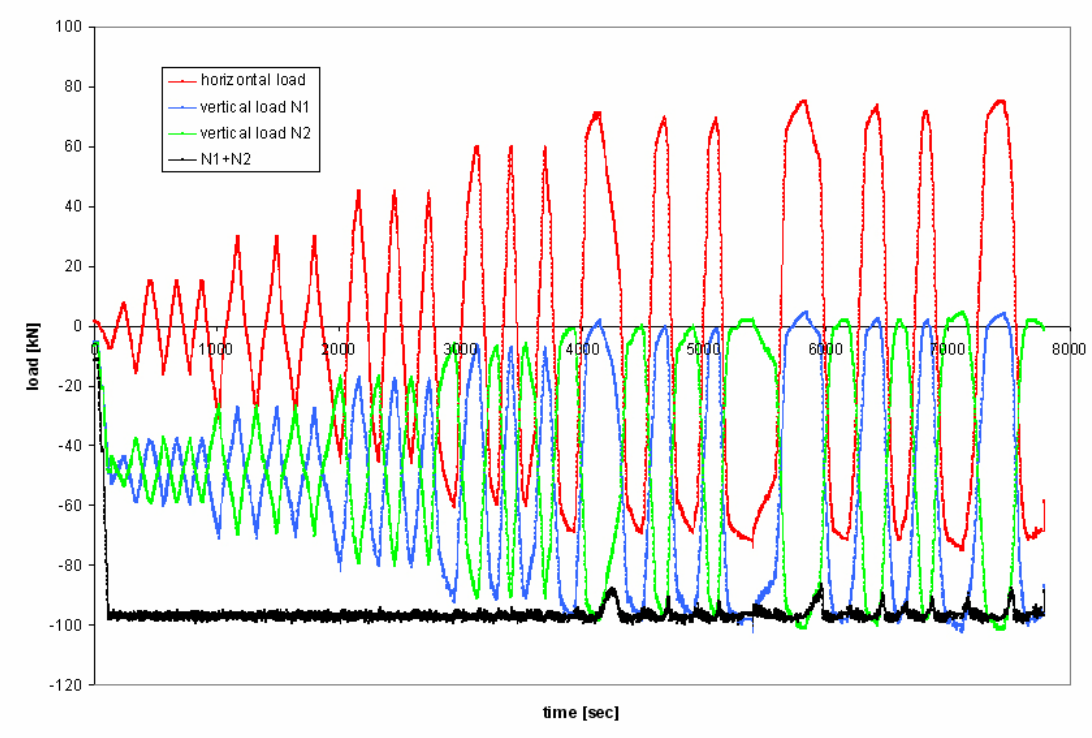

figure A15-3: load history of wall No. 15

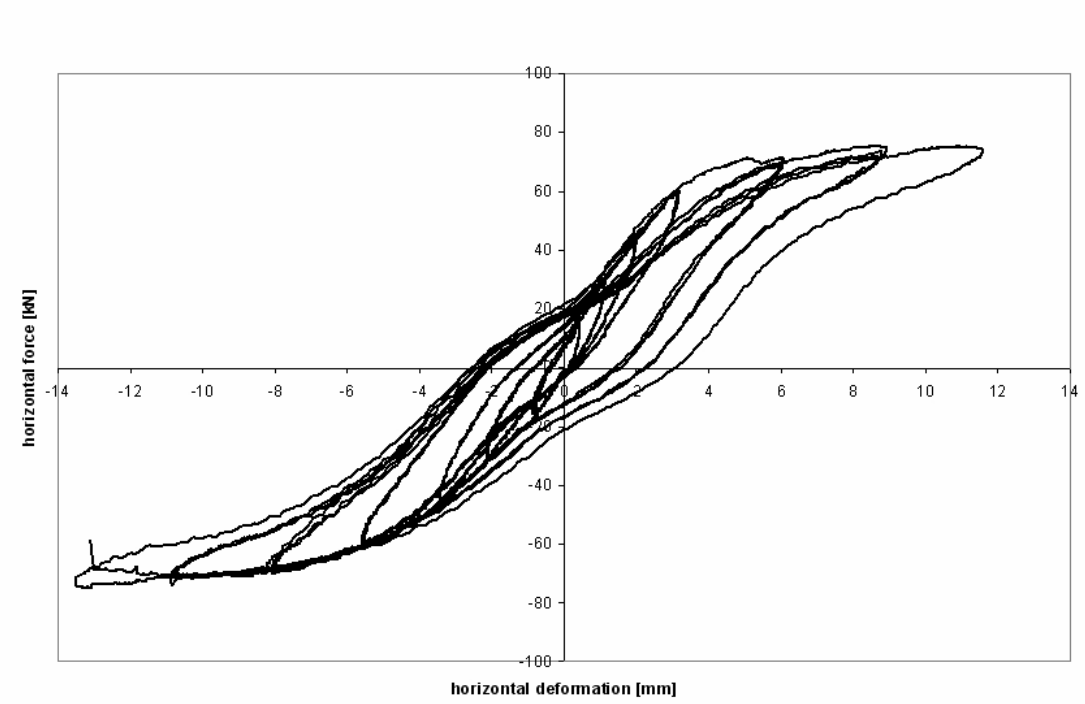

figure A15-4: hysteresis of wall No. 15

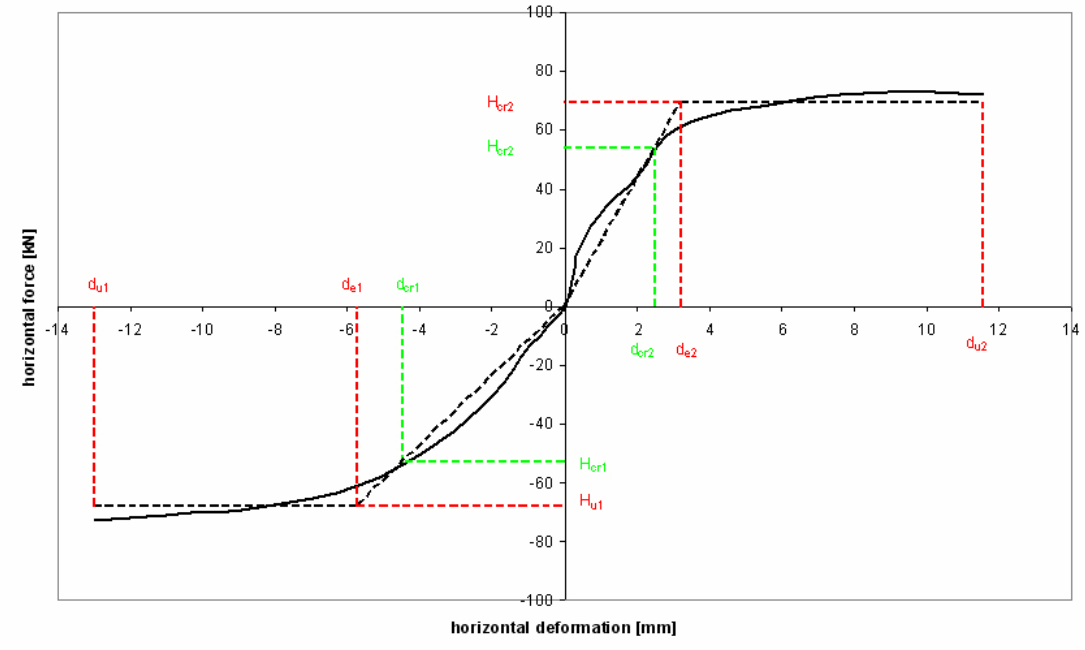

figure A15-5: enveloping curve of wall No. 15

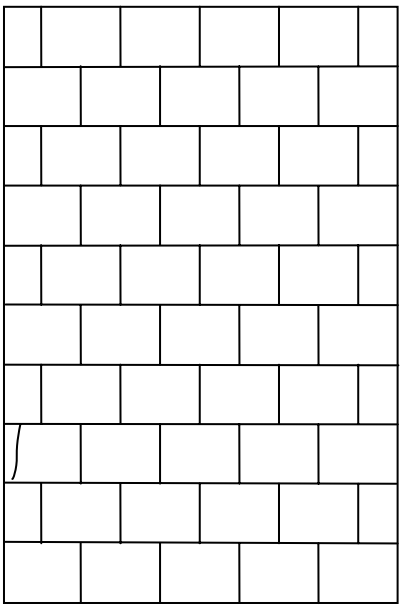

figure A16-1: first cracks at about 86 kN of test No. 16

figure A16-2: crack pattern of test No. 16

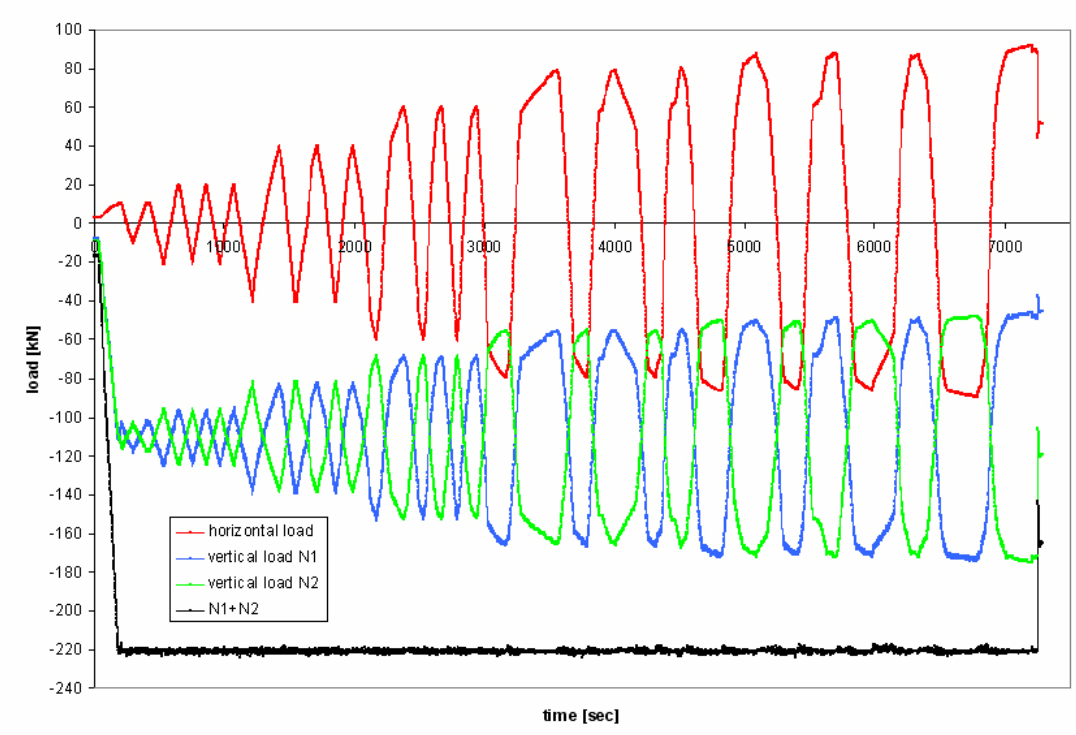

figure A16-3: load history of wall No. 16

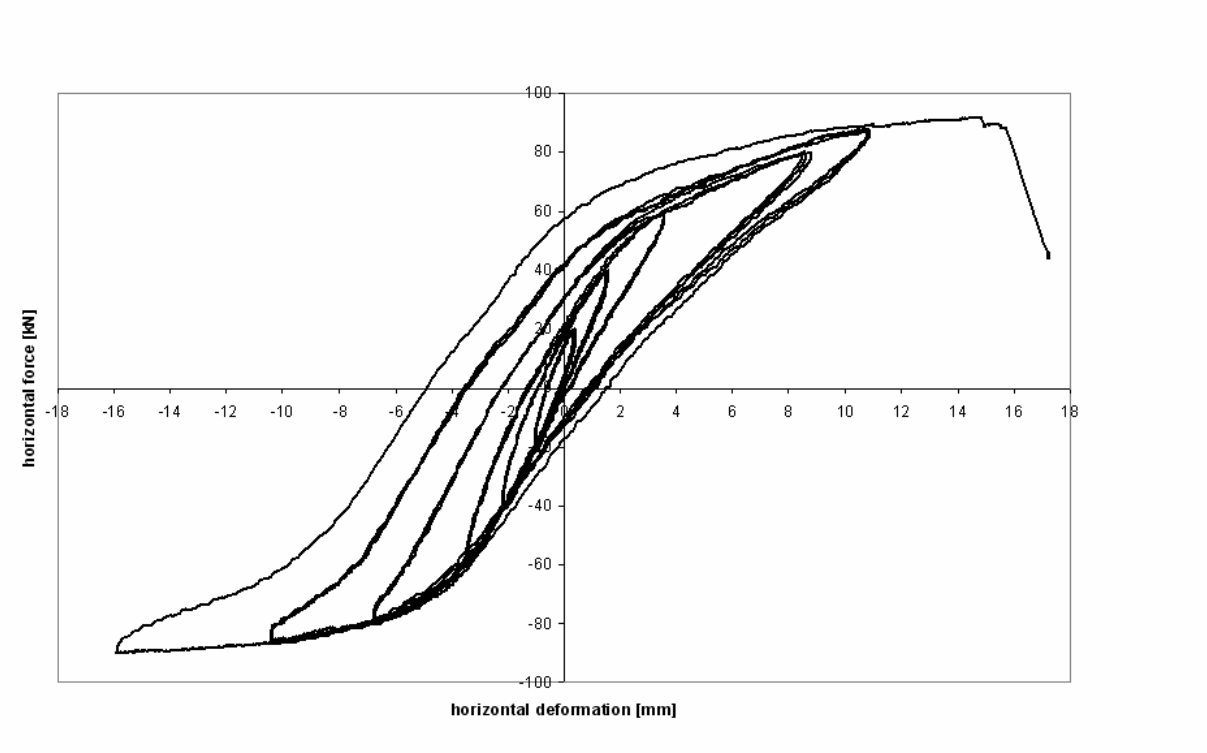

figure A16-4: hysteresis of wall No. 16

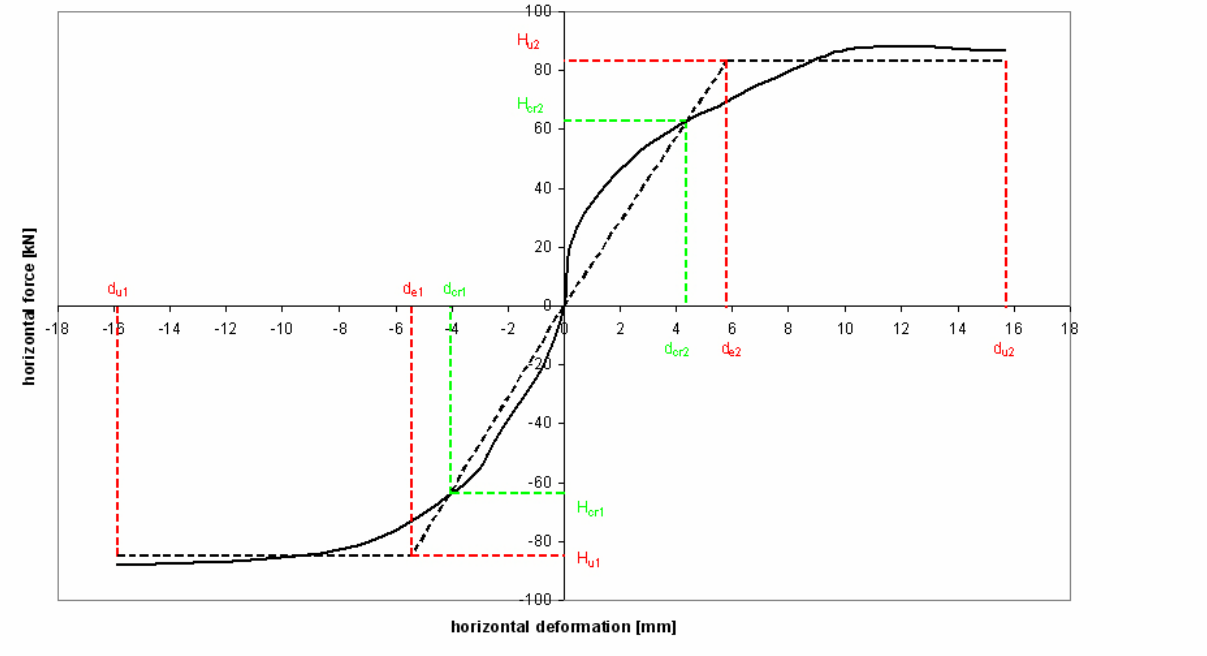

figure A16-5: enveloping curve of wall No. 16

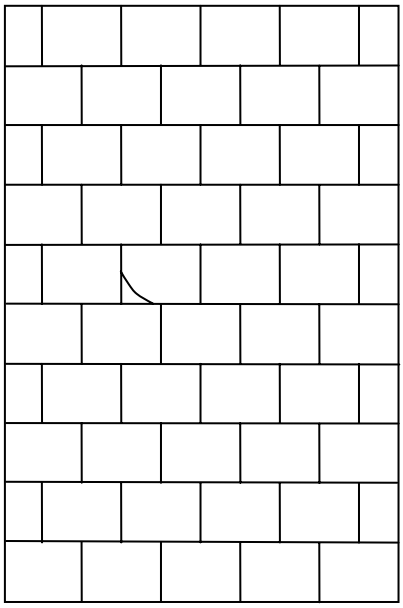

figure A17-1: first cracks at about -81 kN of test No. 17

figure A17-2: crack pattern of test No. 17

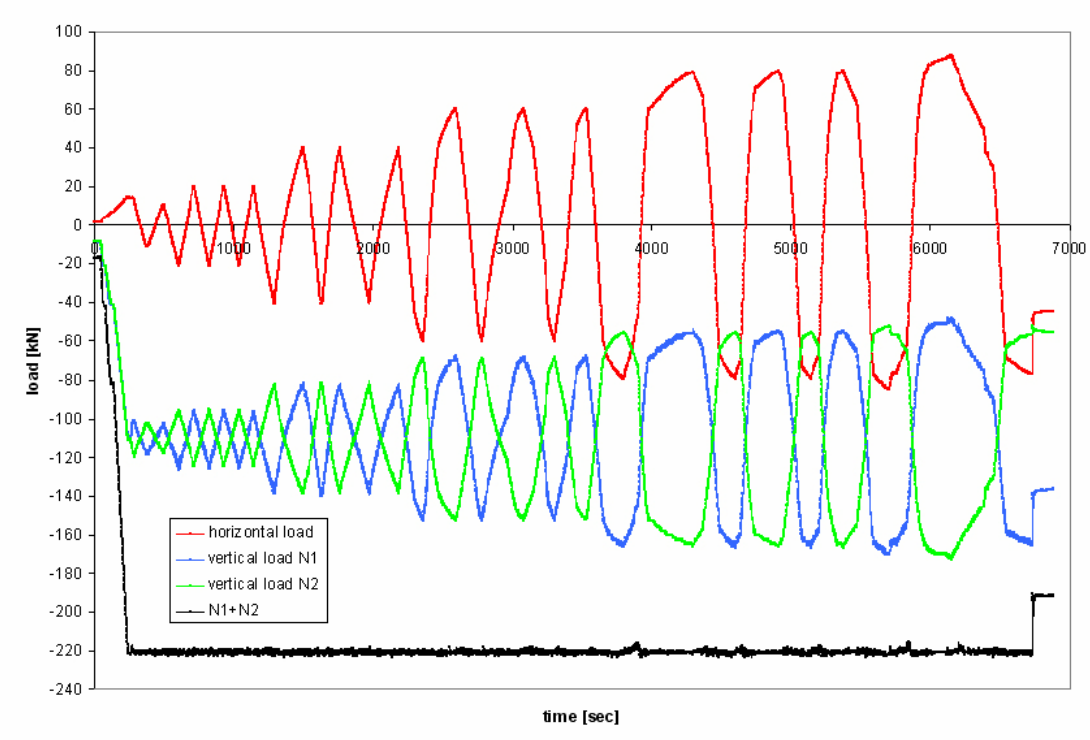

figure A17-3: load history of wall No. 17

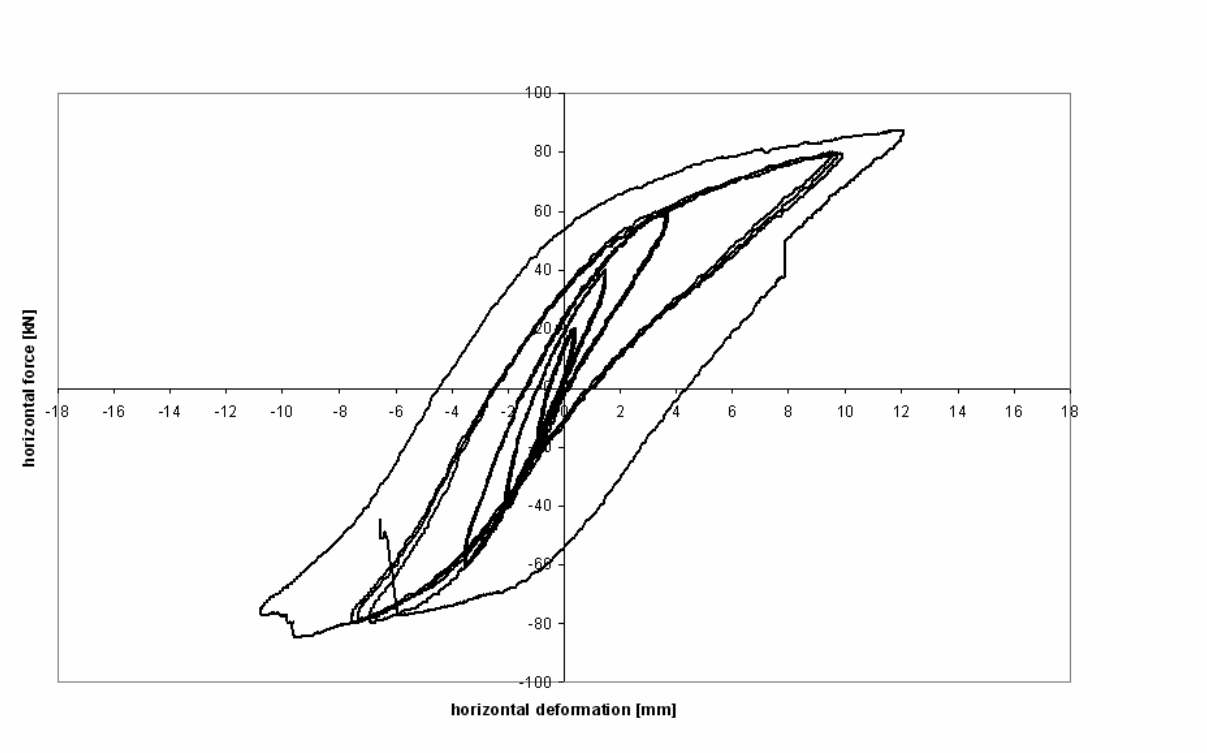

figure A17-4: hysteresis of wall No. 17

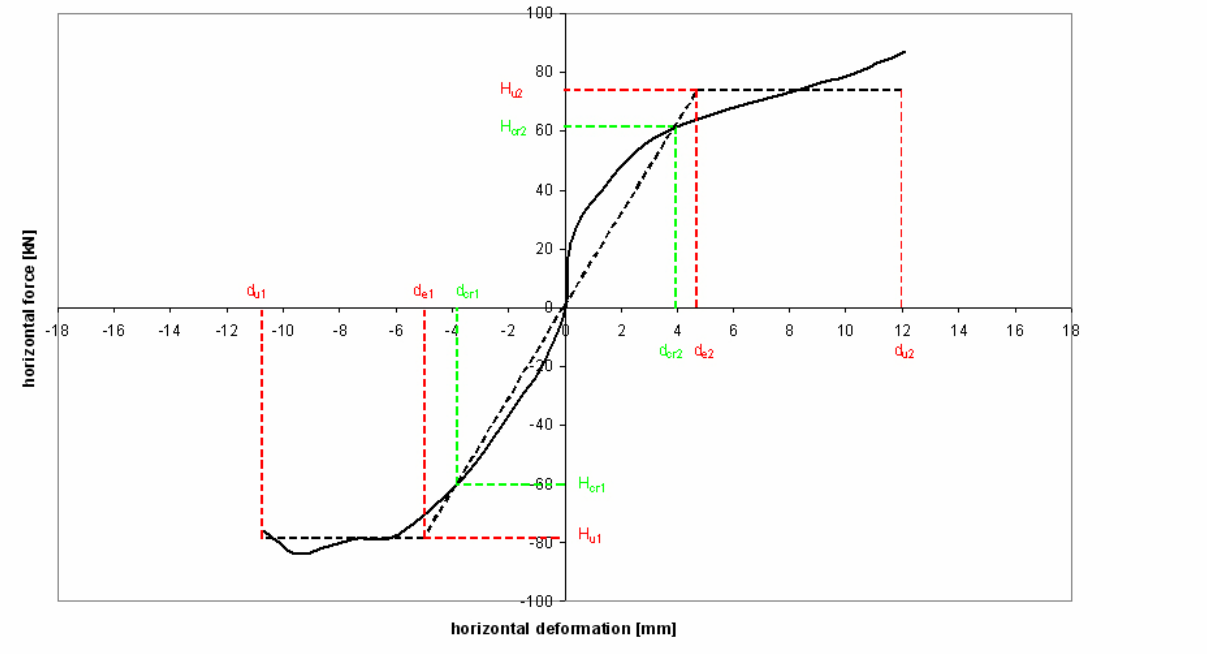

figure A17-5: enveloping curve of wall No. 17

figure A18-1: crack pattern of test No. 18

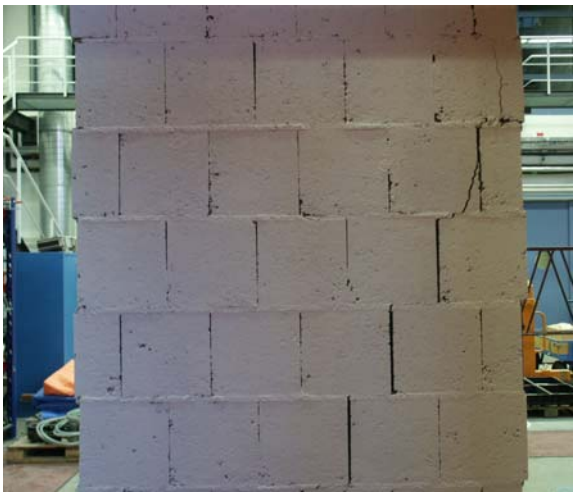

figure A18-2: detail of the crack pattern of test No. 18

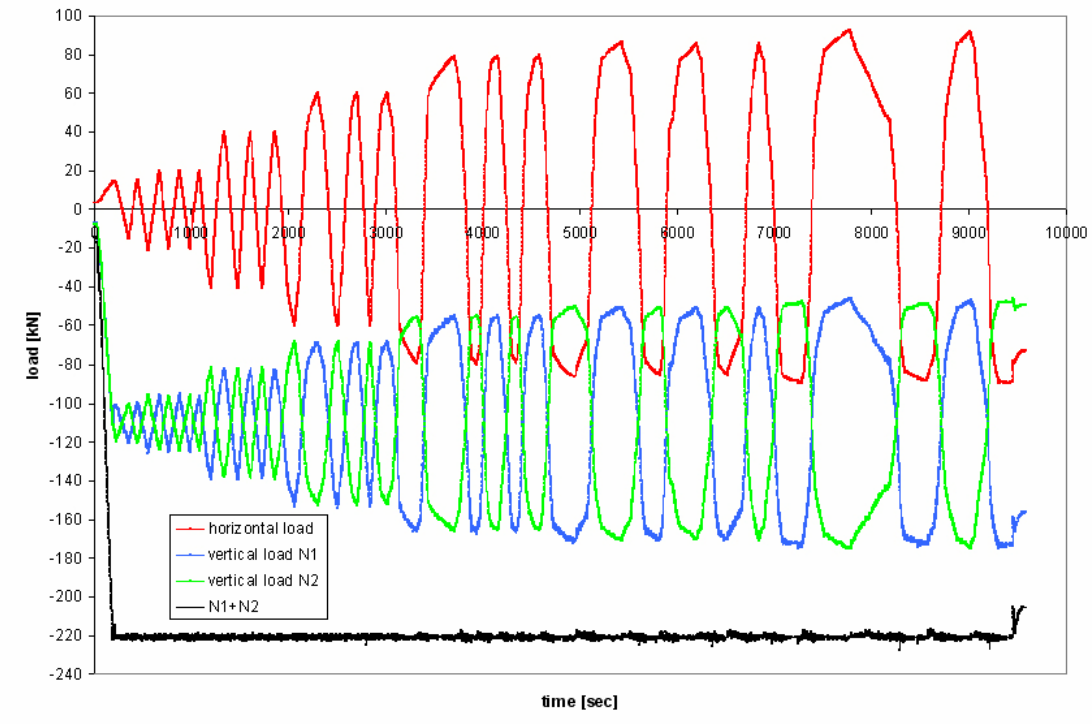

figure A18-3: load history of wall No. 18

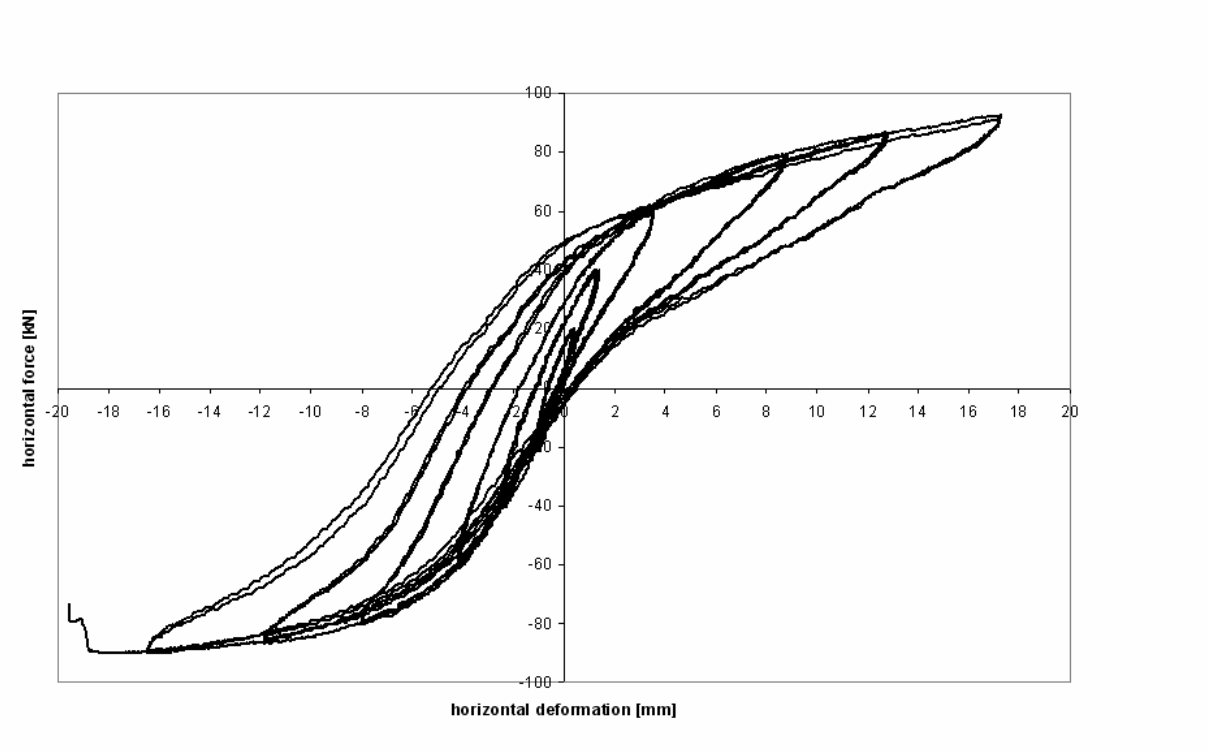

figure A18-4: hysteresis of wall No. 18

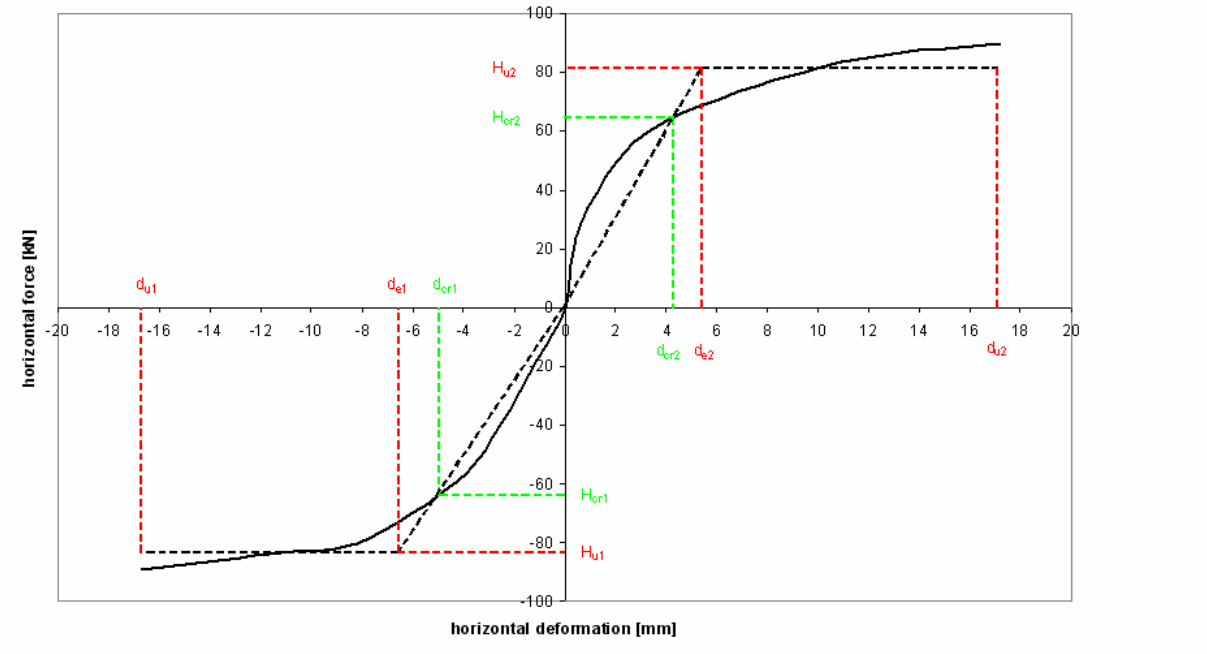

figure A18-5: enveloping curve of wall No. 18

figure A19-1: crack pattern of test No. 19

figure A19-2: detail of the crack pattern of test No. 19

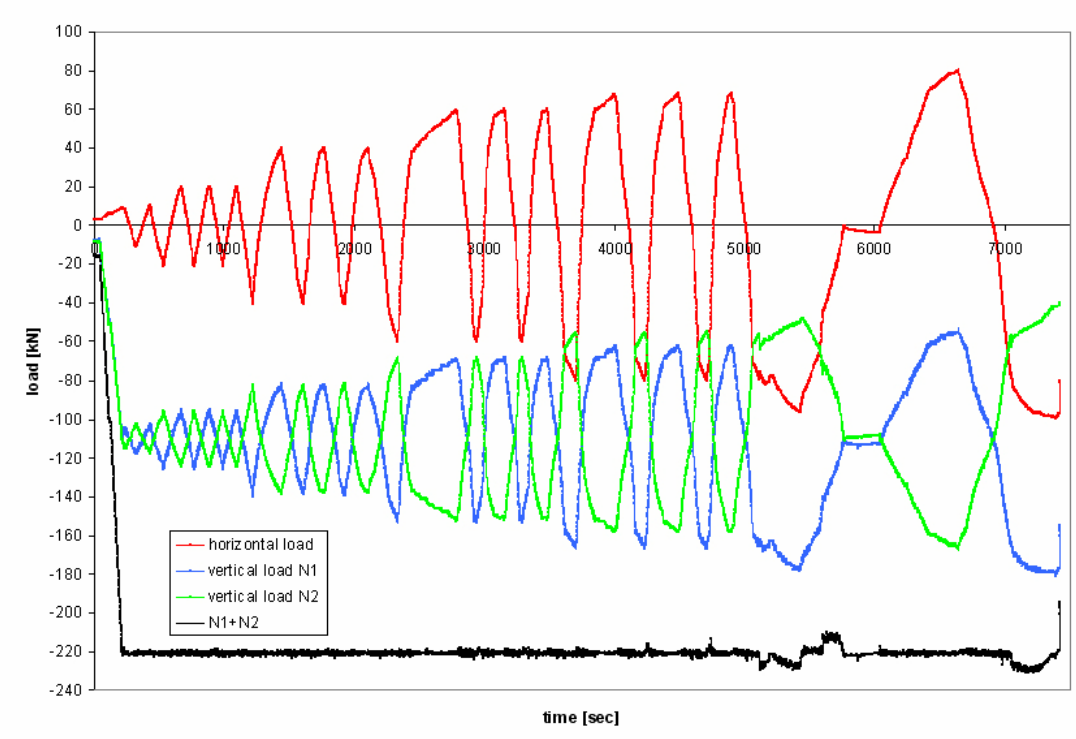

figure A19-3: load history of wall No. 19

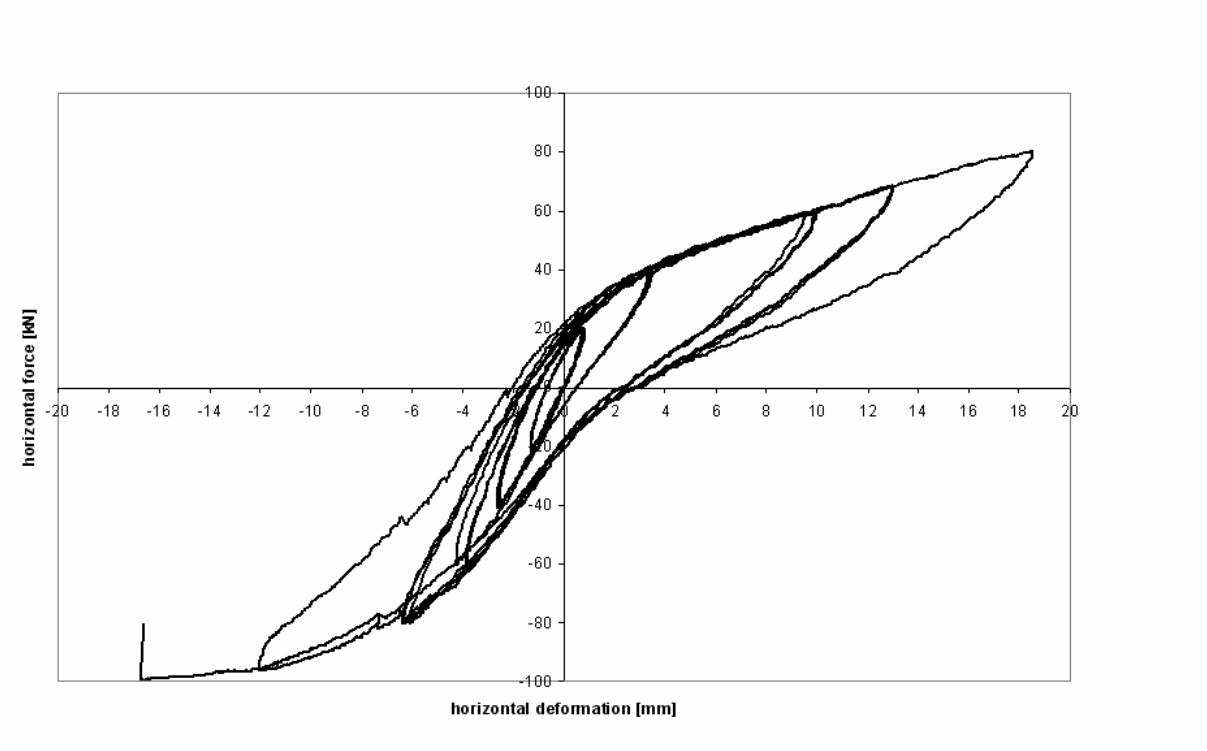

figure A19-4: hysteresis of wall No. 19

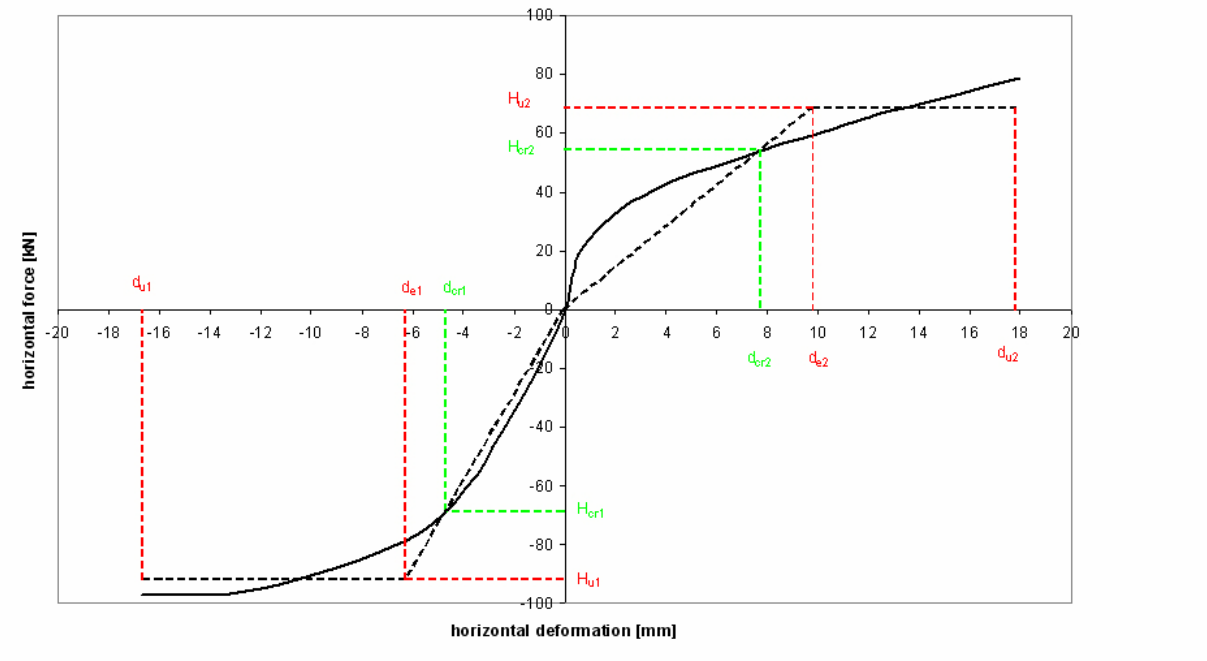

figure A19-5: enveloping curve of wall No. 19

figure A20-1: crack pattern of test No. 20

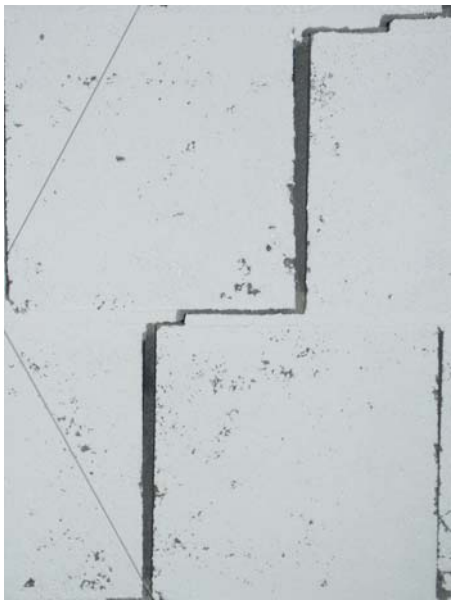

figure A20-2: details of the crack pattern of test No. 20

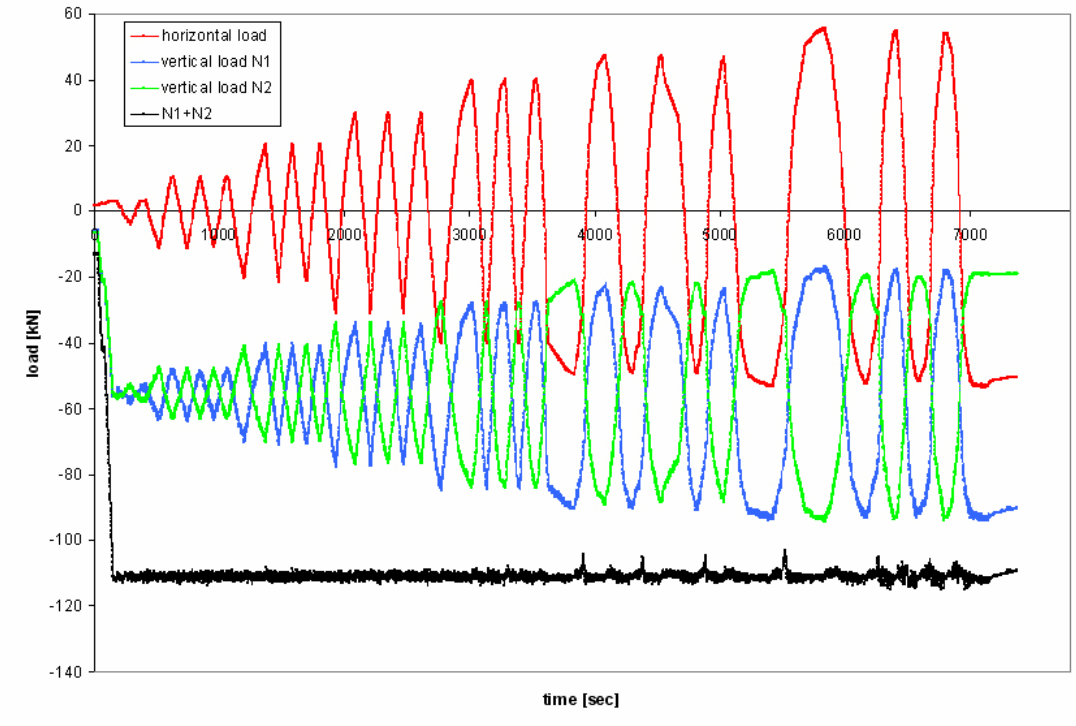

figure A20-3: load history of wall No. 20

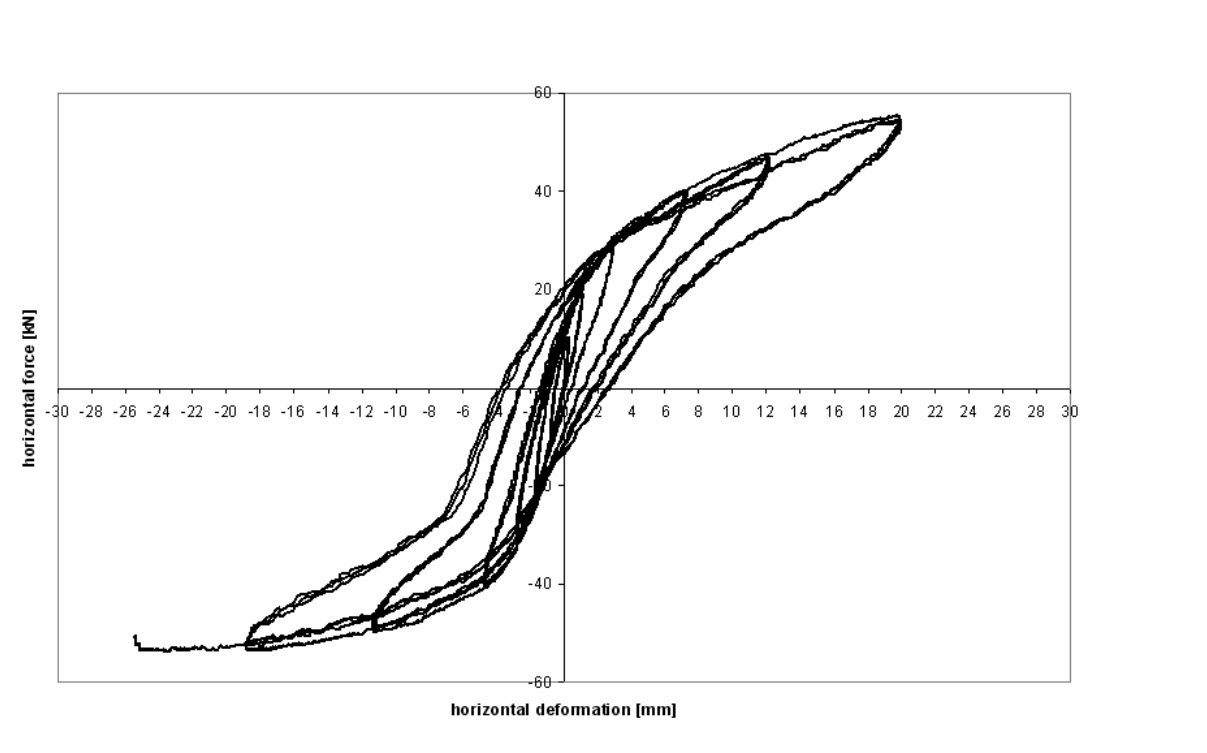

figure A20-4: hysteresis of wall No. 20

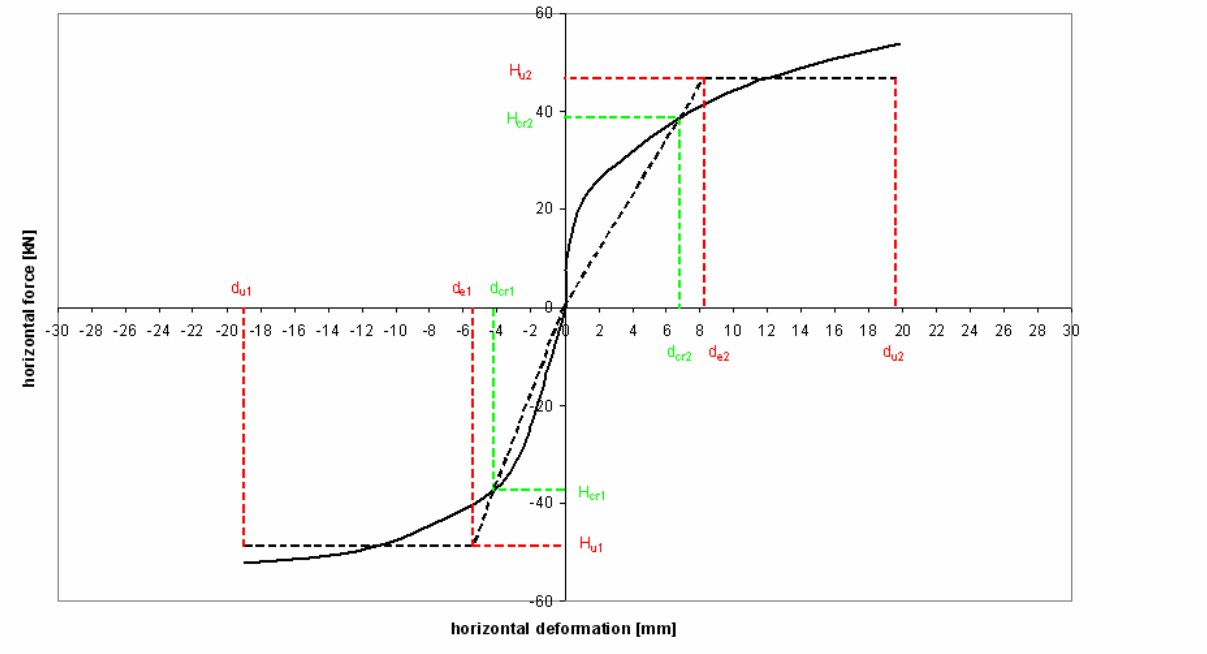

figure A20-5: enveloping curve of wall No. 20

figure A21-1: crack pattern of test No. 21

figure A21-2: gapping of test specimen No. 21

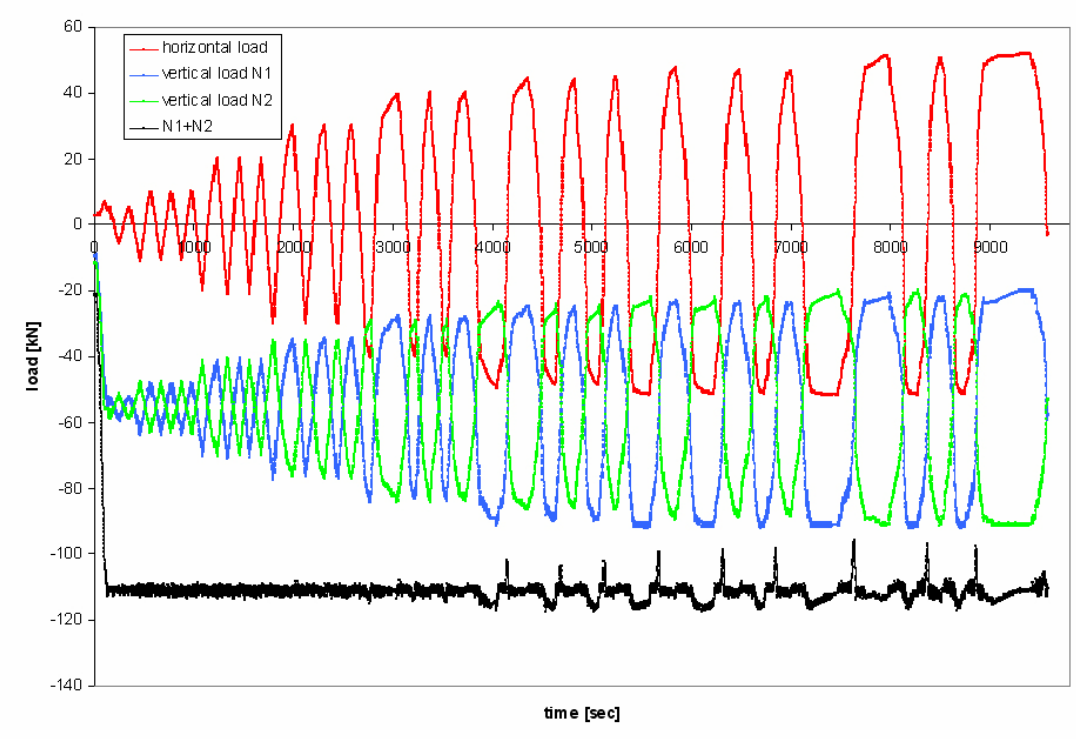

figure A21-3: load history of wall No. 21

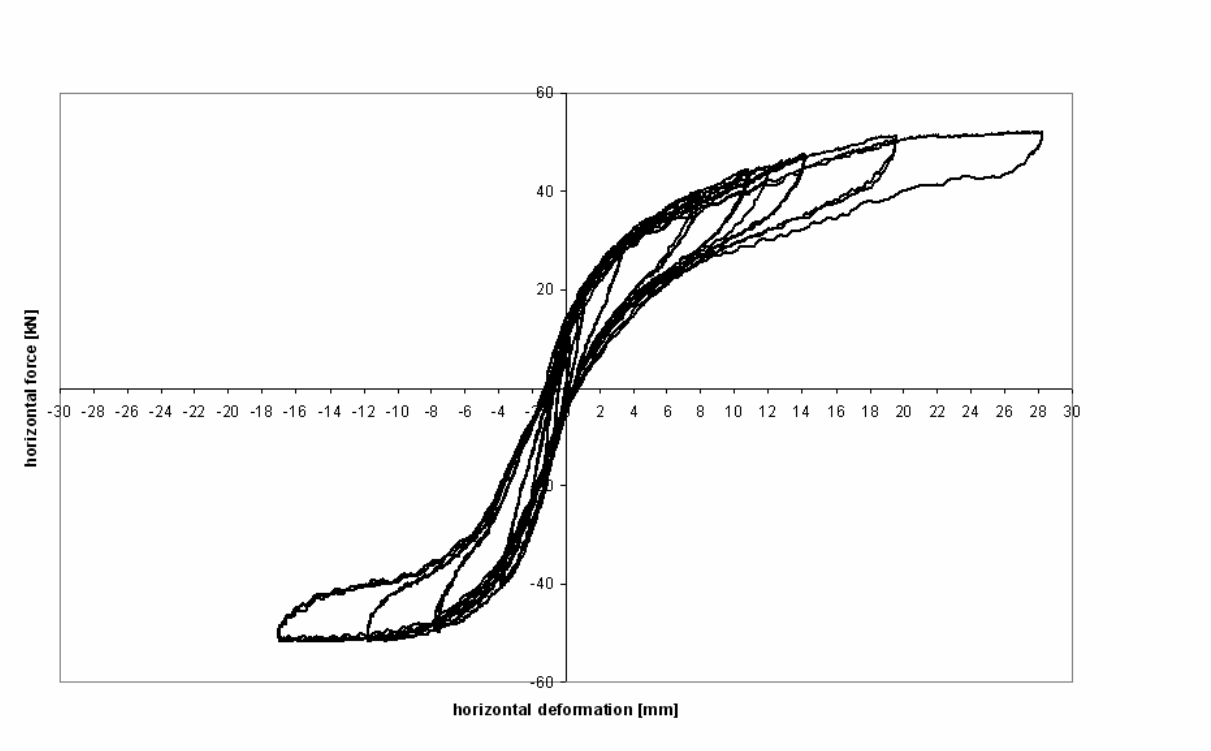

figure A21-4: hysteresis of wall No. 21

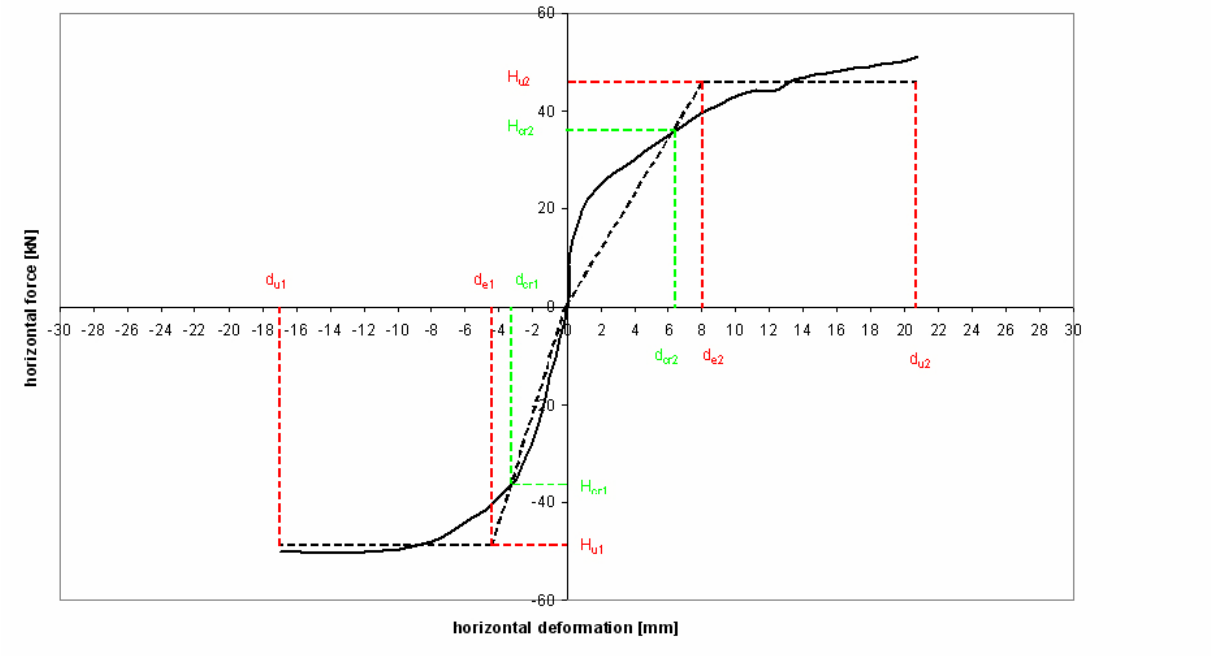

figure A21-5: enveloping curve of wall No. 21

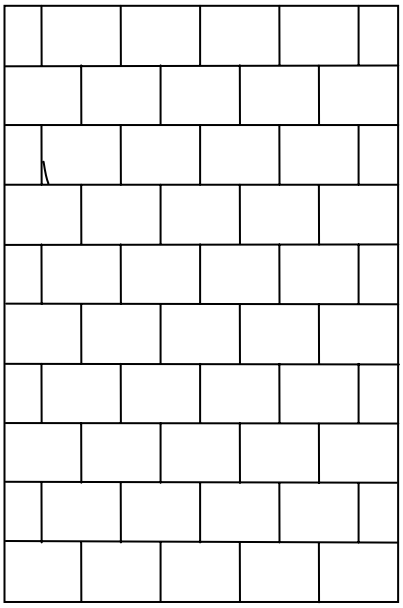

figure A22-1: first cracks at about -48 kN of test No. 22

figure A22-2: crack pattern of test No. 22

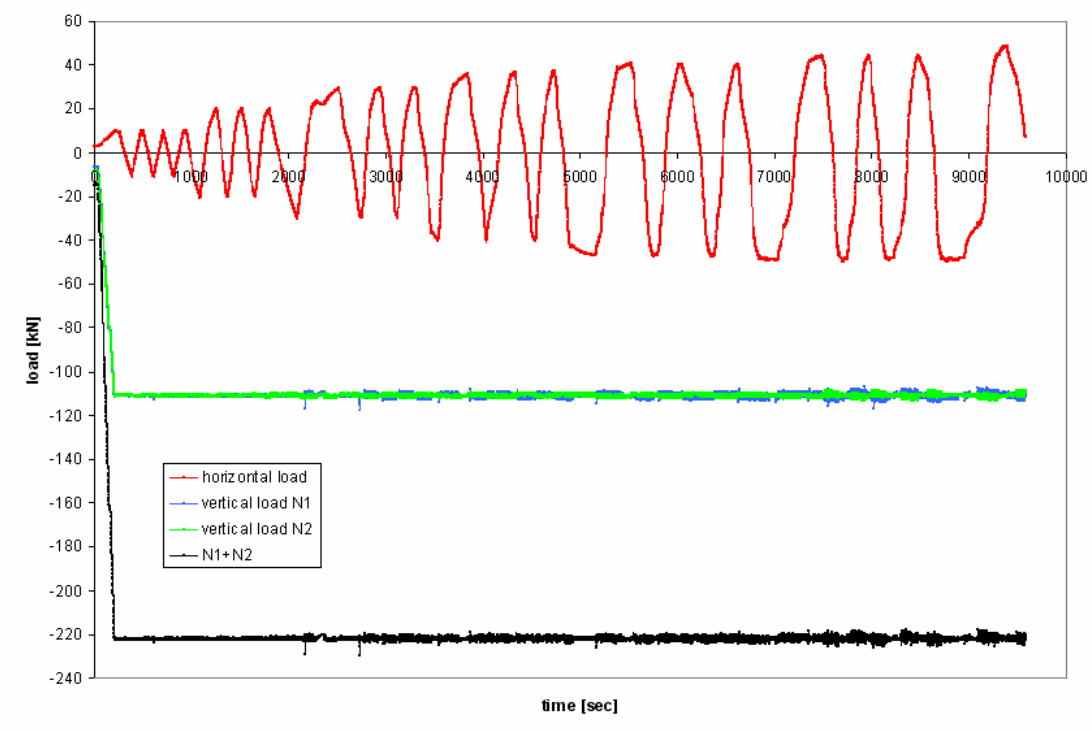

figure A22-3: load history of wall No. 22

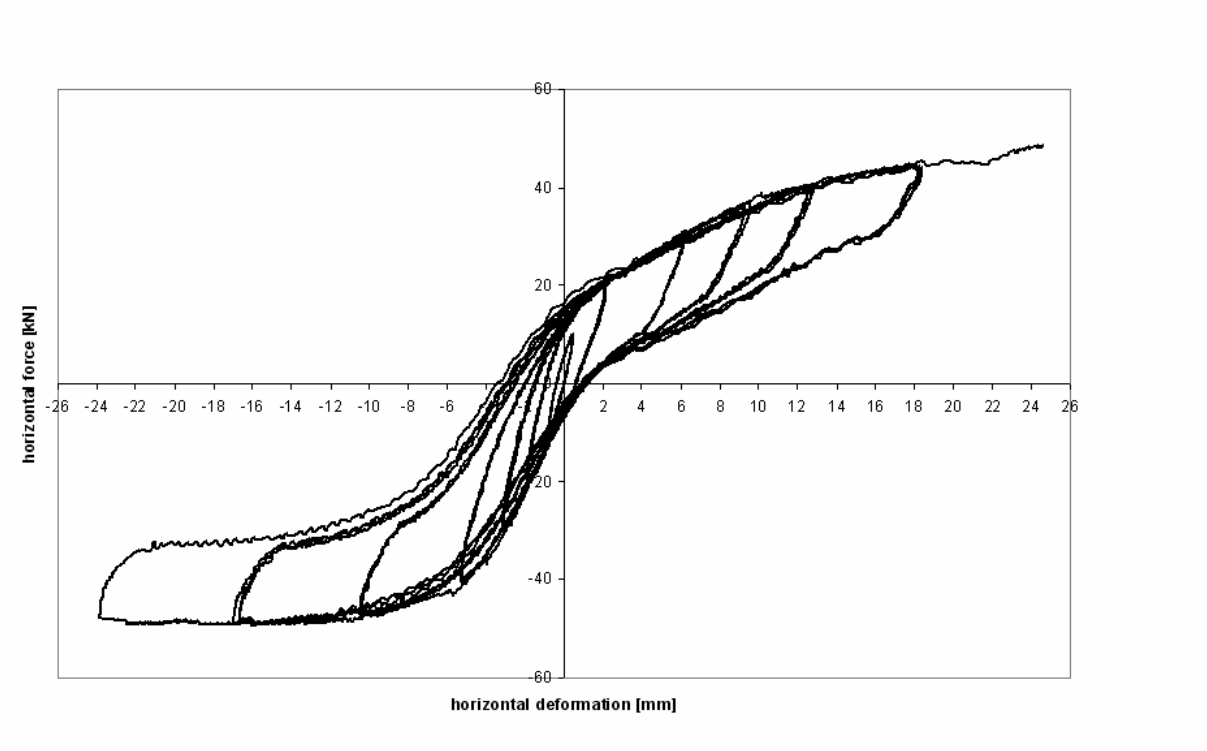

figure A22-4: hysteresis of wall No. 22

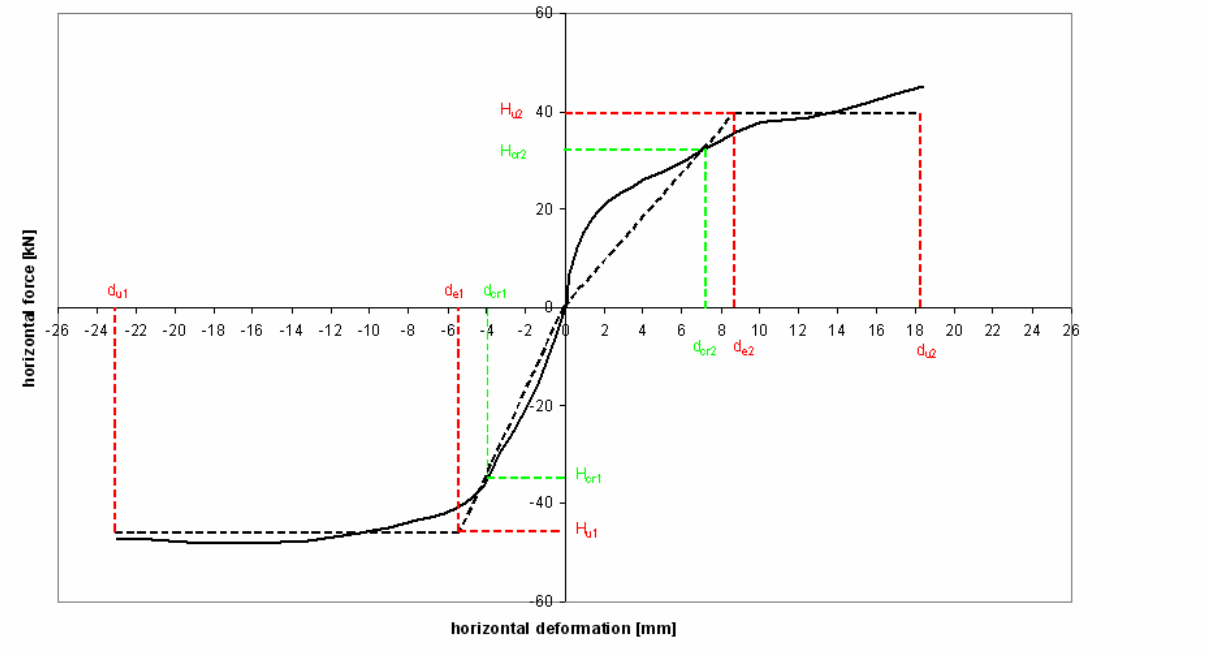

figure A22-5: enveloping curve of wall No. 22

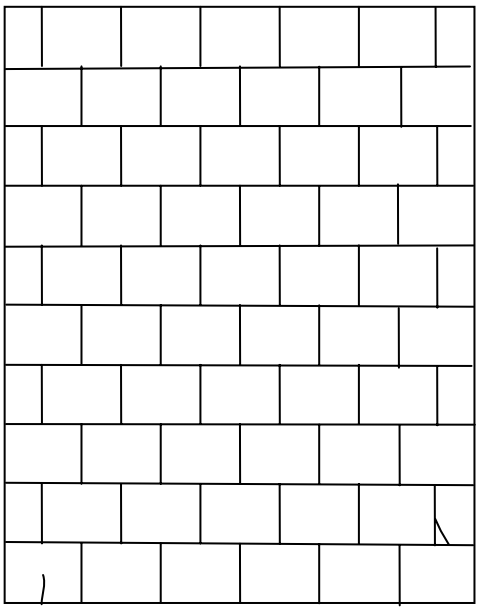

figure A23-1: first cracks at about ±100 kN of test No. 23

figure A23-2: failure of test No. 23

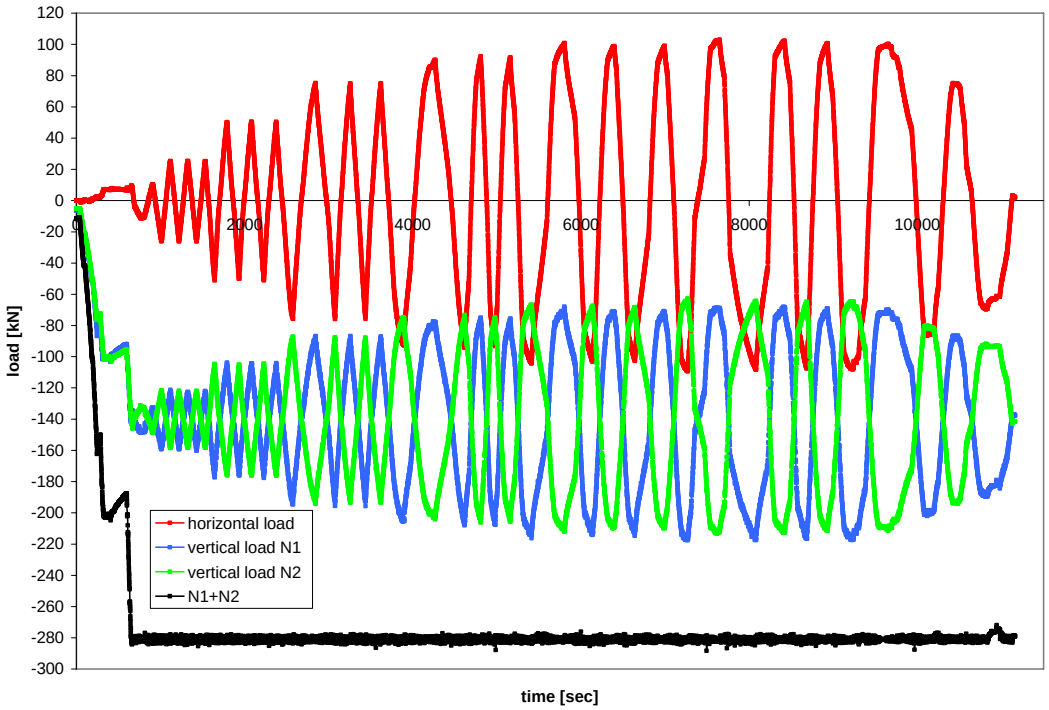

figure A23-3: load history of wall No. 23

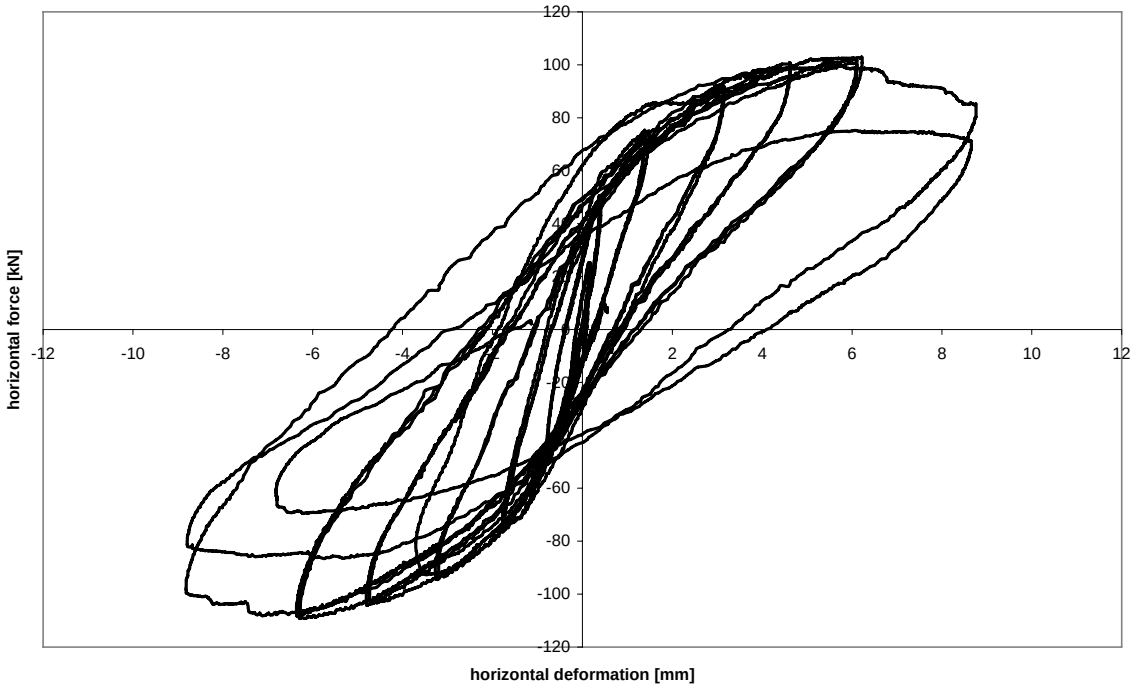

figure A23-4: hysteresis of wall No. 23

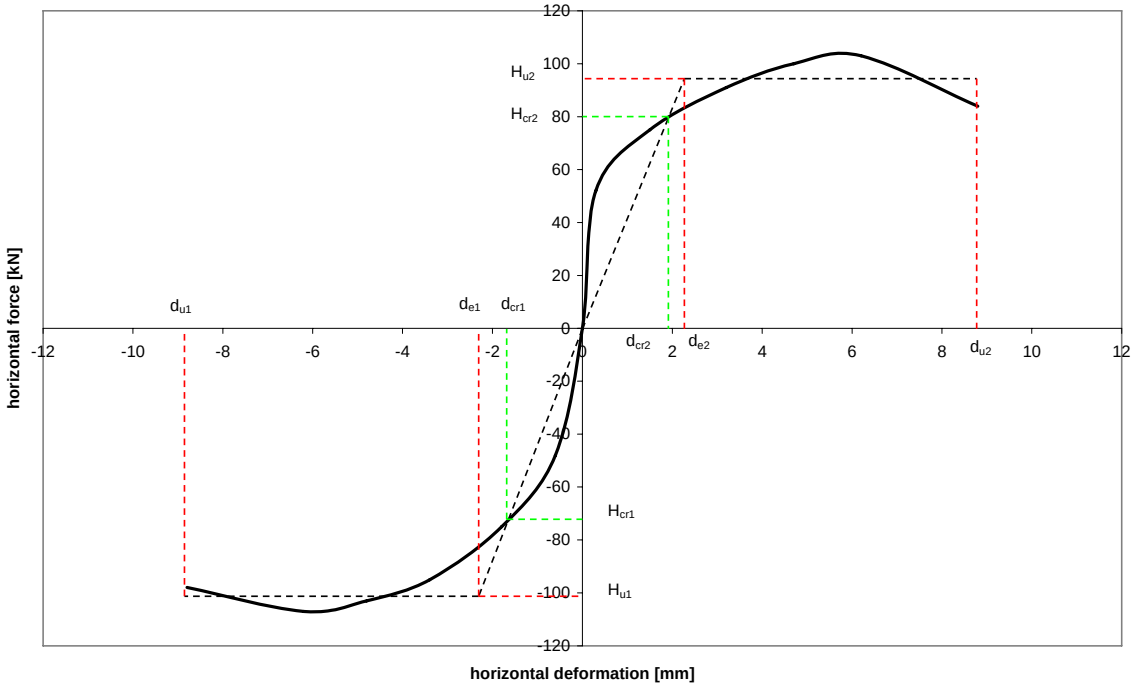

figure A23-5: enveloping curve of wall No. 23

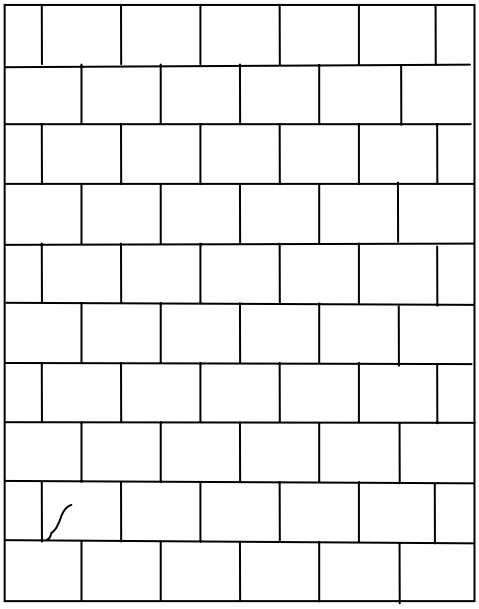

figure A24-1: first crack at about +115 kN of test No. 24

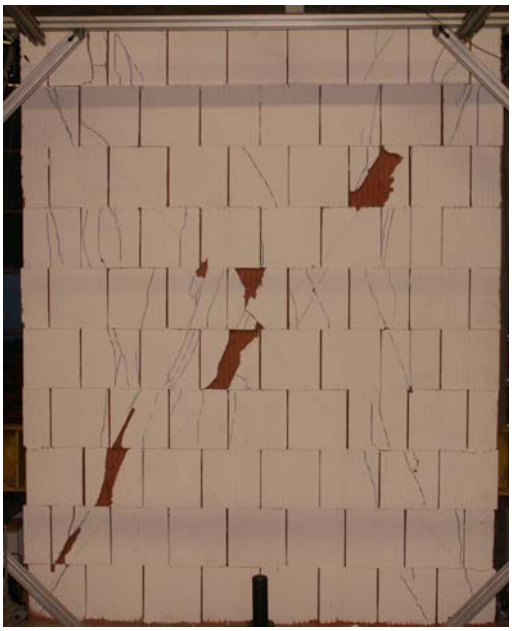

figure A24-2: crack pattern of test No. 24

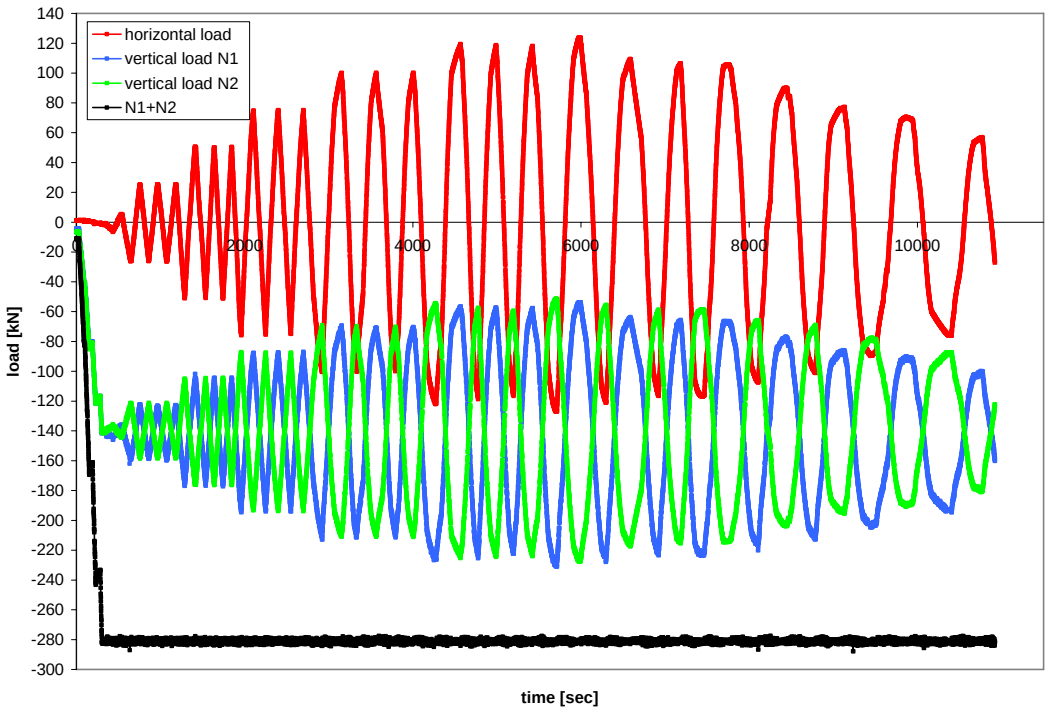

figure A24-3: load history of wall No. 24

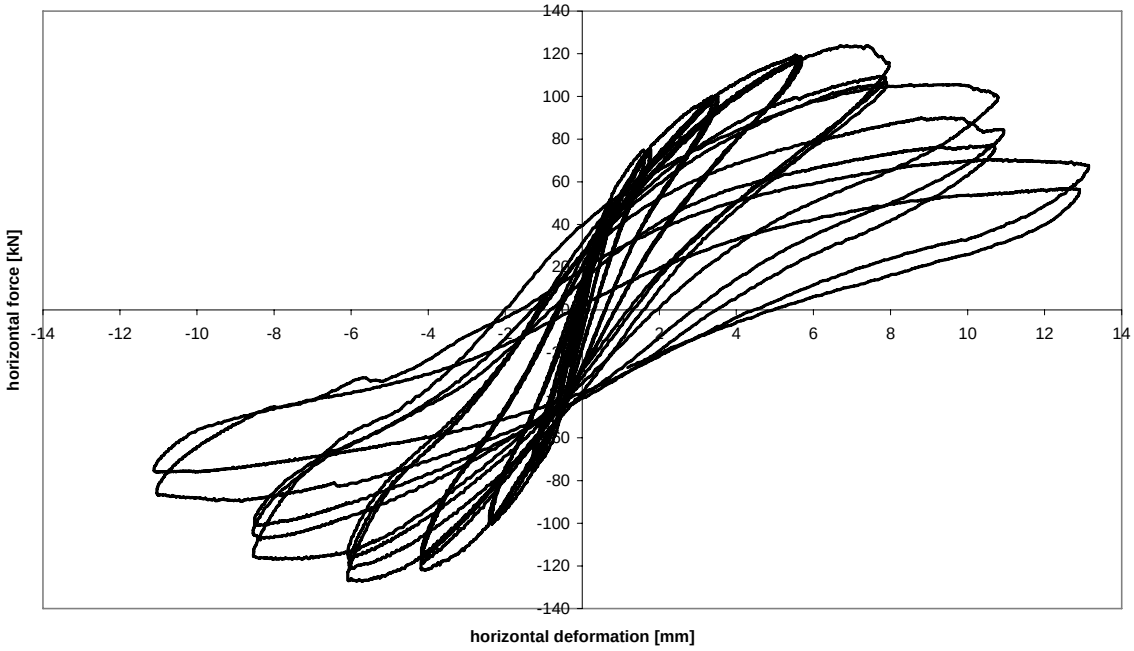

figure A24-4: hysteresis of wall No. 24

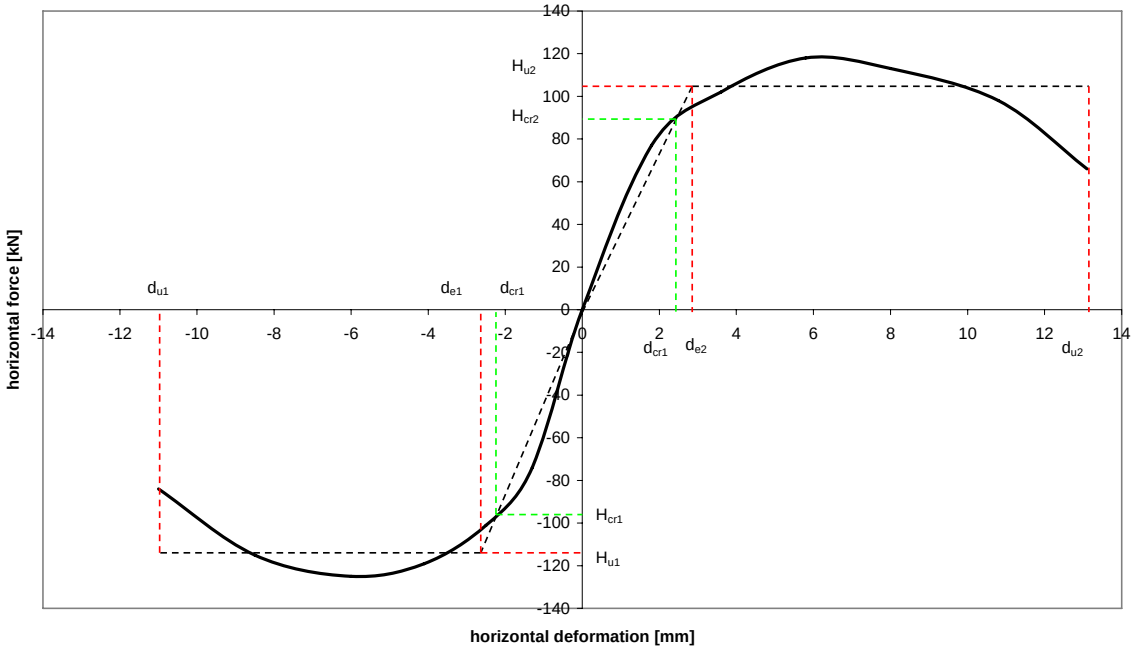

figure A24-5: enveloping curve of wall No. 24

figure A25-1: first crack at the face side of test No. 25

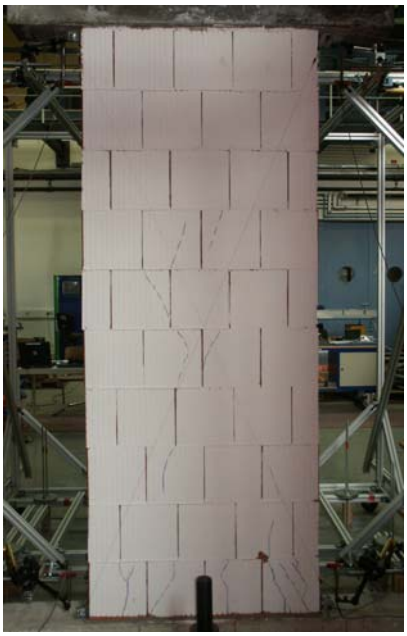

figure A25-2: crack pattern of test No. 25

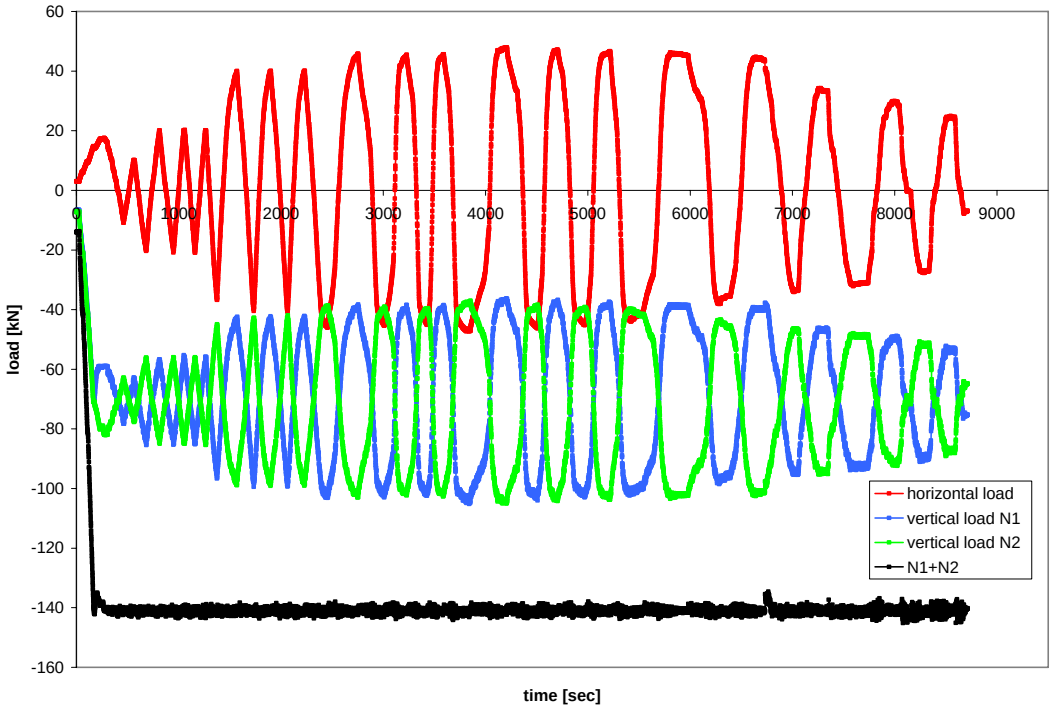

figure A25-3: load history of wall No. 25

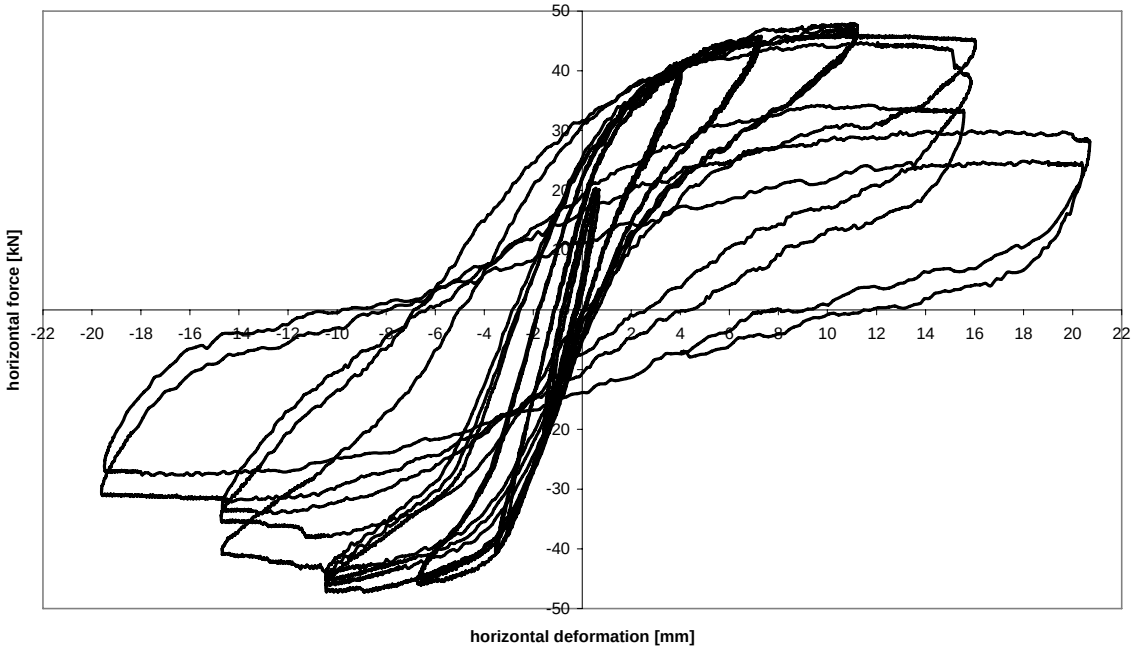

figure A25-4: hysteresis of wall No. 25

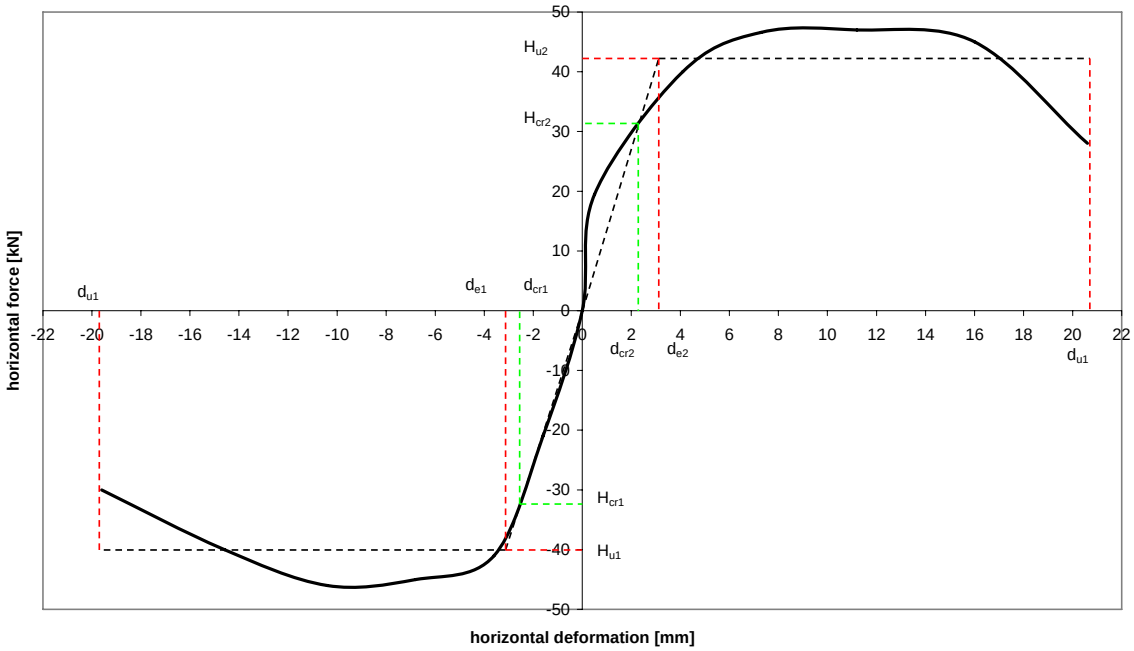

figure A25-5: enveloping curve of wall No. 25